Predetection of Stroke by Using Heuristics and Artificial Neural Networks

By
Andrei Popescu

A Thesis
Presented to School of Graduate Studies and Research
In partial fulfillment of the
Requirements for the degree of

Master of Applied Science

Electrical and Computer Engineering
University of Ottawa

I hereby declare that I am the sole author of this thesis. This is a true copy of the thesis, including any required final version, as accepted by examiners. Also, I authorize the University of Ottawa to lend this document to other institutions for scholarly research.

Abstract

The strokes are an important cause of death for all the people, not only for the aged population.

Sooner a stroke is discovered better chances are for the patient to minimize the damage or even to survive it.

The complexity of strokes reveals clearly the importance of early stroke predetection which are not only helping the doctors but they could literally save lives.

Algorithms for predetection of stroke are diverse, however they are little explored. This thesis is mainly centered on predetection of stroke, based on the inversion of T waves in electrocardiograms.

Two models were proposed in this thesis to help providing efficient predetection of stroke for people suffering of myocardium diseases and myocardial ischemia. The algorithms were tested on data from four electrocardiograms given by a library and five electrocardiograms from five different patients. Filters for noisy signals are also provided in this thesis.

These algorithms can be used as a tool by nurses and doctors but they do not represent a fully automated detection of stroke.

Acknowledgments

This thesis would not have been completed without the help and support I received. I would like to acknowledge all those who have provided me with the opportunity to end this thesis.

I would like to thank my supervisors at the School of Information Technology and Engineering at the University of Ottawa, Dr. Voicu Groza and Dr. Tet Yeap. I am grateful for both the guidance and support they have offered me during my work and the progression of my research.

I would like to thank my parents Olga and Mihai Popescu for all their entire support.

I would like to thank my friends and relatives for their sincere encouragements.

My last thoughts are for my wonderful loved children: Isabela and Sebastian. I deeply hope one day they forgive me for all the time I could not spend with them.

Table of Contents

List of Tables

List of Acronyms

ECG	Electrocardiogram
BP	Blood pressure
SBP	Systolic blood pressure
DBP	Diastolic blood pressure
MAP	Main arterial pressure
AVR	Augmented vector right
AVL	Augmented vector left
AVF	Augmented vector foot
PTT	Pulse Time Transit
OMW	Oscillometric Waveform
BPF	Band-pass filter
RSA	Respiratory sinus arrhythmia
PP	Pulse pressure
NN	Neural Networks

List of Figures

Chapter 1 Introduction

The stroke, the pulse, the heart rate, and blood pressure are frequent subjects of many conversations.

The ***main objective*** of this thesis is to develop reliable algorithms for the predetection of stroke based on patient's change of T wave's polarity at his / her electrocardiogram (ECG).

1.1 Blood pressure, electrocardiograms and strokes

The heart is a muscular organ that has a heartbeat. The resting human normal heartbeat ranges from 60–100 bpm. [1]

The pulse beat was observed by humans for hundreds of years. Once they realized its regularity the scientists became more and more interested about it. [2]

It is stroke and the blood pressure (BP) of human body that presents more interest for this thesis and these are related to different blood vessels. Those vessels are entering and leaving the heart (blood is pumped by the heart and carried by the blood vessels; the vessels that carry blood away from the heart are called arteries and the blood vessels that bring blood towards the heart are called veins).

Blood pressure (BP) represents basically the force of blood against the walls of human's blood vessels. [9]

According to Dr. Faulx, the blood pressure and heart rate often rise and fall together and when a person is facing a danger, most of the times they both jump upwards at the same time. However, if the heart rate rises that does not automatically mean that blood pressure rises. Still elevated heart rate is associated with elevated blood pressure. [3] [19]

Optimal blood pressure is typically defined as 120 mm Hg systolic (the top number, when the arteries rich its highest pressure) over 80 mm Hg diastolic (which is the lowest blood pressure). The hypertension condition is caused by elevated blood pressure. [3]

When talking about heart problems, people fear of hypertension and especially the aged population could be easily spotted here. Hypertension is a common clinical problem and a major risk factor for strokes, cardiovascular diseases, and other risks.

Heart functioning is a complex process. The malfunctioning of heart can lead to stroke. There is an electrical system that controls the heart and uses the electrical signals to contract the heart's walls to pump the blood to human's body (before the blood circulation an electrical activity must occur). This electrical activity is recorded by a device called electrocardiograph that is used to monitor the electrical and muscular activity of the heart and they are producing ***electrocardiograms*** (ECGs). [14]

The measurements of heart's electrical activities are done through recording leads situated on patient's body. [36] A picture about how the signal comes from an ECG can be seen in the next figure:

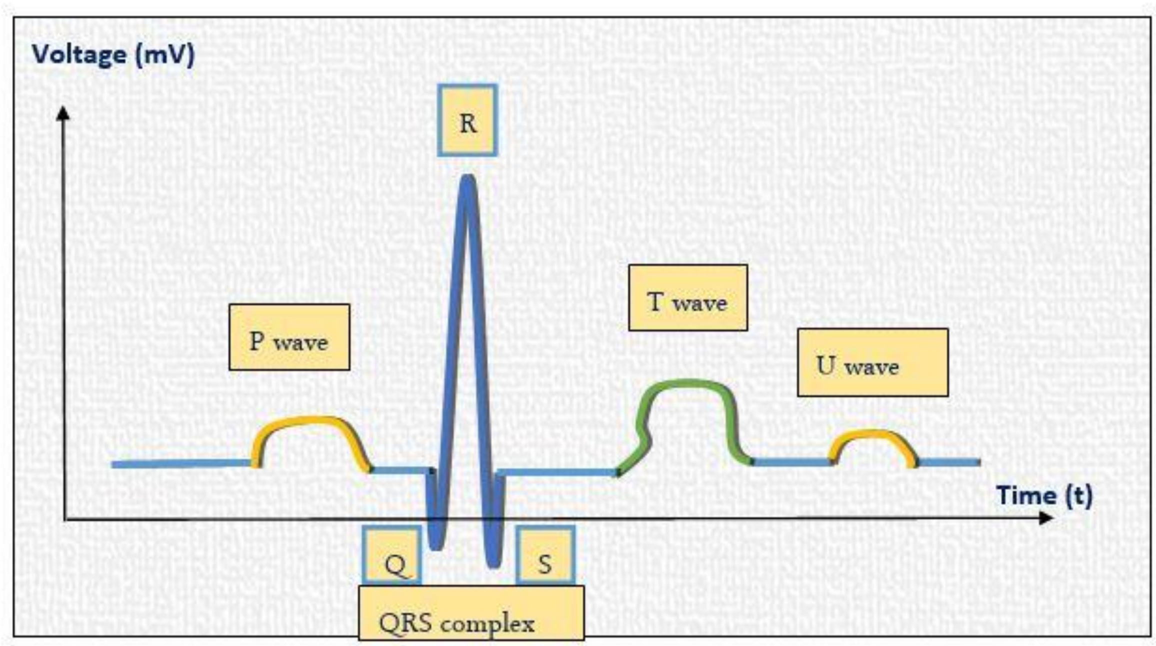

Figure 1.1: A classic electrocardiogram with its specific signals (waves)

More details about ECG and electrodes are provided in chapter 2.

Strokes are perceived as a "brain attack". People are dealing with strokes when the blood flow to an area of brain is reduced or cut off. Then the brain cells begin to die. There are two types of stroke: *ischemic and hemorrhagic* strokes. The problem is that most of the people recovered from strokes have special types of disabilities. The good thing is that up to 80% of strokes can be prevented. [4]

Strokes occur when a blood vessel is blocked by o clot or burns. There are drugs that can produce a powerful clot-busting. [5]

In figure 1.2 it can be seen a representation of a clot right away after a brain artery is split in two. This drawing was realised by using exclusively Microsoft Word Illustration tools.

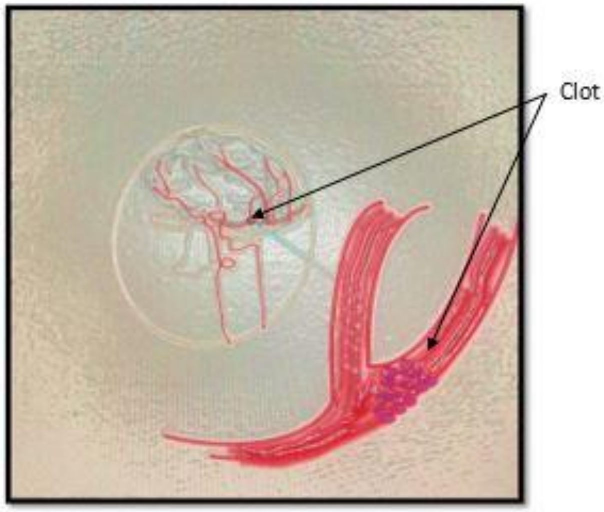

:

Figure 1.2: Ischemic stroke

The ischemic stroke is the most common type of stroke; it is considered that nine strokes out of ten falls into this category. [4] Ischemia is a serious medical problem where some part of your body (e.g. heart or brain) is not getting enough blood, so it is not getting enough oxygen. Ischemia happens because of a blockage in the arteries. [6] As it is showed in figure 1.2, an ischemia stroke occurs when an artery that is carrying blood to the brain is blocked by a blood clot. [4]

Medical world is very interested in finding and administrating the best drugs to remedy the strokes. Everybody agrees there is a limited time in which a clot busting drug can be efficient. It is about only a few hours (for instance not more than 4.5 hours). [4]

Some signs that are preceding a stroke (for example weakness of the body or change of vision in one or both eyes) are probably not leading right away to the certitude of having one. Other signs (such as problems of keeping the balance or walking, difficulties in speaking or understanding others) could lead easier to the presumption that the subject is facing a potential stroke. [6]

The immediate test to verify if somebody is facing a stroke are relatively easy to be followed: the subject can be asked to lift his / her arms or to repeat a simple sentence.

Symptoms that show a possible stroke necessitate immediate medical attention. Sometimes doctors can reduce the damage if they act quickly. Initially doctors administrate oxygen; for a stroke in progress, anticoagulants may be provided but they are not given to patients with high blood pressure. [7]

Removing blockages after a small stroke (e.g. transient ischemic stroke) may reduce the risk of further strokes. [7].

Once the stroke is completed, some brain tissue is dead. Once the blood supply is re-established, it cannot restore its function.

A less commented aspect is that high blood pressure can damage arteries when creating conditions to clog or burst them easily. A weakened artery resulting from high blood pressure represents a much higher risk for a stroke. [8]

The other type of stroke is the hemorrhagic stroke, which can be fatal in comparison with the stroke one. It happens when deteriorated blood vessel in the brain is erupting; this unwanted possibility can be seen in the Figure 1.3:

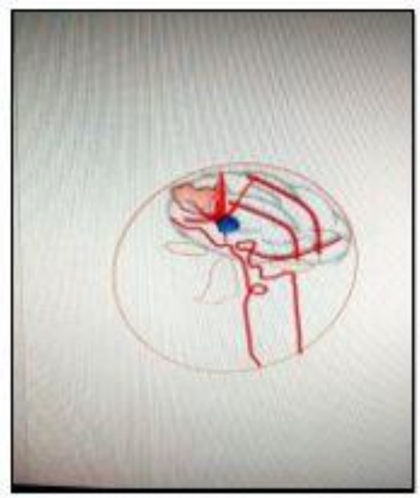

Figure 1.3: Hemorrhagic stroke

It is very difficult to stop the bleeding when it is occurring inside the brain.

An ischemic stroke can be caused by fat substances that are building up in the arteries or by any uncontrolled high blood pressure that causes a deteriorated artery to break.

After a stroke occurs, the rehabilitation starts as soon as the blood pressure, pulse, and breathing have been stabilized. The rehabilitation continues in the hospitals or in rehabilitation centers. [7]

1.2 Motivation of the research

After cancer, the stroke and the diseases of heart are the main causes of death in Canada.

According to the Statistics Canada, stroke and diseases of heart were the third and the second causes of death in 2011, 2012, 2013 and 2014. [67] [68] Over twenty thousand people died in Canada because of stroke in 2011 and 2012. [67]

In Unites States, stroke is the fifth leading cause of death. [69]

Regarding the enormous impact this disease has, the awareness of the population and the exposure to stroke education are considered crucial. [69] Being such an important disease, its prevention is critical, it is extremely useful to have reliable predetection stroke alarms. Finding improved algorithms is relied on signals such as electrocardiograms (ECGs).

It is of interest to build good algorithms that could alert nurses while interpreting an electrocardiogram. Blood pressure is a vital signal and people are often developing hypertension. In this thesis, the hypertension is considered a trigger for stroke. The patients who suffered hypertension are sent to do their electrocardiograms.

Previous work made in this field initially relates primarily to the myocardial infarction detection and secondly to designing artificial neural networks to identify arrhythmias from ECGs.

P. Libby stated that ST segment elevation causes myocardial infarction. {74] Myocardial infarction is associated with significant risk of stroke. [81]

Mohamed Abdelazez et al. wanted to reduce the vast number of false alarms for myocardial ischemia by implementing a system that employs multiple estimates of ST segment deviations. This system makes correlations between estimates (low correlation means there is an inaccurate estimate). During this study, three correlation methods were considered. [75]

V. C. Cavalcanti Roza et al designed an artificial neural network to identify two arrhythmias patterns in the datasets obtained through ECG signals. Two types of arrhythmias were studied in an arrhythmia dataset (AD) and supraventricular arrhythmia dataset (SAD). [76] C-H Lin proposed a method for ECG heartbeat discrimination. In the end, cardiac arrhythmias were recognized. [77]

1.3 Problem Statement

There are algorithms that help people analyzing ECGs to detect heart diseases. [46]

Considering the natural fluctuations that happen in every human body, inaccuracies in predetection of stroke and blood pressure estimations shall be expected. These fluctuations can be caused by a biological and / or artefactual phenomenon (such as stress, reactions induced by diabetes, obesity, etc.). Breathing is one the key elements that induce fluctuations in electrocardiograms and blood pressure estimations. [19] [23] The breathing effects on blood pressure have been intensively studied and they are well known; they usually lead to alterations in the signal recordings. [23]

The manifestation of myocardial ischemia and myocardial infarction goes on when T wave inversion occurs. [73] [39]

Clinical studies showed that during myocardial damage the most repeated change in the ventricular complex is the enlargement of Q wave combined with the negativity of the T waves. [70] It is not only the inversion of T waves that conclude a myocardial ischemia: according to Kevin Channer and Francis Morris this myocardial ischemia can influence the morphology of T waves in several ways: T waves may become flattened, tall, inverted, or biphasic. [73]

The myocardial infarction is known as a heart attack when the blood supply is brutally restricted for a part of the heart. [7]

According to W. Perry Dickinson the majority (e.g. 60%) of deaths occurred to patients who experienced a transient ischemic attack resulted from a myocardial infarction. [65]

The change in T wave's polarity is used for stroke's predetection in this thesis. [81]

Various algorithms are proposed and applied to determine predetection of stroke. Based on the change of the polarity of T waves (see figure 1.1) in this thesis it will be determined if there are cases of any alarm related to stroke's predetection or not. The main steps will include the selection of database from various ECGs, the electrocardiogram configuration, the signal modelling in Matlab, and the mathematical predetection of stroke.

Filters applied to noisy signals on ECGs are tackled later after the development of stroke's predetection algorithms.

In this thesis, the algorithms are implemented in Matlab. Above it was already considered the physiological aspect of ECGs pulse and blood pressure but more mathematical models that define them are to follow.

Figure 1.4 shows a block diagram which provides the main practical steps taken in this thesis. Some of these steps supported by mathematical algorithms. The main goal of this thesis is to provide reliable stroke's predetection alarms for people with myocardium affections.

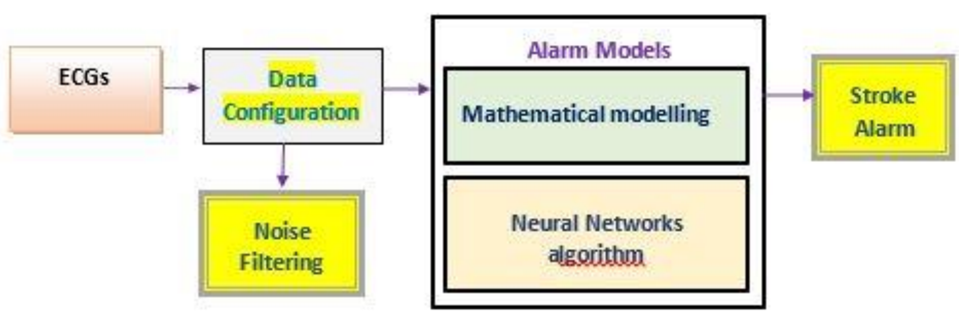

Figure 1.4: Block diagram with the main steps of the thesis

1.4 Contributions

The major contributions of this work are the followings:

- conceived a new mathematical algorithm to detect the polarity of T waves of various ECGs
- used artificial neural networks to classify the electrocardiogram signals for predetection of stroke
- devised a new mathematical equation for oscillometric waveforms
- provided two new mathematical equations that relates the breathing effects on the OMW and ECGs

The major challenge was the use of Artificial Neural Networks on electrocardiograms. The performance is assessed based on comparing the values of eight electrocardiograms produced during those mathematical operations.

At the best of the author's knowledge, providing stroke's predetection alarms for the change of polarity of T waves in an electrocardiogram by using heuristics and artificial neural networks was never explored before by others.

1.5 Thesis overview

In chapter 2 the theoretical basis of this thesis is indicated, including stroke, ECGs, heart rate, blood pressure, signal processing, breathing effects, and artificial neural networks.

In chapter 3 the mathematical models and equations designed for predetection of stroke and ECGs, oscillometric waves, and breathing effects are implemented. Artificial Neural Networks are used for pattern recognition and classification of stroke's predetection as well in chapter 3.

In this research, the theoretical presentation of stroke's predetection algorithms is done in Chapter 2, while their implementation is done in Chapter 3. Both heuristics and neural networks are used in Chapter 3 to get the best approach to these algorithms. The technical data is revealed in Chapter 4.

In chapter 4 technical data about the studied electrocardiograms are shown. Filters are presented in this chapter including Artificial Neural Networks used as estimating tools. In the end of this chapter the two presented models are compared and the most precise is chosen.

Finally, in the last chapter a few conclusions are taken with a summary about the previous chapters. Limitations and future work that can be done in this area are pointed out there as well.

Chapter 2 Literature Review: Blood Pressure, Electrocardiogram and Stroke

2.1 Heart, blood pressure electrocardiograms, and stroke

The history of pulse, strokes, and blood pressure measurement is extremely complex. The begging cannot not be clearly dated and it is not the goal of this study to search the proofs and the original ideas in this field.

2.1.1 Heart

The blood circulation system of the human body (including the heart in the middle) is illustrated in figure 2.1

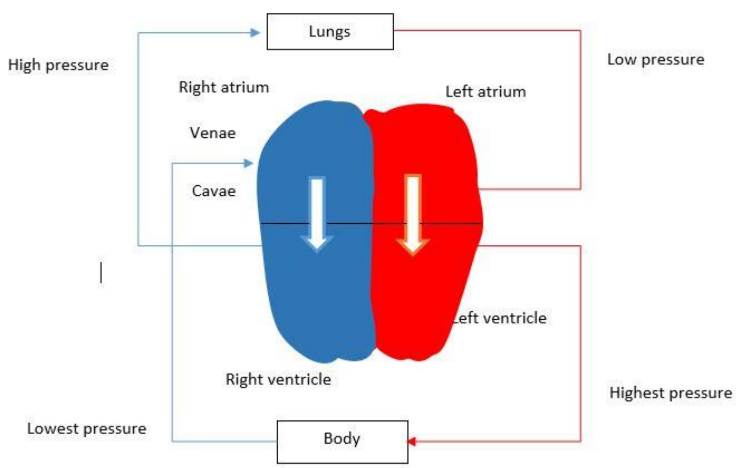

Figure 2.1: Blood circulatory system of the body

2.1.2 Blood Pressure

The interpretation of blood pressure measurement is important. By respect of all the pioneers and scientists who worked in the past and had a huge contribution in the blood pressure measurements, some important dates and devices are mentioned below.

Stephen Hales is the first person known in the history who measured blood pressure by inserting a tube in a horse's artery. A U-shaped mercury manometer ("the Haemodynamometer") was invented in 1828 but the very noticeable first ***non-invasive device*** (which was a vertical manometer with mercury) was introduced by Jules Herisson.

Later other remarkable sphygmanomometers have been invented (e.g. Marey's, Sommerbrodt's, Pond's, Dudgeon's, and Bloch's). [9]

The principle that was behind those sphygmometers was that the blood pressure is equal to the force which is required to compress the wall of the artery. [9]

In 1896, the professor Scipione Riva-Rocci constructed an arm cuff. The main idea was to obstruct the blood flow of the brachial artery. This device could catch the pressure required to inflate the rubber cuff at the moment when the pulse was not palpable distal to the obstruction.

This method was introduced in America in 1901 by Harvey Cushing and improved by H. von Recklinghausen. N.S. Korotkoff was a Russian army surgeon who described the arterial sounds caused by compression. He introduced the method of auscultation in blood pressure measurement. [9]

In 1909 M.V. Pachon introduced an aneroid manometer using an airtight tube responding to changing pressure which popularizes the ***oscillometric method*** and in 1910 I. Gallavardin introduced in France a double cuff to improve the sensitivity of Pachon apparatus. [9]

The **oscillometric method** is based on the principle that the pulsatile blood flow through an artery is creating arterial wall oscillations which are transmitted through the soft tissue to the occluding cuff where they are detected by the piezoelectric sensors as cuff pressure oscillations. [13] The physical procedure itself is to deflate the cuff wrapped around the person's arm.

As the occluding cuff pressure is gradually reduced from above systolic (SBP) to below diastolic (DBP); the SBP, DBP and the mean arterial pressure (MP) can be measured.

A typical blood pressure waveform looks as it follows:

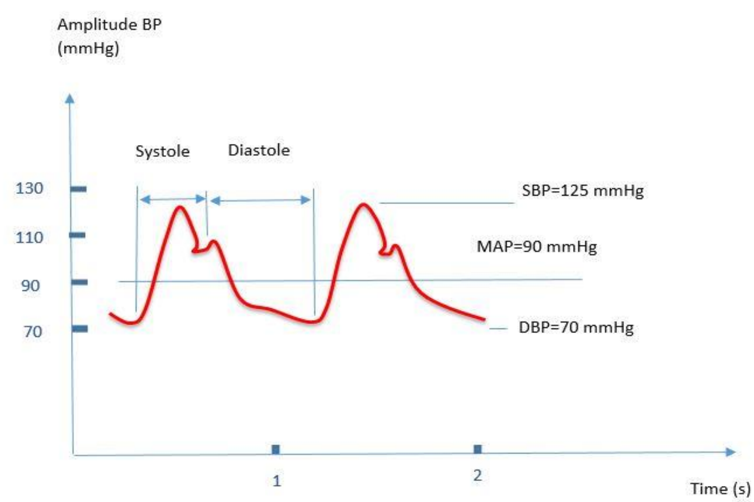

Figure 2.2: Blood pressure waveform

The arterial pressure wave (which can be seen above) is a shockwave that travels much faster than the human ejected blood.

Non-invasive methods are widely preferred. Diastolic and systolic blood pressure can be measured but the both reading cannot be made in the same cycle. The systolic is the top number and represents the force measurement when the heart contracts and pushers out the blood while the diastolic is the measurement when the heart relaxes between beats.

The world of medicine agreed about the risk degrees related to BP. In a lot of articles and medical studies it has been concluded that there are three degrees of risks: low medium and high [3]. All these are well captured in the following table:

Table 1: Low, medium, and high values of blood pressure

Categories	Systolic / Diastolic
Low risk	120 / 80
Medium risk	121-139 / 80-89
High risk	140+ / 90

Also, they agreed there are exceptions to these categories. [1]

In general, the systolic blood pressure should be less than 150 for people *over 80 years of age.* Considering the patients overall medical conditions, a healthcare professional can decide the right pressure for each patient. [10]

Other cardiovascular factors are associated to elevated blood pressure and heart rate.

Patients defined as “pre-hypertensive” with a heart rate ≥ 80 beats per minute were found to have a 50% increase in all-cause mortality. [11]

Health studies must be taken seriously by health practitioners and policy makers and not just by academics and environmentalists. [12]

Medical devices evolved a lot. In nowadays many people with hypertension can measure their blood pressure at home, they don’t need to go to the clinic for this purpose. Blood pressure monitors can be purchased from almost any pharmacy.

A current electronic device used for blood pressure measurement for home users is shown in the next picture:

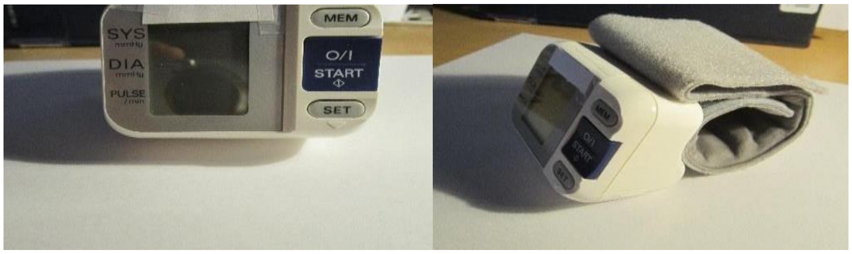

Figure 2.3: Home monitor used to measure the blood pressure and heart rate

These monitors can also measure the heart beat (heartbeat detectors are incorporated inside).

2.1.3 Electrocardiogram waveform ECG

An electrocardiogram (ECG) represents how the electrical current is moving through the heart during one, two or more heartbeats. In the literature, the speed of the heartbeat is the number of contractions of the heart per unit of time, typically stated as beats per minute (bpm). The heart rate is equal or close to the pulse measured at any peripheral point. [3] There are diverse types of electrocardiographs. [64]

Electrocardiography is a simple procedure in which the heart's electrical impulses are amplified and recorded [7]. The pulse's activation is represented by the P wave, then the electrical current flows down to the lower chambers of the heart (the already referred ventricles). The activation of the ventricles is represented by the QRS complex waves. The T wave represents the recovery wave for the electrical current that spreads back over the ventricles in the opposite direction [7].

The P, QRS, and T waves are shown in figure 2.4 are the major waves that present interest for this thesis. As a short conclusion, each wave represents depolarisation (electrical discharging) or repolarisation (electrical recharging) of a certain region of the heart. U waves are not shown in figure 2.4.

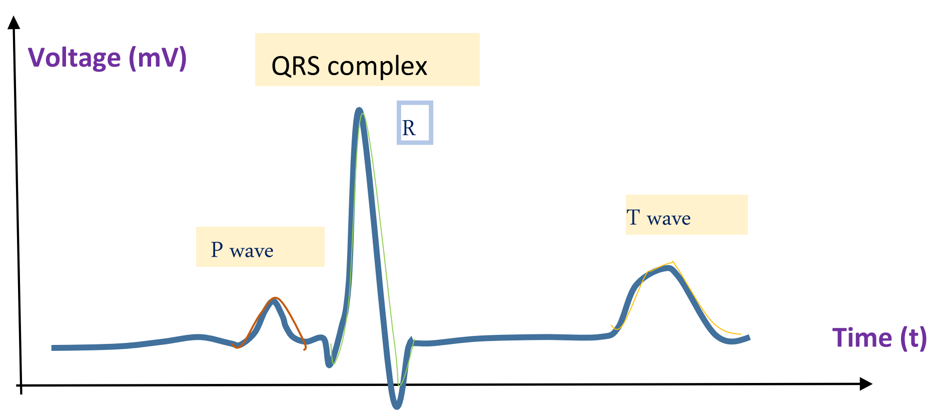

Figure 2.4: The P, QRS, and T waves of an ECG

On a normal ECG, the contour of P, QRS, and T waves are noticeable. A normal ECG from an unknown patient is shown in figure 2.5:

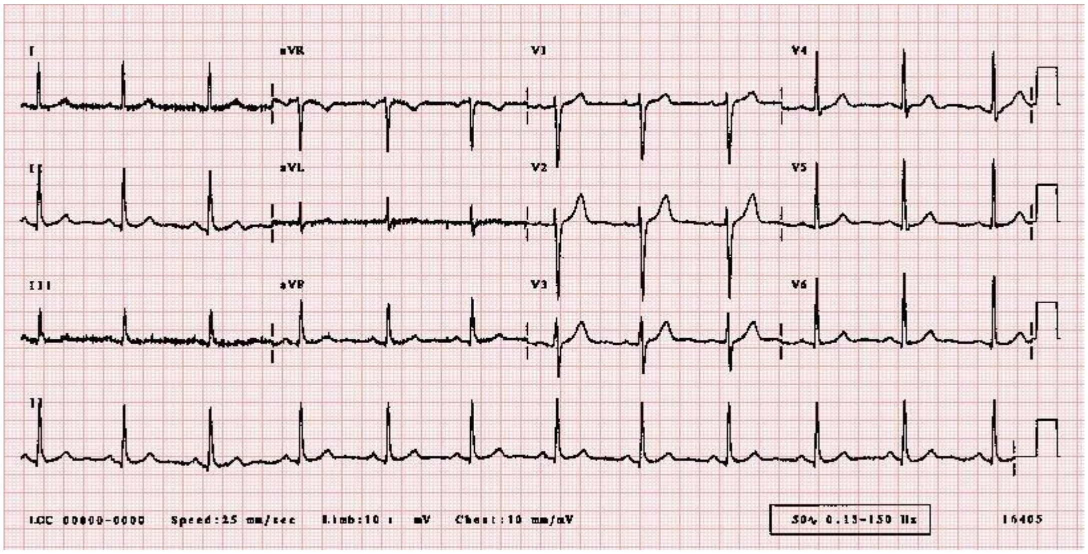

Figure 2.5: A normal adult ECG

Source: ECG Library 1995 - 2014. Dean Jenkins and Stephen Gerred

An electrocardiogram is one of the simplest and convenient way to investigate the heart and it remains an essential part of the valuation of cardiac patients. Generally, an ECG is printed on paper for easier analysis and it is recorded for just a few seconds. A standard cardiac cycle starts with the depolarization of the sinus node known as the heart's main pacemaker. [82] A wave of electrical depolarization extents through the right ventricle. In the heart, the itinerary of transmission of the electrical depolarization from atria to ventricles is through the atrioventricular node. Then the wave of depolarization extents down the interventricular septum into the right and left ventricles (Figure 2.6a). The direction of the depolarization is usually from the superior to the inferior aspect of the heart. [36]

When the wave of depolarization goes towards a recording lead (e.g. an electrode on the patient's chest) this results in a positive deflection and when it goes away from a recording lead this results in a negative deflection. In general, there are 12 lead directions through 10 recording electrodes applied on the patient's skin. Six of them are recorded from the chest overlying the heart, four are recorded from the limbs; it is necessary that each of the 10 recording electrodes is in the correct position to obtain the right appearance of the ECG. [36]

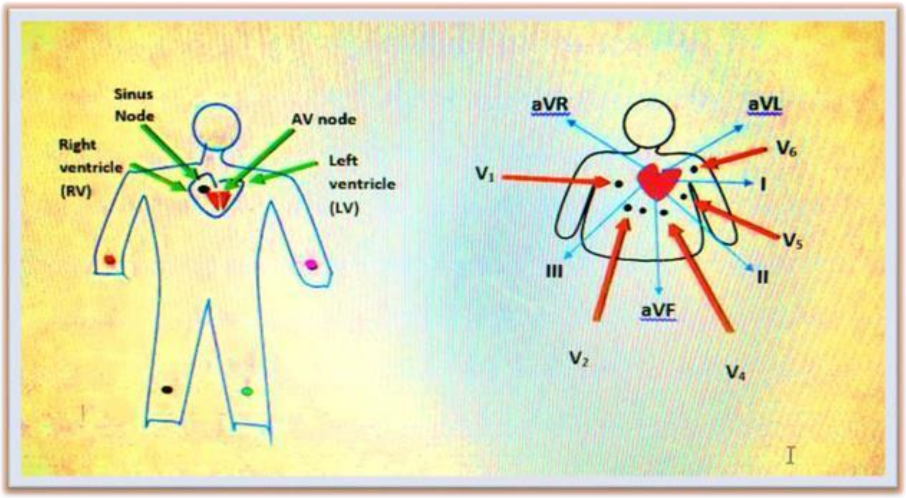

Fig 2.6(a) Fig 2.6(b)

Figure 2.6: Basic electrophysiology of the heart and the electrodes placement

Figure 2.6(a): Basic electrophysiology of the heart and ECG's 4 electrodes placement RA, LA, LL, RL

Figure 2.6(b): Orientation of the six limb leads (in blue) and the orientation of the other six chest leads in relation to the heart (V1-V6)

The ECG is recorded from the limbs that are called leads I, II, III, AVR (augmented vector right), AVL (augmented vector left), and AVF (augmented vector foot – because the electrode is on the foot) and the chest records are called V1, V2, V3, V4, V5, and V5 as it can be seen in Figure 2.6(b). [36]

The six chest leads from the figure 2.6(b) are also called the precordial electrodes. [72]

The other four limb electrodes (see figure 2.6(a)) are located on the following patient's limbs: right arm (RA), left arm (LA), left leg (LL), and right leg (RL-ground). When dealing with an amputee patient, the equivalent electrode is positioned on the nearest region of the chest (such as shoulders or lower abdominal region). [72]

As it can be seen in Figure 2.4, the amplitude of an ECG in its vertical axis is measured in millivolts (mV). In the medical world, the standard is that 1mV is represented by a deflection of 10 mm. The time is plotted on the horizontal axis and one second is the equivalent of 25 millimetres. [36]

The ECG paper is marked with a grid of small and large squares. Each small square represents 40 milliseconds (ms) and 5 small squares represent 200 ms. The roles of P, QRS, and T waves has been mentioned above and it is interesting to add that P wave represents the sum of the electrical signals from the two atria. The depolarization of the ventricles is knowns as QRS complex (as it can be seen in figure 2.4). The *repolarization* of the myocardium is known as the ST segment and the T wave. [36]

The electrocardiograms recordings allow to the specialized personnel to analyses various phases of electrical depolarization and to see if they are in a normal range. The following intervals are in the normal range:

- PR interval which is measured from the beginning of P wave to the first deflection of the QRS complex has the normal range 120-200 ms which corresponds to 3 to 5 small squares (on ECG paper)
- QRS duration (from the first deflection of QRS complex the end of QRS) should be up to 120 ms which corresponds to 3 small squares (on ECG paper)
- QT interval measured from the first deflection of QRS complex to the end of T wave has a normal range up to 440 ms

The electrocardiograms also allow us to approximate the heart rate as it follows:

- for 5 large squares, there are 60 beats per minute (bpm)
- for 3 large squares, there are 100bpm
- for 2 large squares, there are 150bpm

All the up-mentioned values are for a normal ECG [36].

Recently smartphones were provided with apps and HW extensions that allow people found out they can see their electrocardiograms on their androids. For example, the Heart Monitor named AliveCor can be attached to an android and through a couple of sensors is helping the clients see their ECGs. Once the device is attached to the android, the only thing that clients need to do is pressing the two sensors with their two fingers from their two hands.

Another interesting new application by the same AliveCor is Kardia which is a mobile device that can record client's ECG. The Kardia Bands Adds EKG Tech to Apple Watch. This product uses ultrasound technology and various algorithms to detect cardiac arrhythmia conditions that could cause stroke and if the heart rate is normal or not. Basically, there is a button attached on a band that surrounded client's wrist that needed to be pressed for a few seconds. [15]

Diverse methods were used to eliminate the pulse artifacts in oscillometric records when needed. When the blood pumped into the circulation system, the pressure wave is propagating along the arteries away from the heart. [37]

When the heart beats, the blood is pumped into the circulation system and a pressure wave is applied along the arteries away from the heart. Pulse wave analysis studies showed some key factors that determine and affect the shape of pulses. Those factors can be physiological, pathological and psychological such as growth, stress level, physical fitness, foods, heart rate, exercise, body height, gender and diseases. [32] A crucial factor related to the blood's velocity is the stiffness of the arterial walls. The most common ways used in the last 20 years to measure how fast the pressure wave propagates are:

- pulse transit time
- pulse wave velocity

The ***pulse transit time*** represents the time it takes the wave to propagate from the heart to a specific point on the body (e.g. a finger). [37]

Traditionally the pulse transit time has been defined as being the time that passed between the blood being emitted from the heart and the arrival of the pulse at an extremity. [37]

Two physiological signals are used to determine the up-mentioned points in time and the ECG can be used to infer the point at which the heart beats. The most used peaks are the peaks from QRS complex. [37]

Figure 2.7 shows how pulse transit time (PTT) technique makes it possible to trace beat-to-beat pulse using the QRS complex of an ECG.

Two physiological signals were used to determine that PTT: electrocardiogram and the photoplethysmography. This photoplethysmography is a low-cost optical technique used to make measurements at the patient's skin surface. [38]

The peak of the R-peak of the QRS complex is a very good indicator for the origin of a blood pressure pulse as it can be seen in figure 2.7.

A photoplethysmography trace shows a major rise when the pressure wave arrives. [37]

Figure 2.7 shows how the pulse transit time is measured. {19] [37] [38]

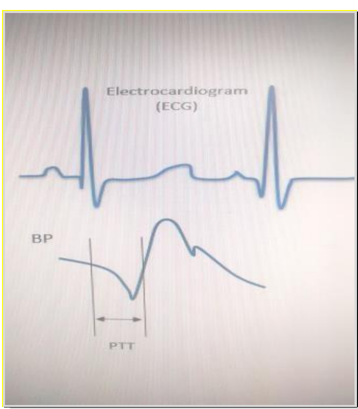

Figure 2.7: Plot of ECG showing how it relates to BP: Pulse Time Transit (PTT) measured from the R peak of QRS complex

PTT values are calculated in software from digitized version of the traces and can be calculated once per heartbeat. Consequently, if PTT can be correlated with Blood Pressure, then beat−by−beat arterial pressure readings are possible. [18]

It is important to realize that with age, the rapport PTT and blood pressure is not constant, it will change. [37]

The ***pulse wave velocity*** is the speed at which the wave propagates. This is correlated with PTT. [37]

2.1.4 Myocardial infarction and Stroke

As it was stated before, the ECG is a very good instrument for “the valuation of cardiac patients”. It is essential for the identification of disorders of the cardiac rhythm and for the diagnosis of abnormalities of the heart such as myocardial infarction. [39]

The P wave is positive because of atrial depolarisation, and the T wave represents the repolarisation of the ventricular myocardium. [39] The region of myocardium survey varies between V1 and V4 (as it can be seen in Figure 2.6(b)). Looking at that region, namely leads II, III, and AVF, changes are produced in the leads by infarction. [39]

The T wave normally has a positive polarity. If the polarity of T waves changes it is considered that there is a T wave inversion which may be caused by one of the following: myocardial ischemia, myocardial infarction, ventricular hypertrophy, and digoxin effect. [39]

The ST segment is measured from the end of S wave to the beginning of the T wave (Figure 2.4). It is the transient period in which no more electrical current can be passed through the myocardium. [39] This segment presents interest for the study of myocardial infarction and ischemia; it is the commonest manifestation of myocardial ischemia. Another manifestation of myocardial ischemia happens when T wave inversion occurs. [39]

In the “New England Journal of Medicine” it was reported in 2003 a case of a 52-year-old man with acute myocardial infarction. He was brought to the hospital because of chest pain. It was observed that he had hypertension and the ECG showed the ST segment depression and T wave inversion. [71]

Other probable causes that may inverse the T wave do not present any interest for this thesis. The heart is an irreplaceable organ that pumps blood throughout the human body and that is very important: for instance, when the blood flow to the brain is disrupted the brain cells can go dead or be damaged mainly because of absence of oxygen. Brain cells can also be damaged if bleeding occurs in the brain. Neurologically speaking, these complications are called ***cerebrovascular disorders*** because of the brain and blood vessel involvement. [7]

Insufficient blood supply to parts of the brain for short periods causes ***transient ischemic attacks***. If the blood supply is restored quickly the brain cells don’t die as it happens in a ***stroke***. Strokes are the most common cause of disability neurologic damage. Stroke is the term used for a clinical syndrome that consist of focal cerebral infarction (ischemic stroke) and focal hemorrhage in the brain. High ***blood pressure*** and atherosclerosis are the ***major risk factors*** for stroke. [7] [40]

Because more and more people are aware of importance of controlling the blood pressure and high cholesterol the rate of strokes has dropped in the recent years.

The blood can be blocked by small pieces of calcium or fatty material that are building up on the arteries' wall. Blood is supplied to the brain through two pairs of large arteries: the carotid artery and the vertebral artery that are bringing the blood from the heart. These large arteries empty into a circle of smaller arteries. The tests that can identify a stroke are the computed tomography and the magnetic resonance imaging. [7]

Hypertension is a very important precursor of ischemic stroke and intracerebral hemorrhage. Hypertension has also an aggravating and accelerating but nonspecific impact on degenerative cerebrovascular maladies. [40]

In an ischemic stroke, a blood clot blocks a blood vessel. A blood clot formed in the heart can travel through the arteries to the brain. The result is an embolic stroke. Also, a sudden drop in blood pressure can severely reduce the blood flow to the brain. A stroke resulted because of low blood pressure is severe and elongated. This state can occur when an individual loses a lot of blood from an injury for example. [7]

There is an open discussion about the relation between the stroke and blood pressure and there are many opinions about this matter. After lengthy and complex studies, very convincing evidence came out: an effective way to primarily and secondarily prevent stroke is to control the hypertension. [41]

After acute ischemic stroke, an elevated blood pressure is frequent to many patients. [41]

2.2 Algorithms for blood pressure and electrocardiogram signal processing

Over time, many attempts have been made to illustrate or model pulses and determine heart signals. In the past, it was accepted that a physiological signal is difficult to be reproduced; still in the last dozens of years advanced techniques have been made to describe the bio-signal components of pulses.

The most common methods are Fourier transform and frequency analysis. [16] [17]

In this chapter, the theoretical basis of oscillometric waveforms, breathing effects, electrocardiograms, strokes, and artificial neural networks are described.

The oscillometric method is implemented by most of the automatic blood pressure measurement devices. [17] It is interesting to see how the blood pressure relates to heart rates, electrocardiograms and, in the end of this study, strokes.

2.2.1 Oscillometric Waveform (OMW)

In chapter 2 there was mentioned the cuff pressure when referring to BP.

To resume, the baseline pressure is induced by the device attached to the patient's arm and it is a pressure combined with the pulse pressure and that finally gives us the cuff pressure deflation curve as it can be seen in figure 2.8.

The sensors in the cuff will sense the pressure oscillations of the arterial walls through the cuff deflation. Later, the values of systolic (SBP), main arterial pressure (MAP), and diastolic pressure (DBP) are given by the oscillations amplitudes.

The cuff pressure deflation curve will be considered first. This will be followed by a few Electrocardiograms presentations. Often cuff pressure is approximate as a straight line, as it can be seen in picture 2.8.

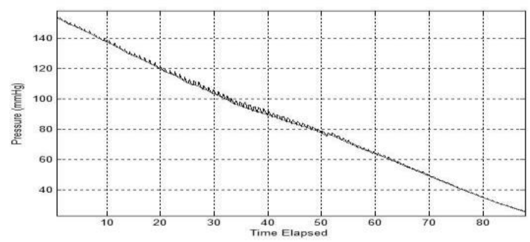

Figure 2.8: Plot of Cuff Pressure Deflation Waveform

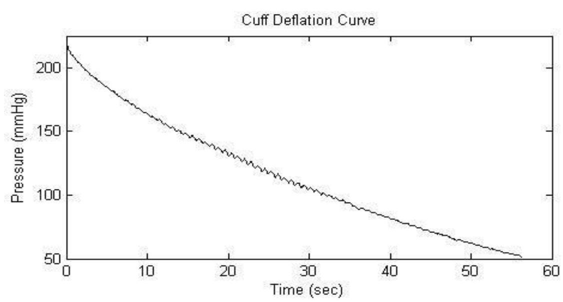

Figure 2.9: Another way to represent the cuff pressure deflation curve

In the oscillometric recordings, the oscillometric pulses look like as a series of low amplitude pulses that are imposed on a slow decreasing trend. [20]

There are various methods to extract the oscillometric waves (OMW). Two effective methods that are presented are filtering and detrending.

For filtering a band-pass filter (BPF) was designed with cut-off frequencies of 0.5 Hz and 20 Hz. Basically, the cuff pressure is filtered to take out the trend line and suppress the higher frequency noise from the recorded cuff pressure deflated waveform. Usually the low cut-off of the band pass filter is set between 0.3-1 Hz. In figure 2.10(a) it can be seen a plot of the recovered OMW by using the filtering method. {19]

The oscillometric pulses are determined after subtracting the cuff pressure from a baseline that represents either the deflation cuff pressure or the regular pressure decrease and this is referred as the detrending method. [21]

A very efficient way to separate the deflation from the blood pressure pulsation is acquired by a segmentation data process into impulses. The deflation signal is calculated by interpolation of data between subsequent segment borders. [22]

If the decreasing cuff is properly estimated by detrending, each pulse of the OMW starts from zero so none of OMW's points should be negative (as it can be seen in Figure 2.10(b)). [19]

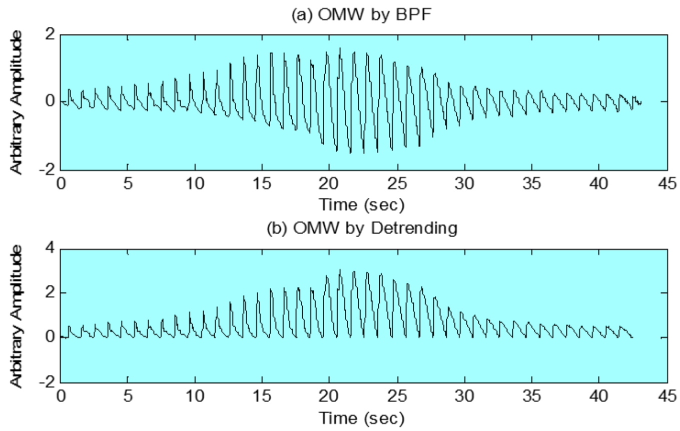

Figure 2.10: OMW extracted by (a) filtering method and (b) detrending method

2.2.2 Breathing effects

A change in the intra-thoracic pressure is associated with breathing effects related to the central and the peripheral blood pressure measurements. [23] It has been proved that the systolic and diastolic pressure vary phasically with both inspiration and expiration cycles. The breathing depth also affects the pulse rate and the R wave amplitudes from the electrocardiograms.

Kitney underlined in 1979 the two essential parameters needed to achieve stable oscillations referring to the non-linear element and the time delay. This model was used, among other applications, to study the respiratory sinus arrhythmia (RSA) which is a natural variation in heart rate due to the human breathing. [24] [25] In 1982 Selman et al. studied the effects of the tidal volume and respiratory frequency on RSA. [24]

Silu Chen stated that the breathing effects "have never been studied in oscillometric recordings before". [19]

When referring to heart waves and to the blood pressure, as suggested in the above paragraphs, a point of interest is revealed by the effects of respiration on amplitude and frequency modulation.

Blood pressure could be displayed as the cardiac output multiplied by the resistance to blood flow by the blood vessels. [26] Cardiac output is the volume of blood pumped into the arteries from the heart per minute. This volume of blood is straight associated to blood pressure.

The most significant changes in amplitude are the result of the interaction between the cardiac output and the intra-thoracic pressure. The variations in the amplitude and pulse to pulse intervals of blood pressure and heart waves are influenced by both the depth and frequency of the respiration. [19]

Once the breathing effects are revealed in this chapter, a huge importance is given to electrocardiograms including the waves that can be found inside. In the observed electrocardiograms, the physical influences of respiration result in amplitude variations. The respiration generates an apparent modulation in the direction of the cardiac electrical axis. [27]

On a healthy 51 years old man, the breathing effects can be seen on the first electrocardiogram presented in this thesis, with a particular attention on R waves (which have the highest amplitudes). A yellow line was drawn to unite the R peaks from lead I and a red line was drawn to unite the R peaks from lead II.

Figure 2.11: Respiration-induced modulation of QRS waves amplitudes

To obtain a clear ECG (without annoying variations), it is recommended that the patient lies down and no movement is allowed during the registration which takes between 5 and 10 minutes. [66]

2.2.3 Modelling of pulses

Modern devices that are measuring blood pressure, such as oscillometric devices with automated cuff yields (as shown in Chapter 2, figure 2.3), are using sophisticated mathematics and simple or combined algorithms. Most of the existing algorithms are searching the differences in pulse pressure and artery stiffness. [28]

An important assumption in this thesis is that a good mathematical algorithm applied for electrocardiogram waves isn't necessary good when employed on oscillometric waves.

In nowadays there is a strong economic competition between the producers so it is understandable that some of those algorithms are guarded trade secrets. Most of the companies, labs, researchers are exhausting a specific model that is tried with a matrix of different systolic and diastolic pressure values. [28]

The OMW were modelled by involving Fourier series to decompose the waveforms into a series of sinusoidal waveforms, Gaussian function, or linear combinations of trapezoidal waveforms.

Especially because of R peaks high amplitudes and often frequencies variations, the Fourier series are not used to model the heart waves (nowhere in this thesis).

Numerous algorithms were used for oscillometric blood pressure estimation, OMW extraction, peak detection (including the R peak detection), and oscillometric waveform envelope. [19] [29] [18]

Hersh et al. proposed that the OMWE has the shape of a Gaussian function. [30]

M. Forouzanfar offered a sum of two Gaussian functions was proposed to model the oscillometric waveform envelope. The results were compared against the polynomial fits. [29]

George B. Moody et al. describe an interesting signal-processing technique which derives respiratory waveforms from electrocardiograms, allowing reliable detection of respiratory efforts. [27]

An interesting approach was initiated by David Abolarin. He could model the OMW waves by using sum of sinus. [18]

His fitting model is a weighted sum of sinusoids to several pair harmonics. A sinusoidal is a continuous moving waveform that has positive and negative half-cycles that are generally symmetrical with respect to a reference. [31]

David Abolarin used Matlab function ***lsqcurvefit*** as a model to estimate and handle the errors. His model describes a series of quantitative measures of amplitudes and phases.

His simplest form of the model function is expressed as:

$$Y = dc + A_0 * \sin(2\pi ft + \varphi_0) \qquad (2.1)$$

In equation (2.1) *dc* is a constant component, A_0 is the amplitude, π =3.14157, *f* is the heart frequency, *t* is the time and φ_0 represents the phase. [18]

After giving a few inputs, his response data model is given as:

$$Y = dc + A_0 * \sin(2\pi ft) + A_1 * \sin(4\pi ft + \varphi_1) + A_2 * \sin(6\pi ft + \varphi_2) + A_3 * \sin(8\pi ft + \varphi_3) \quad (2.2)$$

In equation (2.2) coefficients A_0, A_1, A_2, and A_3 represent the amplitudes, *dc* is the component of the signal and φ_1, φ_2 and φ_3 are phases. David Abolarin noted *dc* as being the mean blood pressure (or mean arterial pressure – MAP). The φ_0 phase was assumed to be zero. [18]

Looking at equation (2.2) it can be concluded that the sum of sinusoids is expressed as a Fourier series and it could be represented as:

$$y = a_0 + \sum_{k=1}^{n} a_k \sin(k\omega t + \varphi_k) \qquad (2.3)$$

Fourier series can also be well expressed by a sum of sinusoids and cosines also as Fourier series in the following form:

$$y = a_0 + \sum_{k=1}^{n} [a_k \cos(k\omega t) + b_k \sin(k\omega t)] \qquad (2.4)$$

In equation (2.4) the parameter a_0 models a constant intercept (dc component), a_k and b_k are the amplitudes, ω is the fundamental frequency, and *n* is the number of harmonics in the series. [18]

Different waveforms have obviously different frequencies and specified amplitudes. The new model in this thesis was inspired by the equation (2.4). The best possible parameters that are adjusting the OMW pulses are determined on a pulse-to-pulse basis.

The discrepancies between the original OMW (data) and the model sum of sinusoids is expressed as residuals and are the unknown parameters.

After studying different breathing effects two theoretical models are proposed. In the future, for a better accuracy, more researches are needed.

The breathing effects were studied within numerous labs. When revealing the blood pressure measurement techniques, Andrew Nara et al. studied the respiratory effects on those blood pressure measurements. It was revealed that the artery pressure waved are enveloped in a sinusoidal signal. The systolic and diastolic pressure vary phasically with both inspiration and expiration as a direct result of the pressure changes in the chest [23]

Intrathoracic pressure approximates the atmospheric pressure. In the arteries, blood pressure variation is not due directly to the pressure changes in the chest cavity but rather to the effects of the changes on left ventricular stroke. Because of this indirect change of pressure, the amplitudes of the sinusoidal signal have smaller values. The spontaneous respiration augments venous return during inspiration. The positive, controlled pressure ventilation (which is a mechanical one) reduces the venous return during inspiration. [23]

When dealing with the electrocardiograms it is easy to see that the expansion and contraction of the chest (which obviously accompanies respiration) are causing results in motion of chest electrodes and this is reflecting in R peak amplitudes. [27] The sinusoidal wave has a similar shape as it can be seen in figure 2.12.

The OMW waves could be seen in Andrei Nara et al. but in Silu Chen's thesis as well. [23] [19].

The expected breathing effects can be seen in the figure below:

Figure 2.12: Breathing effects on oscillometric waves

To obtain an accurate signal, the breathing signal must be extracted and that could be done by applying a band pass filter around the breathing frequency. The filter must be tuned to the frequency of breathing.

A better method of appreciation of the OMW was initiated be V.Z. Groza, M. Mafi et al [39]. The blood pressure was determined by using pulse morphology. More exactly the pulse morphology was employed to obtain an estimation of systolic and diastolic pressure. The suggestion made in the mentioned article is that changes in pulse morphologies of the deflation waveform is comprising essential information about blood pressure and cardiovascular condition of human beings. [32]

The morphology of pulses is referring to the shape of those pulses through a cardiac cycle. The parameters of the pulse contour can provide significant diagnostic information about the cardiovascular system. [33]

The changes in amplification and shape of the arterial pulses in an OMW as they travel away from the heart were also mentioned by David Abolarin [18].

Previously the oscillometry was revealed as a non-invasive method of acquiring the blood pressure. Other methods through the pulse waveform can be obtained are tonometry and photoplethysmography. When using the tonometry an ascending aortic pressure wave is generated from arterial pressure and it is recorded by planation tonometry in the radial carotid artery. [34]

The other non-invasive method, photoplethysmography is an optical one used to detect the blood volume changes in the microvascular bed of tissue. [35] It comprises two components: a pulsatile waveform that is attributed to the changes in the blood volume with each heartbeat and a varying slowly baseline that is combining low frequency fluctuations mainly due to respiration. [35]

There are reports of sudden deterioration of patients' health after aggressive BP reduction.

Oliveira-Filho et al. explore the relationship between acute BP reduction and three-month result in patients with acute ischemic stroke. They evaluated 115 patients within the first 24 hours of ischemic stroke signs and the association between BP lowering and poor outcome. The degree of BP reduction remains an independent predictor of poor outcome. The authors demonstrated a nearly dual augmented risk of poor outcome for every 10% decrease in systolic BP reduction in the first twenty-four hours, regardless of whether antihypertensive treatment was given. [41]

Vemmons et al studied the correlation between acute blood pressure values with findings in the setting of acute stroke. In cardio embolic stroke, history of hypertension, stroke severity, haemorrhagic alteration and brain oedema were related with higher 24-h blood pressure. They also correlated death due to brain injury and brain edema with high initial blood pressure levels. [42]

Even though sever hypertension during a critical ischemic stroke is an indicator of poor prediction there is no undoubted evidence that rapid lowering of elevated BP is beneficial for the patients; on contrary, there are published reports about patients in whom neurological depreciation was linked with precipitous falls in BP. The risk of causing harm suggested that rapid lowering of BP is best avoided during the critical phase of an uncomplicated ischemic stroke. [40]

Specific drugs can be used to lower the blood pressure. When questioned about how far should BP be lowered, the answer given by most of the authorities agreed that mean arterial blood pressure (MAP) should be reduced by about 20% to 25% over 24 hours. [40]

The studies mentioned above plus most of medical studies underline the importance of the heart and brain well-functioning represents for the human body. Within those studies, the normality of high and low blood pressure plays a crucial role. Precision in BP measurements has an enormous importance for patient's treatment. It was revealed that a BP estimation error of as little as 5% can conduct to a 25% increase risk of morbid consequences such as stroke and myocardial infarction. [43]

A. Ball-Llovera developed an algorithm for automated measurements of BP using the oscillometric method. Mathematical methods have been applied to calculate BP, including SBP and DBP. [44]

Perfetto et al. advanced an algorithm to detect systoles and diastoles from non-invasive continuous BP signals in head up slope curves. The algorithm does not depend on the history of the signal. It can detect the searched parameters changes in the signal. [45]

Artificial neural networks were applied in the recent past to estimate BP and ECG classifications. [46]

Mohamad et al. implemented a ratio-independent method and algorithm using Artificial Neural Networks to determine blood pressure from extracted features of oscillometric pulses.

[18] [43] A mathematical model of oscillometry was derived to describe the interaction between the cuff and the artery and to build a model for PTT based on coefficient-free estimation of blood pressure. [43]

Colak et al. developed a neuro-fuzzy approach to determine the BP values. The membership functions of their algorithms are determined by using neural networks. [47]

Gratze et al. worked to develop and evaluate an algorithm for non-invasive, real-time, beat to beat monitoring of stroke index, BP, and total peripheral resistance index which has a menu driven interface suitable for unskilled staff. A meta-analysis was included for the evaluation of autonomic function which encompassed spectral analysis of heart rate, blood pressure, stroke index and total peripheral resistance index and the calculation of baroreceptor reflex sensitivity. [48]

The testing procedure proposed in this thesis is the following: first the blood pressure is checked and if the patient has hypertensions he / she must perform ECG. If the T waves are inversed then it results a stroke's predetection alarm.

This procedure is described by the following block-diagram:

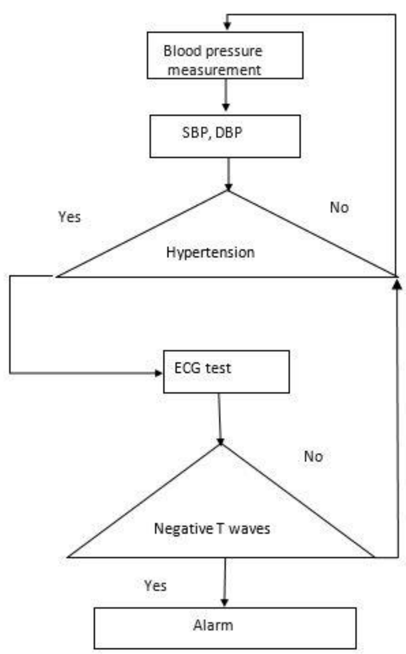

Figure 2.13: Block-diagram for testing stroke procedure

2.3 Artificial Neural Networks

2.3.1 The foundation of Neural Networks

Consciously, the first discipline that could be associated with Neural Networks would be the neurosciences (other sciences associated with neural networks are mathematics, computer science, or engineering).

The human brain computes differently than a computer, considering how the neurons are performing when processing information (e.g. human vision or numerical pattern recognition) or when performing certain computations (e.g. motor or industrial process controls). [49}

Neural Network is a machine designed to model how the "brain" performs specific tasks. [49]

In term of composition, the human brain is simply a network with interconnected neurons. A neuron has an *axon* (which is as a pulse generator and the transmission line), *soma* (which is the center of the nerve and it is emitting pulses), *dendrites* (seen as a pulse receptors), and *synapses* (which are making the connections between neurons). The receptors convert stimuli from the human body into electrical impulses that convey information to the brain (or to the net). The most common type of synapse is the chemical one. [49]

The general assumption (after excluding the dead neurons) is that each neuron does some (numerical) computing. This assumption was made so that computers can be used to imitate this structure. [49]

It is interesting to know that most neurons encode the outputs as a series of specific voltage pulses. [49]

The brain's structure is unique and is nowhere re-created with artificial neural networks. They are primitive in comparison with the interregional circuits in the brain.

A nonlinear model of a neuron

The neuron is the most fundamental unit that is operating into a neural network. This neuron is an information-processing unit. [49]

When revealing the model of a neuron, the synapses are the *connecting links* and each link has attached a *weight* on it [49].

In the next figure, the model of a neuron *k* will be build. The input signals that are connected to neuron *k* are all multiplied by *synaptic weights* w_{kj} (as it can be seen in figure 2.14). The synaptic weight of an artificial neuron may have positive and negative values (which obviously is never the case of synaptic human brain). All these weighted input signals are ending into an *adder* which will sum them, this operation being described as a linear combiner. Right after the adder it must be an activation function for limiting the amplitude of the neuron's k output. The normalized amplitude range of an output is closed to an interval [0, 1] or [-1, 1] and most of the times, the neuron includes an externally applied bias, which in denoted b_k. [49]

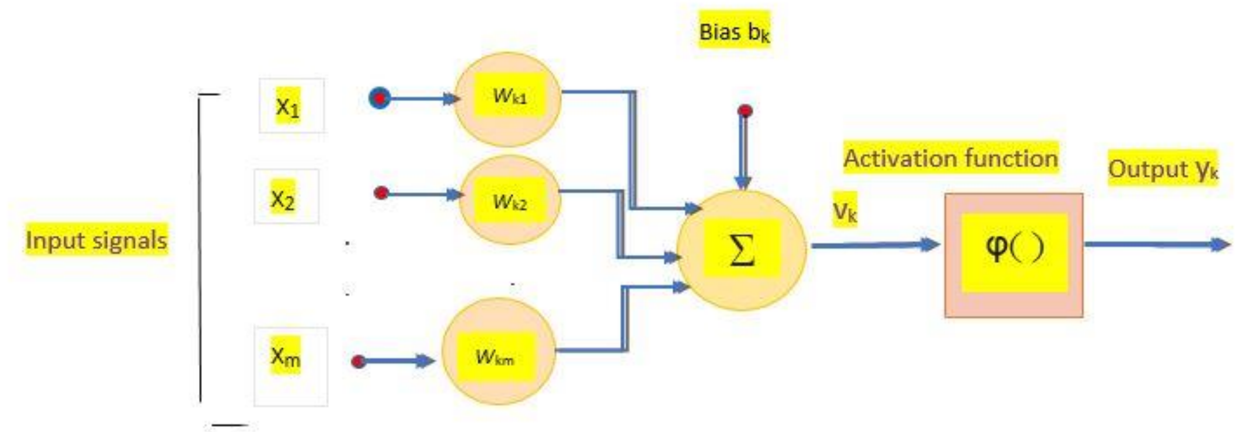

Figure 2.14: A nonlinear model of a neuron

This model is generating the following mathematical equations:

$$u_k = \sum_{j=1}^{m} w_{kj} x_j \qquad (2.5)$$

$$y_k = \varphi(u_k + b_k) \qquad (2.6)$$

$$v_k = u_k + b_k \qquad (2.7)$$

The function u_k is a linear combiner output due to the input signals. The bias b_k is an external parameter of the artificial neuron k. [49]

There are three types of activation functions: Threshold, Piecewise-Linear, and Sigmoid functions.

These functions are perfectly described in the following figures:

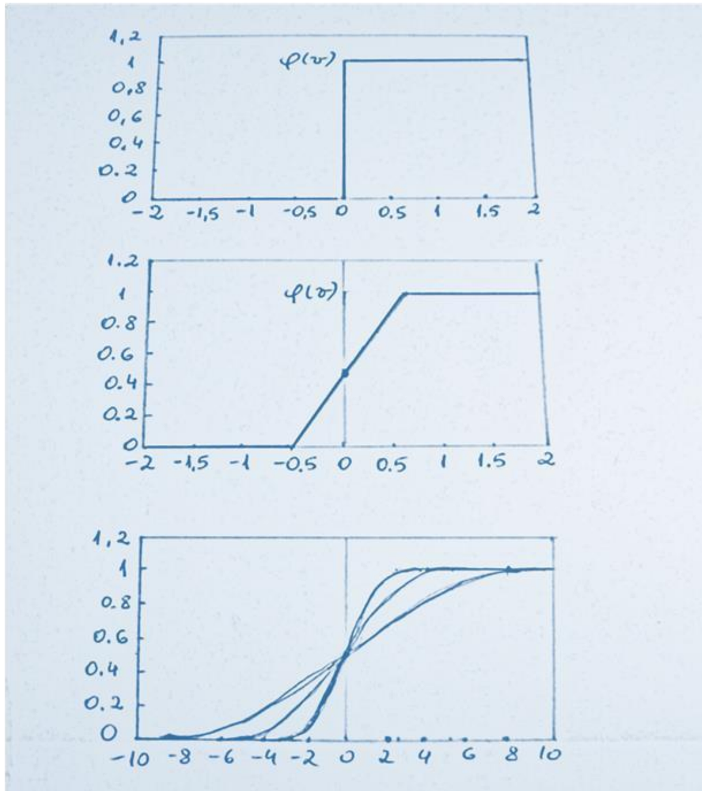

Figure 2.15: Threshold, Piecewise, and Sigmoid functions

a) <u>Threshold Function</u>

This type of function which is known as the *Heaviside* function is described by the following equations:

ϕ(v)=1, if v>=0 (2.8)

ϕ(v)=0, if v<0 (2.9)

b) <u>Piecewise-Linear Function</u>

This function is described by the following equations:

ϕ(v)=1, if v>=+1/2 (2.10)

ϕ(v)=v, if +1/2 > v > -1/2 (2.11)

ϕ(v)=0 if v =< -1/2 (2.12)

As it can be seen in Figure 2.15, the amplification factor is assumed to be unity.

c) <u>Sigmoid Function</u>

The last function from Figure 2.15 is defined by the following equation:

$$\varphi(v) = \frac{1}{1+\exp(-av)} \tag{2.13}$$

This s-shaped function is the usual form of activation used in the construction of artificial neural networks and it is an increasing function. The parameter "*a*" that is revealed in equation (2.13) is the *slope parameter* of the sigmoid function. [49]

Neural networks are dynamic systems and there is *feedback* whenever the output of an element in the system influences somehow the input applied to that element. In this way one or more closed paths are risen so that the transmission of signals around the system is a complex one. Neural networks are known as recurrent networks. [49]

There are several ways in which a neural network architecture can be build. The way in which the neurons of a neural network are structured is deeply linked with the learning algorithm that is used to train that network. During this study, it was noticed that the learning algorithms are complex and variously structured.

The dynamic behavior of neural networks is most of the time complicated because the networks are usually nonlinear. It is obvious that this behavior is controlled by the weights (a good example of weights was shown is figure 2.14).

The generally accepted fundamental classes of network architectures are the following: the single-layer feedforward networks, the multilayer feedforward networks, and recurrent networks.

i) Single-Layer Feedforward Networks

This is the simplest form of a layered network that contains only one *input layer* of source nodes that projects onto an *output layer* of neurons (but not vice versa). It is illustrated in figure 2.16 in case of three neurons in the input and output layer. [49]

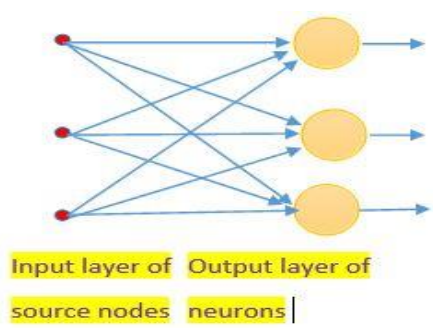

Figure 2.16: Network with a single layer of neurons

ii) *Multilayer Feedforward Networks*

This is a network distinguished itself by the presence of one or more *hidden layers* (the computational nodes that correspond to those layers are called *hidden neurons*). [49]

The hidden neurons intervene between the external input and the network's output in a convenient and useful manner. In Figure 2.17 it is illustrated a multilayer feedforward network with 4 inputs and a single hidden layer of 3 hidden neurons. The output has two neurons in this case. [49]

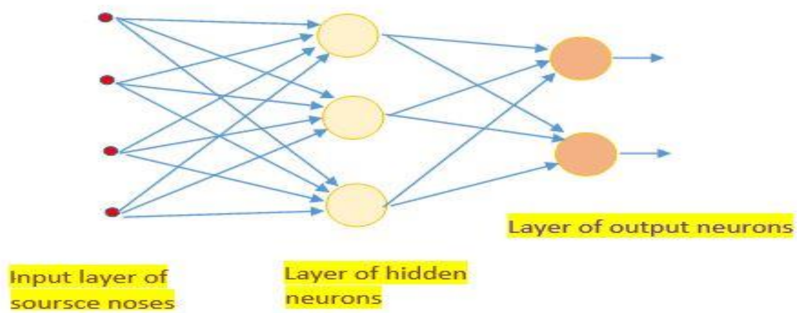

Figure 2.17: Feedforward network with hidden layer and one output layer

The four inputs represent the four source nodes.

The represented source nodes supply the elements of the activation pattern which is the *input vector*. This vector represents the input signals applied to the neurons from the hidden layer. The hidden layer is the second layer in figure 2.17. The output signals from this layer are the input signals from the third layer which is the layer for the output neurons. The output layer is the final one. In this example, the neural network is fully connected that means that every node in each layer is connected to every other node in the adjacent forward layer. If some of the connections links are missing (thing that is perfectly possible in other cases) then the network is a partially connected one. [49]

The knowledge of a neural network refers to the stored information or used models used for various purposes. It is important the type of information used and the way this information is encoded. This information contains the known facts (referred as prior information) and the measurements obtained by the sensors to probe the environment. The known facts are defined by values taken on by the free parameters of the network. In this project, the free parameters are represented by the ECG's amplitudes measured in millivolts.

2.3.2 The learning process

A neural network learns from it environment through a process of adjustment applied to its synaptic weights and eventually bias levels. The first learning rule is *the error–correction learning*. [49]

Considering a neuron *k*, driven by a signal vector *x(n)*, produced by one or more hidden layers, with an output signal $y_k(n)$, the error-signal is given by the difference between the desired response $d_k(n)$ and the output signal $y_k(n)$:

$e_k(n) = d_k(n) - y_k(n)$ (2.14)

This error-signal activates a mechanism of control with the purpose to finally apply a sequence of corrective adjustments to the up-mentioned synaptic weights. [49]

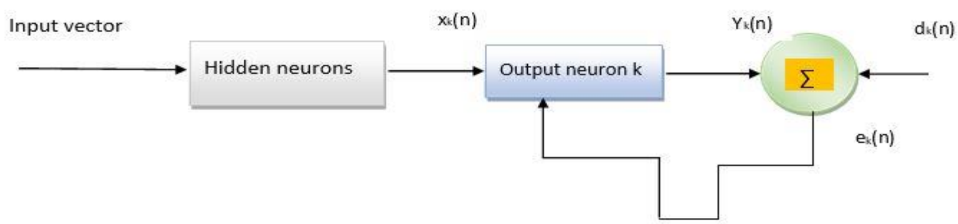

Figure 2.18: Error-correction learning

2.3.3 The Backpropagation Algorithm

This algorithm is very popular. It is largely used and very suitable for medical applications. [60]

The goal of backpropagation is to model a given function to optimize the internal weights of an internal signal so that the neural network can learn how to correctly map inputs to outputs and therefore to produce an expected output signal and reduce the output error. [79]

The algorithm has two major phases: in *the first phase*, the input data (from the input signals) propagates to each layer of hidden neurons and generates output data from the output layer with fixed synoptic weights. This process is called forward-propagation and it has three phases: node activation, node transfer, and the propagation. [79]

The neuron's activation is calculated as the weighted sum of the inputs (it could be the row of a training dataset). The neuron's transfer is done by a transfer function (e.g. sigmoid function). Forward propagating an input is straightforward. [79] If the output data is different from the targeted output data then an error is calculated. [49]

The error energy for a neuron *k* is

$$\xi(n) = \frac{1}{2}\sum_{k \in C} e_k^2(n) \qquad (2.15)$$

In equation (2.15), *C* is a set that includes the neurons from the output layer of the network. The average squared error energy can be determined by summing ξ (n) for the all neurons *n* in the output layer:

$$\xi_{av}(n) = \frac{1}{N}\sum_{n=1}^{N} \xi(n) \qquad (2.16$$

The error is calculated between the anticipated outputs and the outputs forward propagated from the network. [79]

All the free parameters (such as weights and biases) are included in the function ξ (n). [49]

In *the second phase,* once the error-correction rule is used (see figure 2.18), the error signal is produced. The error signal is propagated back to the network (this time from the output layer to the input layer) to modify the weights in the backward process. New trained backpropagation networks will give reasonable outputs for new similar input data. The goal is to minimize the error for each output node and the network as a whole. [49]

The error energy ξ is a measure of learning performance. [49]

The network is trained by using multiple iterations of a training dataset to the network. For each row of data the inputs are forward propagated, the error is backpropagated and weights are updated. [79] The error is expected to decrease very little after the new up-dated weights are used for the first time. After repeating backpropagation process hundreds or thousands of times the error may become very little (e.g. less than one decimal) [80]

Backpropagation can be used for classification and regression problems. [79]

In this study, the back-propagation algorithm is used in the next chapter when dealing with the pattern recognition tool from Matlab.

2.3.4 Pattern Recognition

Before performing a pattern recognition task, a neural network should undergo first a training session. During this session input patterns are repeatedly presented. In general, each pattern belongs to a specific category. Later, when new patterns are presented to the network, this network can identify the class of that pattern. [49]

Pattern recognition performed by a neural network is a statistical progression. It is used in Chapter 3 when classifying the T waves from all the electrocardiograms.

Chapter 3 Methodology for Predetection of Stroke

3.1 Mathematical models describing OMW and breathing effects, predetection of stroke and ECG

When the blood pressure signal is expressed as a sum of a Fourier series, then conditions of linearity and periodicity must be satisfied. [50]

As mentioned in chapter 2, the mathematical new equation for blood pressure in this thesis was inspired by the equation (3.1) and the parameters adjusting the OMW pulses are determined on a pulse-to-pulse basis.

As shown in Chapter 2 (in *2.2.3 Modelling of pulses*), the OMW modelling can be built by using Fourier series is as it follows:

$$Y_0 = MAP + A_0 * \cos[(2\pi f t) + \varphi_0] + B_0 * \sin[(2\pi f t) + \varphi_1] \quad (3.1)$$

Where: MAP = main arterial pressure

A_0 , B_0 = amplitudes

f = heart frequency

t = time

φ_0 , φ_1 = phases

The developed data model is given as:

$$Y_1 = MAP + A_0 * \cos[(2\pi f t) + \varphi_0] + B_0 * \sin[(2\pi f t) + \varphi_1] + A_1 * \cos[(4\pi f t) + \varphi_2] + B_1 * \sin[(4\pi f t) + \varphi_3] \quad (3.2)$$

The φ_0 phase is assumed to be zero, φ_1, φ_2, and φ_3 are distinct phases and the time (t) is measured in milliseconds.

To provide a new model for the OMW, the curve returned by the UFIT from the Silu's study is considered. [19]

Once the OMW new model is finished, the study is oriented on ***predetection of stroke*** and the analysis of ECGs. A new ECG mathematical modelling will be provided and, at the end of this chapter, neural network pattern recognition is implemented.

In Silu's study the data was collected as follows: the measurements were recorded by using a digital blood pressure monitor UFIT TEN-10 that belonged to Biosign Technologies Inc.

The digital UFIT device was applied to the left wrist of the subject and raised to heart level. Another cuff was attached on the upper left arm also at heart level. After the UFIT recordings took place, the discrete derivative of the blood pulse pressure (PP) was processed.

The recording of blood pressure with UFIT was followed by the reading of SBP and DBP by two professional trained nurses after one minute of pause. [19] [51]

These nurses' readings were performed by auscultation using the cuff on the left upper arm.

The recordings were taken from 85 subjects (37 were female and 48 were male) by following a specific procedure (designed in the line with the SP10 standard, that was established to provide safe practices for automated sphygmanometer performance evaluation. The gender and the ages of the subjects were also recorded with their first name for identification purposes.

The maximum difference between readings of these two nurses was no more than 2 mmHg; the SP10 standard requires the mean difference to be no more than 5 mmHg [19]

In Chapter 2, it was shown an OMW signal recorded from one subject undergoing uncontrolled breathing with pulses identified. The OMW amplitude envelope was cleaned by a high pass filter.

The OMW signal produced by the UFIT device for one patient is presented in Figure 3.1:

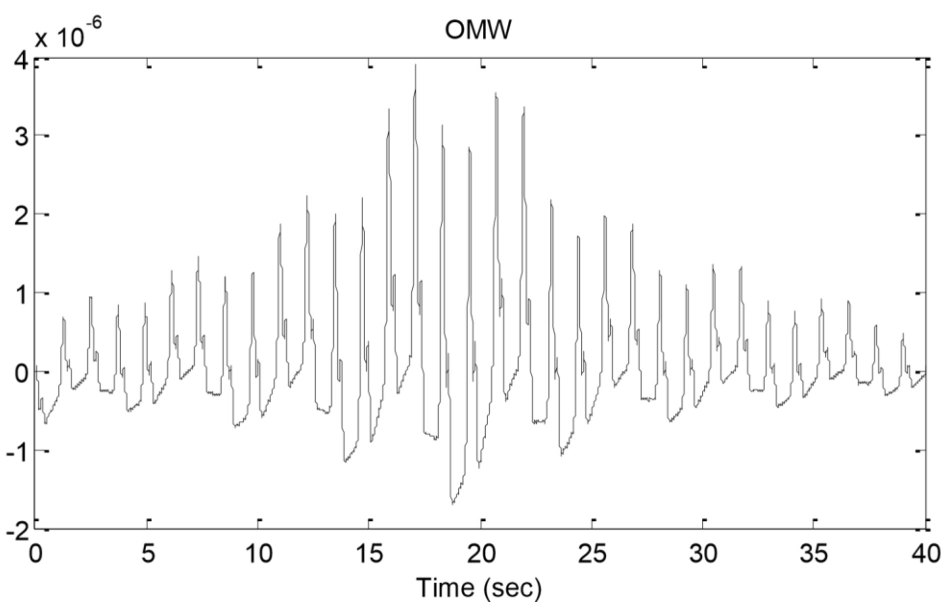

Figure 3.1: The recorded OMW extracted by the UFIT

The amplitude of the vertical axes is given by the amplitude measured by the UFIT device.

From the electrocardiogram and OMW five signals were extracted and they showed similar behavior (see figure 3.2). [19]

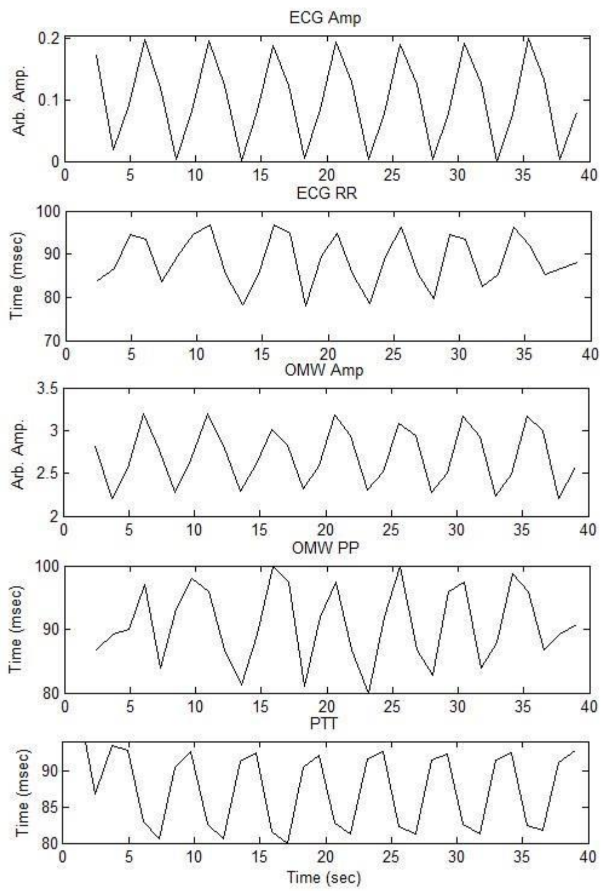

Figure 3.2: Five signals extracted from ECG and OMW

For new mathematical modelling, the third signal (OMW PP from figure 3.2) was used as a primal model. In this signal, the pulse pressure (PP) is clearly identified. [19]

As stated in Chapter 2, Mr. David Abolarin used function *lsqcurvefit* to estimate the BP. His model labelled a series of quantitative measures of amplitudes and phases. [18]

The sum of sines model fits periodic functions is described by the following equation:

$$Y = \mathrm{a}_0 + \sum_{i=1}^{n} a_i \sin(b_i + c_i) \qquad (3.3)$$

In equation (3.3) a_0 represents the amplitude, *b* is the frequency, *c* is the phase constant for each sine wave term, and n is the number of terms in the series and $1 \le n \le 8$. [52]

Least Square problems have an objective function expressed as:

$$\min_{x} \quad \|F(x)\|_2^2 = \min_{x}\left(\sum_i F_i^2(x)\right) \tag{3.4}$$

The variable x must be placed between lower and upper bounds:

$$lb \leq x \leq ub \tag{3.5}$$

In *lsqcurvefit* function *lb* and *ub* are the vectors representing the lower and upper bounds. The intention was to find the appropriate vector x that is a local minimizer to a function that is a sum of squares (as described by equation (3.4)). In this LSQ problem the minimizer was the parameter vector for which the sum of the squares of the lengths of the discrepancies between the constructed model and the observations given by the digital device was minimized. [18]

The most common type of linear regression is a least-square fit. [53]

When it is about data fitting, a data model describes the relationship between the predicted variables and the response variables. In his study, M. David Abolarin proposed a mathematical algorithm adapted from Matlab as follows:

- *lb* and *ub* as constrained bounds
- MAP, A_0-A_3, Phi_1-Phi_3 were the estimation parameters
- X_0 was the starting point

It was demonstrated it is possible to fit a nonlinear model by using directly the *Statistics Toolbox nfit* function or the *Optimization Toolbox lsqcurvefit*. Fitting necessitates a parametric representation that transmits the response data to the predictor data with one or more coefficients.

The differences between the original oscillometric waves and the given sum of sinusoids model was expressed as residual and they were considered unknown parameters. The result of the mentioned fitting process was an estimate of the model coefficients. Those coefficients are obtained by minimizing the summed square of residuals. [18] The dataset used by M. Abolarin was acquired from volunteers at the University of Ottawa by Dr. Saif Ahmad. In total there were ten persons (six males and four females) without any history of cardiovascular diseases. After implementing the mentioned algorithm, M. Abolarin obtained all the necessary coefficients. [18]

Another possibility to fit a nonlinear model is to apply a function in the *Curve Fitting Toolbox*.

The basic acquisition data is processed before fitting. Before modelling the relationship between any pairs of quantities of data, it is not a bad idea to perform correlation analysis to determine if there is a linear relationship exists between these quantities. [53] When dealing with OMW waves, it was revealed that there is no linear relationship between these mentioned quantities.

Mathematically speaking, the main purpose is to find the maximum and the minimum of a real function with a few variables by choosing the best elements with respects to some criteria.

The fitting tools assist users to fit data so they can calculate coefficients and plot the model on top of their data. Curve fitting models (even those with specific constraints) can be done using functions in the Optimization Toolbox. [53]

In our case, the OMW is presented in figure 3.1. The chosen model in this study is related to the selected function in the *Curve Fitting Toolbox*. The model is given by the needed computing values shown in the equation (3.2).

Oscillometric components can be analyzed by means of Fourier analysis of oscillatory time dependent functions.

Once the data is input into the system, the chosen function is *cftool*. It processes OMW and ECG signals in Matlab R2016.

The best option offered by this toolbox (e.g. Fourier series, exponential or Gauss model, or sum of sines) must be considered so that it gives the best fit for the plotted points. [54] In this application, the observed output *y* data, where *x* data and *y* data are vectors. Both vectors must have the same size.

As indicated in the beginning of Chapter 3, the Fourier series were used for the OMW dataset. In our case the use of other models such as Gaussian or exponential would not be possible because we could have negative variables as a response.

Once the measured data is entered we want to try to fit a curve trough the measured points. For the Fourier model, there could be up to sixteen parameters. The best fit (as it is shown in figure 3.3) for our model is the following:

$$Y_2 = f(x) = a_0 + a_1 * \cos(xw) + b_1 * \sin(xw) + a_2 * \cos(2xw) + b_2 * \sin(2xw) + a_3 * \cos(3xw) + b_3 * \sin(3xw) + a_4 * \cos(4xw) + b_4 * \sin(4xw) + a_5 * \cos(5xw) + b_5 * \sin(5xw) + a_6 * \cos(6xw) + b_6 * \sin(6xw) \quad (3.6)$$

For this equation, in Matlab R2016 the calculated coefficients are the followings:

a0 = 2.677

a1 = -0.005956

b1 = 0.007989

a2 = -0.0527

b2 = -0.01417

a3 = --0.04741

b3 = 0.03877

a4 = -0.07887

b4 = 0.0.68

a5 = 0.3227

b5 = -0.1369

a6 = 0.08214

b6 = 0.006487

w = 0.1324

The picture of the fitting curve can be seen below:

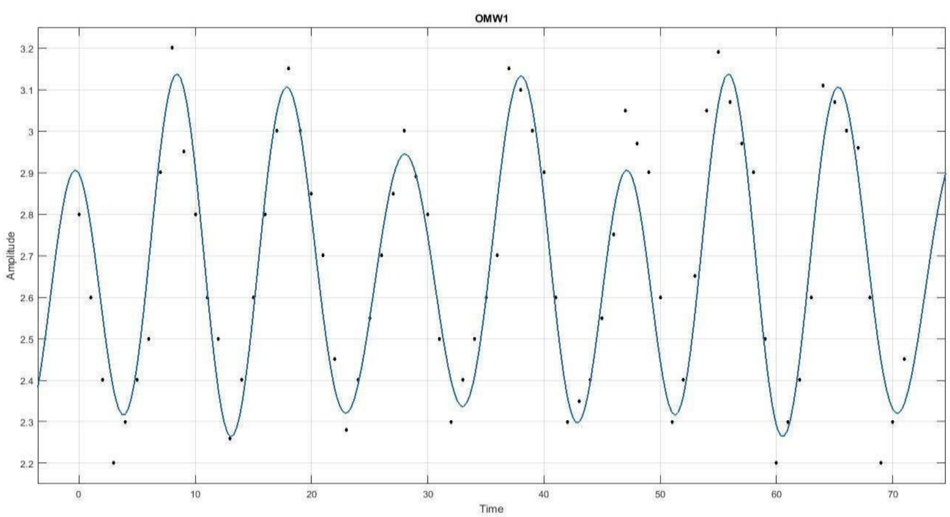

Figure 3.3: The fitted curve for the OMW PP extracted signal

For the Fourier model, this is the best obtained fit for OMW PP extracted signal. The blue line is following the measured implemented data.

It is assumed that output data was measured with little or no error. Once the graph is plotted, the goodness of this fit is evaluated by plotting the residuals. From this point the systolic and diastolic blood pressure can be estimated. Successful attempts were made in time and different algorithms have been used (such as maximum amplitude algorithm or slope based criteria. [18].

In Figure 3.3 the breathing influence is reasonably noticeable. In this study, there are offered two theoretical models offered to stress this breathing effect.

3.1.1. First mathematical equation describing OMW and breathing effects

The first thing that is considered is the calculated mathematical equation (3.6) derived from the curve fitting equation.

As it was mentioned before, the OMW waves must be enveloped in a sinusoidal signal and that is bringing the following equation:

$$Ybr_1(x) = a_0 + [a_1 * \cos(2\pi f_{BP}x + \varphi) + b_1 * \sin(2\pi f_{BP}x + \varphi) + a_2 * \cos(4\pi f_{BP}x + \varphi) + b_2 * \sin(4\pi f_{BP}x + \varphi) + a_3 * \cos(6\pi f_{BP}x + \varphi) + b_3 * \sin(6\pi f_{BP}x + \varphi) + a_4 * \cos(8\pi f_{BP}x + \varphi) + b_4 * \sin(8\pi f_{BP}x + \varphi) + a_5 * \cos(10\pi f_{BP}x + \varphi) + b_5 * sin(10\pi f_{BP}x + \varphi) + a_6 * \cos(12\pi f_{BP}x + \varphi) + b_6 * \sin(12\pi f_{BP}x + \varphi)] * \sin(2\pi f_b) \qquad (3.7)$$

It is known that people's breathing could be between eight and twenty breaths per minute. In this case, it is considered a person who is breathing with eight respirations per minute and that means it gives a 0.125 Hz frequency.

For this equation, the following parameters were considered:

- Breathing frequency (f_b):
- BP frequency (f_{BP})
- Phase (phi) is taken into consideration zero

The resulting plot for equation (23) is given by figure 3.4:

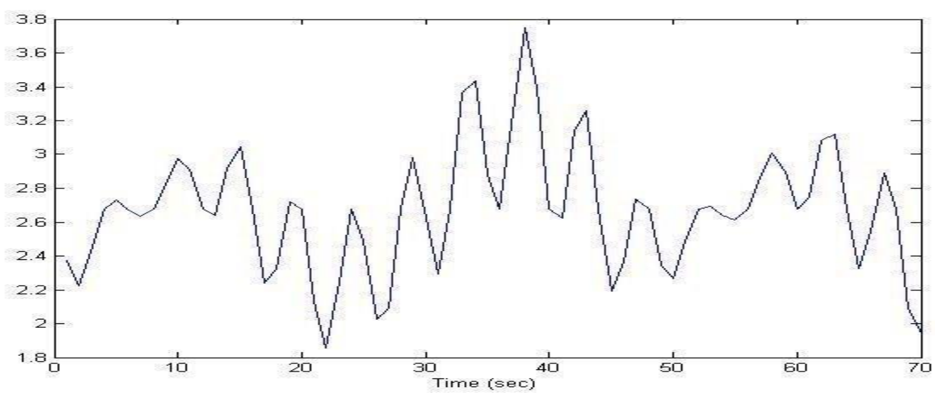

Figure 3.4: The breathing effect over OMW1

In this model, the blood pressure is directly related to the heart rate. Medical textbooks explain that the normal respiratory rate for adults is 12 breaths per minute at rest while older texts provide smaller values such as 8 breaths per minute. The respiratory rate for people when they are ill people is a lot higher (e.g. 20 breaths per minute). [55]

For the simplicity of calculations, it could be considering a person who has 60 beats per minute; sixty beats per minute give a frequency equal to 1 Hz. In our case, we followed the heart rate that was disclosed in figure 3.2.

3.1.2 Second mathematical equation describing OMW and breathing effects

The second mathematical equation is just an improved one. Basically, the sinusoidal signal has a different format and it is better following the envelope waves and variations.

The second mathematical equation that is considered in this thesis is the following:

$$Ybr_2(x) = a_0 + [a_1 * \cos(2\pi f_{BP}x + \varphi) + b_1 * \sin(2\pi f_{BP}x + \varphi) + a_2 * \cos(4\pi f_{BP}x + \varphi) + b_2 * \sin(4\pi f_{BP}x + \varphi) + a_3 * \cos(6\pi f_{BP}x + \varphi) + b_3 * \sin(6\pi f_{BP}x + \varphi) + a_4 * \cos(8\pi f_{BP}x + \varphi) + b_4 * \sin(8\pi f_{BP}x + \varphi) + a_5 * \cos(10\pi f_{BP}x + \varphi) + b_5 * sin(10\pi f_{BP}x + \varphi) + a_6 * \cos(12\pi f_{BP}x + \varphi) + b_6 * \sin(12\pi f_{BP}x + \varphi)] * [3 + \sin(2\pi 0.1666)] \qquad (3.8)$$

The significant difference for this second model is not only that the equation is multiplied by (3+sin (2*pi*x)) but also the frequency of the respiration will be 0.1666 which corresponds to 6 respirations per minute.
The plot obtained is given in figure 3.5:

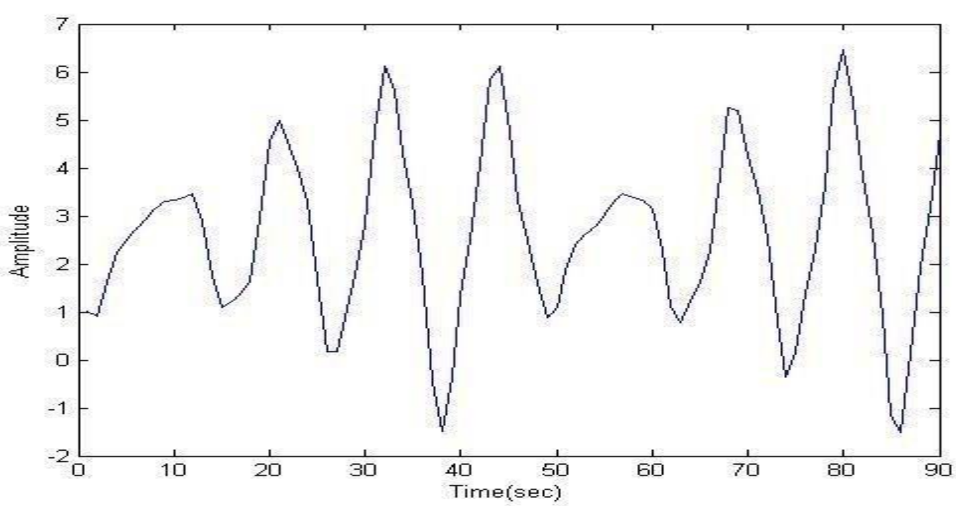

Figure 3.5: Another way to model the breathing effect over OMW1

As expected and indicated in Chapter 2, the breathing effects add noticeable changes in the wave's configuration (as exposed in figures 3.3, 3.4, and 3.5).

3.2 Mathematical Modelling of ECG and Predetection of Stroke

For the mathematical modelling of the ECGs it is preferable to have one clear format and this is the format showed in figure 2.4 in Chapter 2.

From now on in all the mathematical ECG configurations, calculations, and interpretations the *lead I* from each electrocardiogram is exclusively considered. The other *leads* are ignored.

The first ECG is coming from a 70 years old healthy patient and the next few ECGs are taken from the ECG Library 1995 - 2014 Dean Jenkins and Stephen Gerred. This library represents a useful collection of real ECGs recordings. [56]

For standard operations, it used a function called partial fraction expansion. [57] The best way to plot the electrocardiograms waves is by using either Interpolant either Smooth Spline features.

The Spline does not look like a classical function it is a piecewise function. In one dimension, at least, it can be written as a collection of polynomial segments. Usually it is about cubic polynomials. They are joined together to be sufficiently smooth across the break points. But there is no single, simple function that could be captured.

A mathematical interval (e.g. [a... b]) is subdivided into sufficiently small intervals [ξj..ξj+1], so that the limits of this interval a = ξ1<··· <ξl+1 = b. On each such interval, a polynomial pj of relatively low degree can provide a good approximation to the function f. This can even be done in such a way that the polynomial pieces blend smoothly, i.e., so that the resulting patched or composite function s(x) that equals pj(x) for x∊ [ξjξj+1]. Any such smooth piecewise polynomial function is called a spline. [54]

A spline in ppform is often referred to as a piecewise polynomial. The piecewise polynomials and polynomial splines are just two different views of the same thing. As explained above the ppform of order k provides a description in terms of its breaks ξ1...ξl+1 and the local polynomial coefficients cji of its l pieces (e.g. a cubic spline is of order 4 requires four coefficients to specify a cubic polynomial). [54]

$$p_j(x) = \sum_{i=0}^{k} (x-\xi)^{k-i} * c_{ji}, \ \ j = 1{:}\,l \qquad (3.9)$$

The <u>*smoothing spline*</u> *s* is constructed for the specified *smoothing parameter p* and the specified weights w_i when these weights are requested. [54]

The smoothing spline is achieved by minimizing the following equation:

$$p\sum_i w_i(y_i - s(x_i)) + (1-p)\int\left(\frac{d^2s}{dx^2}\right)^2 dx \qquad (3.10)$$

If the weights are not specified, they are assumed to be 1 for all data points. [54]

The parameter p is defined between 0 and 1. The p = 0 produces a least-squares straight-line fit to the data, while p = 1 produces a cubic spline interpolant. [54] Because smoothing splines have an associated smoothing parameter, you might consider these fits to be parametric in that sense. However, smoothing splines are also piecewise polynomials like cubic spline or shape preserving interpolants and are considered a nonparametric fit type.

With the data collected from each patient first the graph will be constructed by using smoothing spline function from curve fitting tools (as suggested above, the Interpolant function would work as well).

Once the graphic is built, an algorithm is applied to check if there is any potential stroke (cause by a myocardial infarction) alarm.

For every analyzed ECG, the following algorithm is applied:

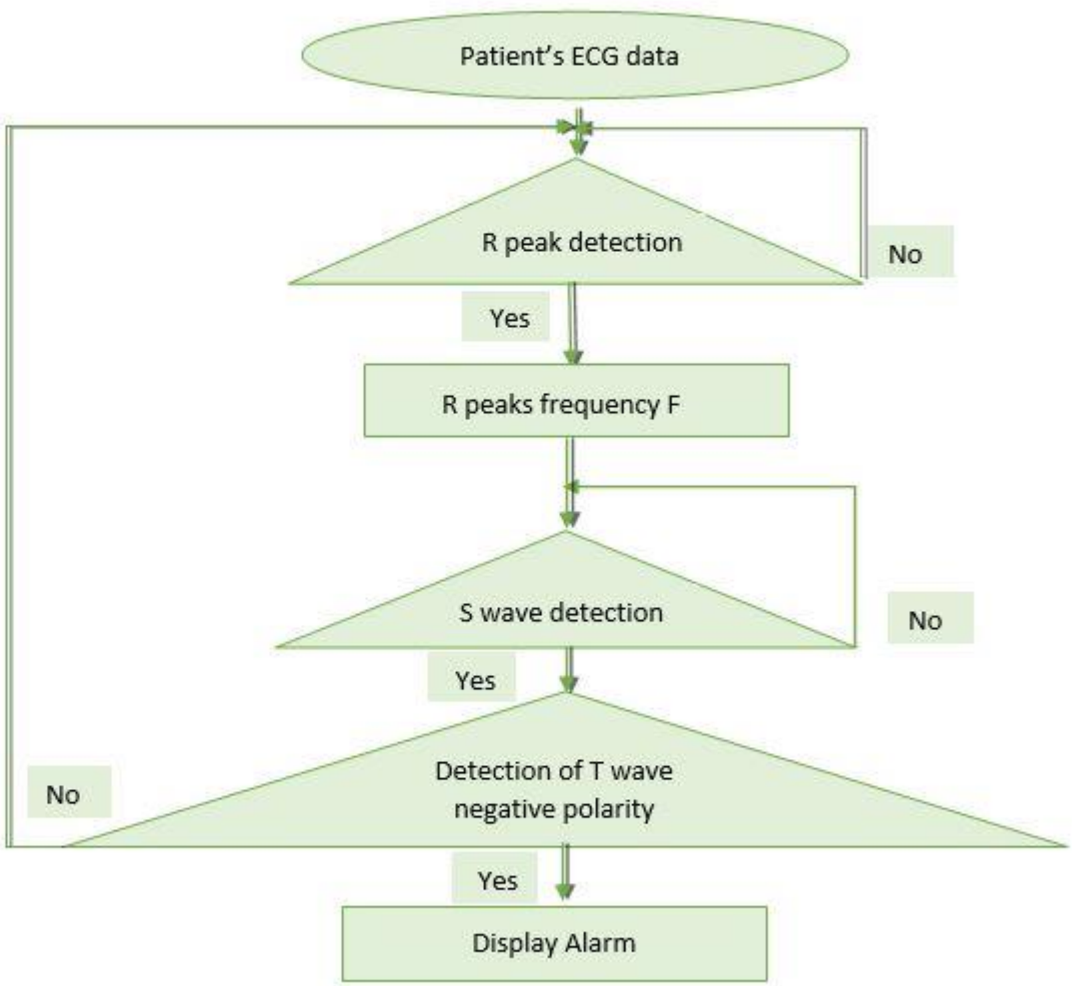

Figure 3.6: Algorithm for predetection of strokes

The first electrocardiogram analyzed here belongs to a seventy years old healthy patient. The ECG was realised in December 2016 at MedLife International Health Care Clinic in Ploiesti, Romania. The recordings devices that are used there for electrocardiograms are the *Electrographs ECG1200G*.

When using the ElectrocardiographECG1200G device it is possible to fine-tune its sensitivity by way of the adjusting button and switching among 2.5, 5, 10, 20, and 40 mm/mV. When needed the paper speed can be adjusted as well. There are filters such as AC, EMG, and DFT that can also be switched to obtain a good accuracy. This device can display the information from the last 10 patients. [58]

Other than smoothing spline function used for the graphs, one period of each ECG is modelled by using a sum of two ratio functions as it follows:

$$f(x) = f(x1) + f(x2) = \frac{\sum_{i1}^{n} r_{i1} \; *x^{i1+1}}{\sum_{j}^{m} q_{j} * x^{m-j}} + \frac{\sum_{k1}^{t} r_{k1} \; *x^{k1+1}}{\sum_{l}^{u} q_{l} * x^{u-l}} \qquad (3.11)$$

In the ECG's graph one unit from the amplitude will be equal to 10 mV and 25 units from the horizontal axis correspond to one second. The *lead I* from the man's ECG is shown as well. This electrocardiogram is named ECG_M (it belongs to patient "M"); the *ym* function is associated to ECG_M. The complete ECG of patient "M" is shown in Appendix A.

After processing the patient's data and using Smoothing Spline function, the following result is obtained:

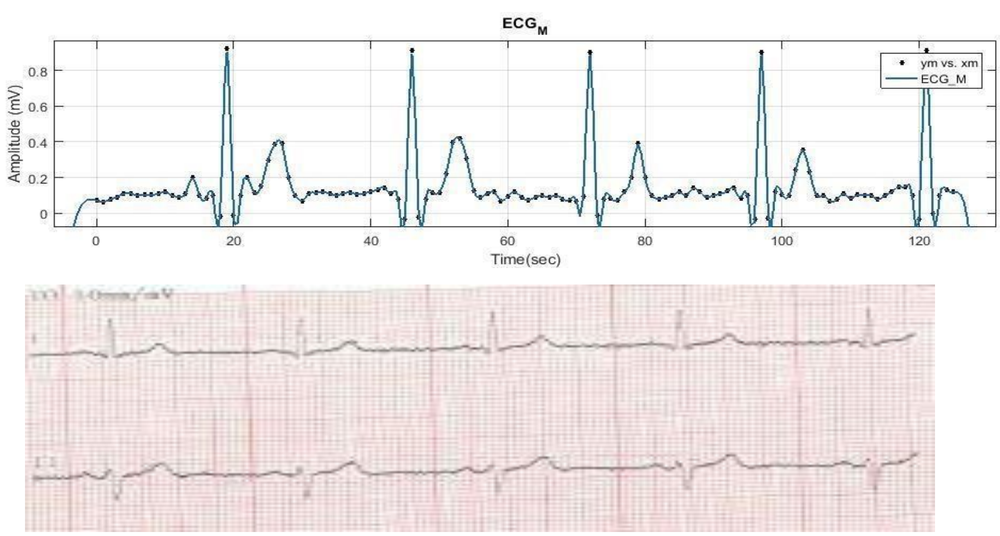

Figure 3.7: First patient's ECG given by (a) Matlab graph and (b) the original lead I

The first period mathematical modelling of the above ECG that is using the two functions from the equation (3.11) is given by the following two graphs:

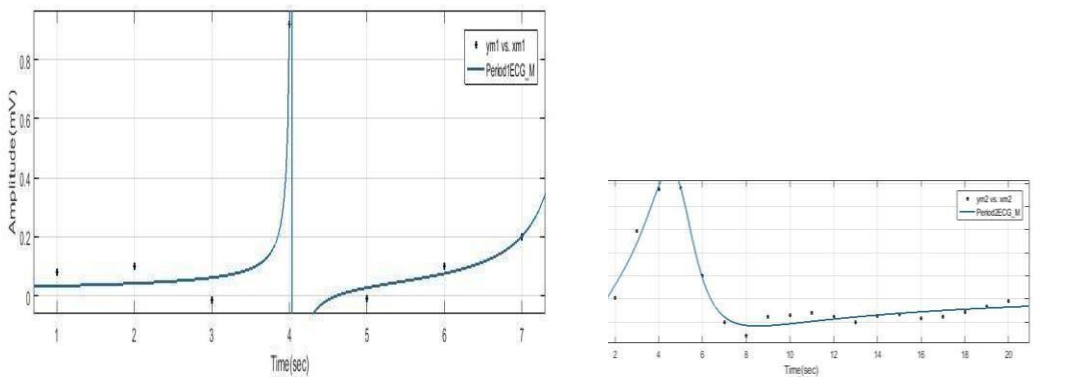

Figure 3.8: First period's ECG modelling by using rational function

As stated in Chapter 1, at this point the main objective is to apply the algorithm mentioned in figure 3.6 to determine if there is a stroke's predetection alarm or not. After determining that the frequency of this ECG is F = 0.9259 Hz the algorithm is not giving any stroke's predetection alarm which is the right result since there is no T wave negative polarity.

The other patient went to CMI private clinic (the full name of the CMI is CABINET MEDICAL INDIVIDUAL DR. MARINOIU MIHAELA MARIA) in Ploiesti, Romania. That was the place where his ECG was released.

It is the ECG of a 64 years old man who is suffering diastolic dysfunction relaxation delayed type. The factors that can contribute to altered left ventricular diastolic function are hypertrophy and ischemia. [59]

Despite the increased cardiovascular risk, the patient does not suffer from myocardial infarction. The determined frequency of his heart beat is 1 Hz and the algorithm is not giving stroke's predetection alarm in this case either.

There is no T wave negative polarity so there is no alarm.

As it happened for the first patient, the *lead I* of his ECG and the graph resulted by using Smoothing Spline function, is presented below:

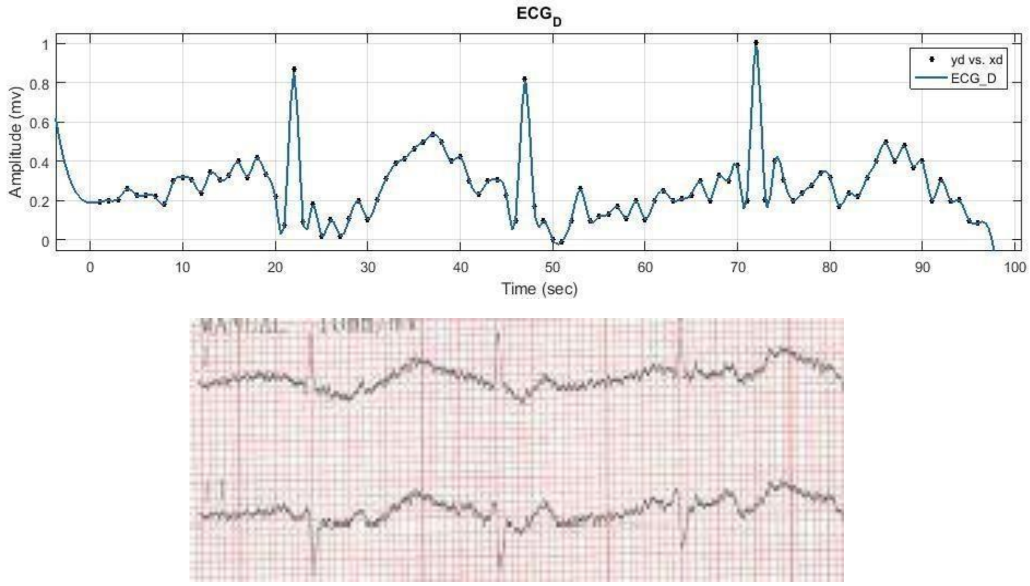

Figure 3.9: The ECG of a 64 years old man given by (a) Matlab and (b) by the original lead I&II

A very interesting ECG is given by the ECG Library 1995-2014: Dean Jenkins and Stephen Gerred; it is from a 79 years old man who is suffering an acute myocardial infarction. This ECG is giving a very good opportunity to see if the algorithm is functional. For the 79 years old patient the lead I of his ECG and the graph is presented below:

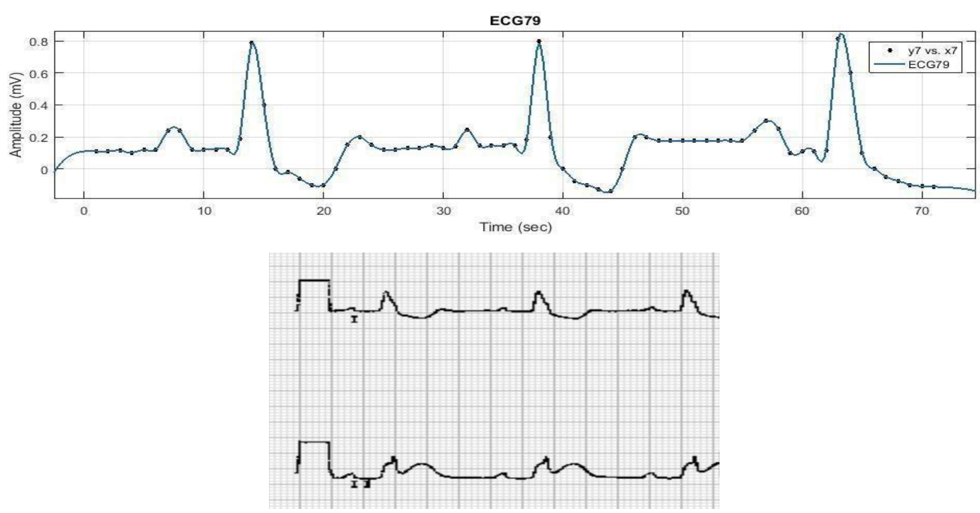

Figure 3.10: ECG of a 79 years old man suffering of acute myocardial infarction given by (a) Matlab and (b) by the original ECG lead I and II

Source: ECG Library 1995 – 2014: Dean Jenkins and Stephen Gerred

Once the mathematical algorithm is run, the 'Alarm' is displayed. The frequency of R peaks is 1.0417.

The next ECG belongs to a 39 years old healthy lady.

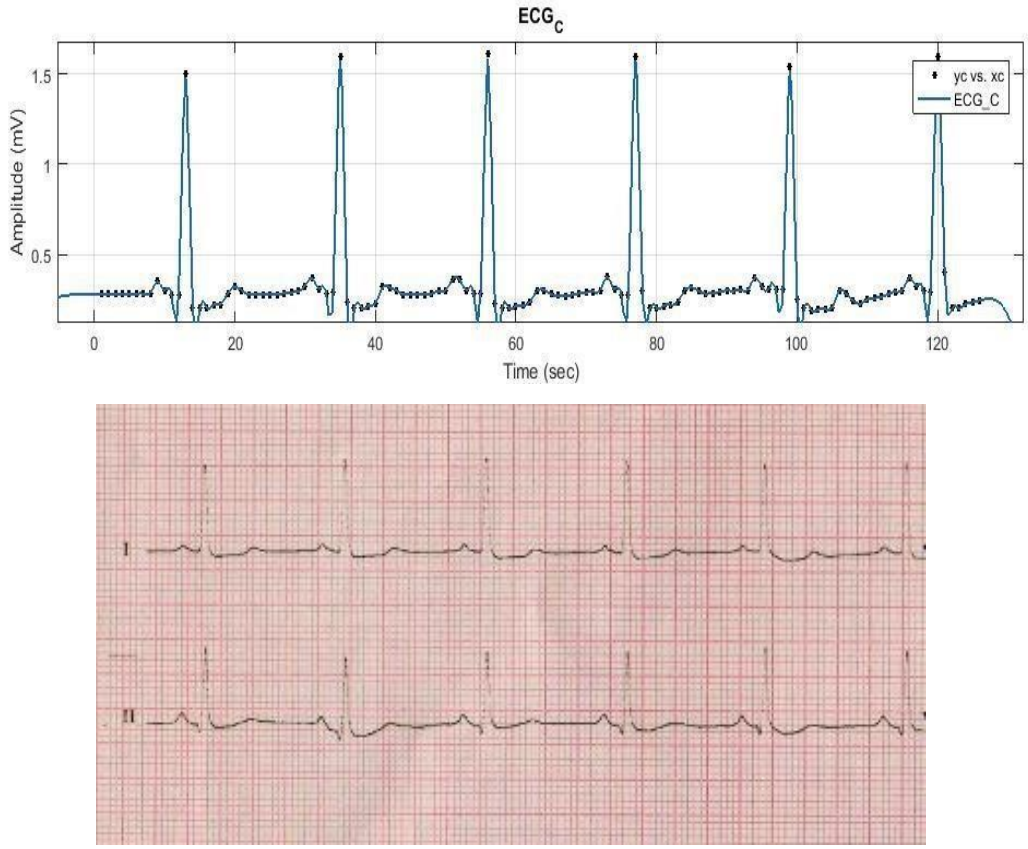

Figure 3.11: ECG of a 39 years old healthy lady given by (a) Matlab graph and (b) by the original ECG lead I&II

The frequency of R peaks is 1.1364 Hz. In the figure 3.11 there are 6 peaks that are seen in the *lead I*. Another particularity of this ECG is that P waves have a higher amplitude than T waves.

Another interesting case is the one of an 84 years old lady with hypertension (left anterior hemi block). This ECG was also taken from ECG Library 1995-2014: Dean Jenkins and Stephen Gerred.

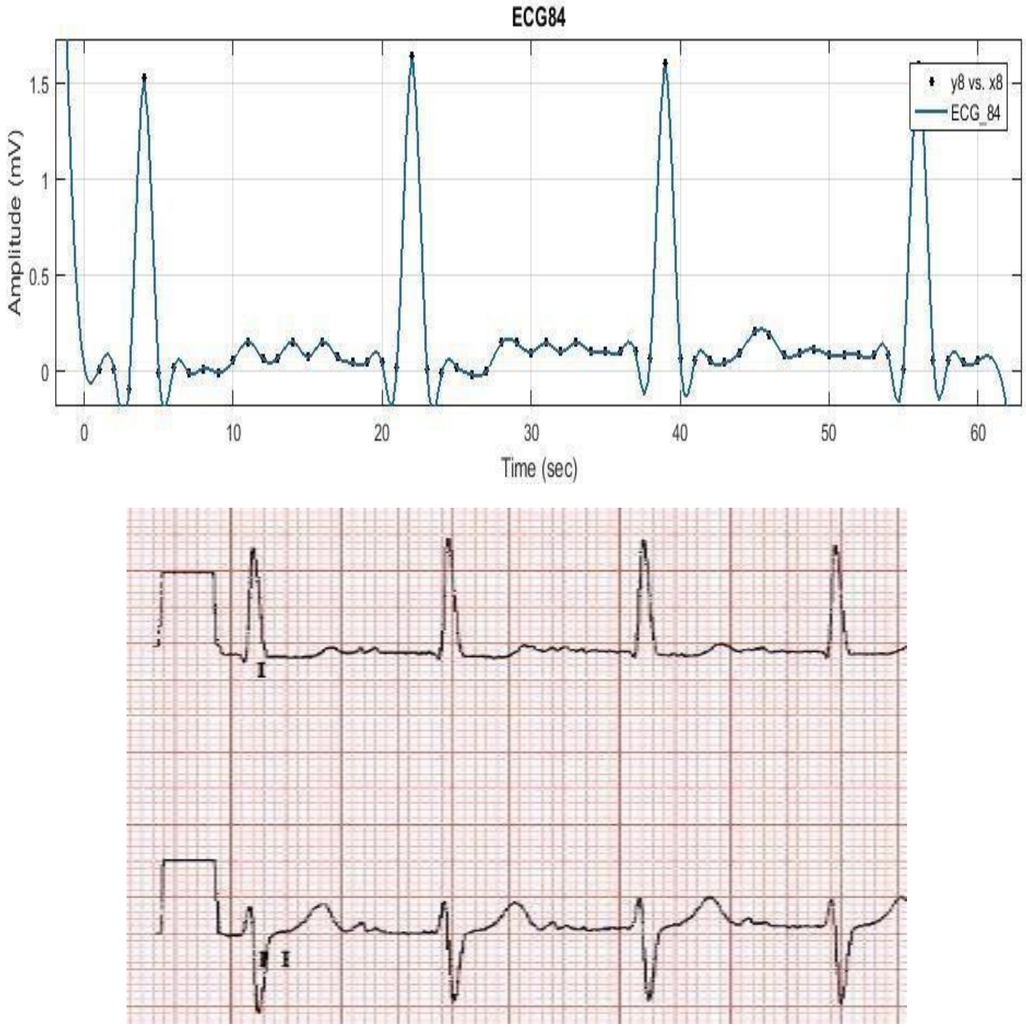

Figure 3.12: ECG of an 84 years old lady with hypertension given by (a) Matlab and (b) by the original ECG lead I&II

Source: ECG Library 1995 - 2014. Dean Jenkins and Stephen Gerred

The heart rate frequency is higher than the other ECGs: 1.3889 Hz. The algorithm does not display any alarm because the T polarity is positive.

An interesting study is done on a 55 years old man's ECG with a crushing chest pain (this ECG is taken from ECG Library 1995-2014: Dean Jenkins and Stephen Gerred).

Because of his low heart rate during the analyzed period, there are not too many noticeable R peaks.

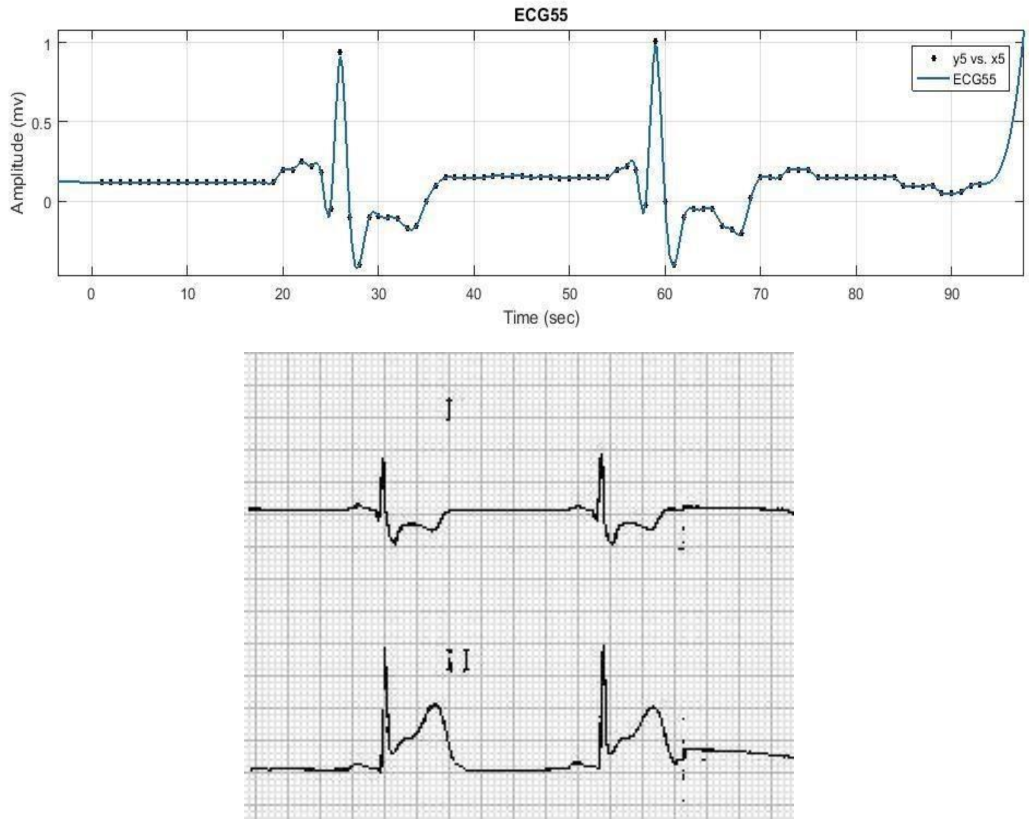

Figure 3.13: ECG of a 55 years old man with crushing chest pain given by (a) Matlab and (b) by original ECG lead I&II

Source: ECG Library 1995 - 2014. Dean Jenkins and Stephen Gerred

This patient's heart rate is lower than in the other cases: F5= 0.7576 Hz. Since the T wave of his ECG is negative, the algorithm will cause the display of 'Alarm'. In the reality, this patient is suffering of acute inferior myocardial infarction as it is attested in the Dean Jenkins and Stephen Gerred 1995-2014 ECG library.

The ECG of a patient whose age is close to the last revealed patient is reviewed next. It is about a man who is 51 years old.

The notable difference between the last two patients is that the 51 years old man is healthy.

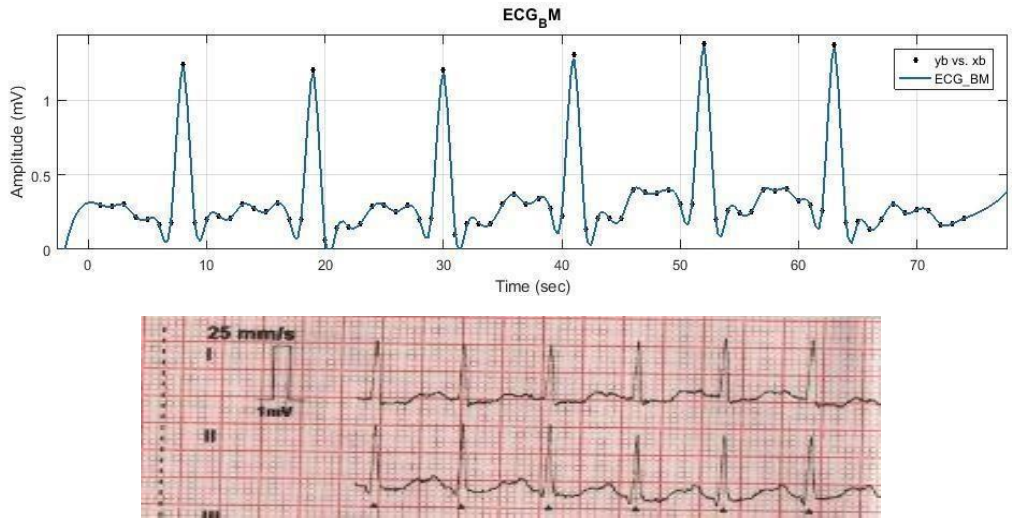

Figure 3.14: ECG of a 51 years old healthy man given by (a) Matlab graph and (b) by the original ECG lead I&II

This is one of the rare cases when the T waves seem to have the same amplitude as the P waves. The frequency of his heart rate is 2.2727 Hz.

His heart rate is almost two times bigger than what was seen for the other patients but the alarm is not displayed because there is no T negative polarity.

The last analyzed ECG belongs to a 94 years old lady. Considering her beautiful age, it will be no surprise to realize that her health is not at its best. She did not want to reveal any aspect about her health. Her wish is respected in this thesis.

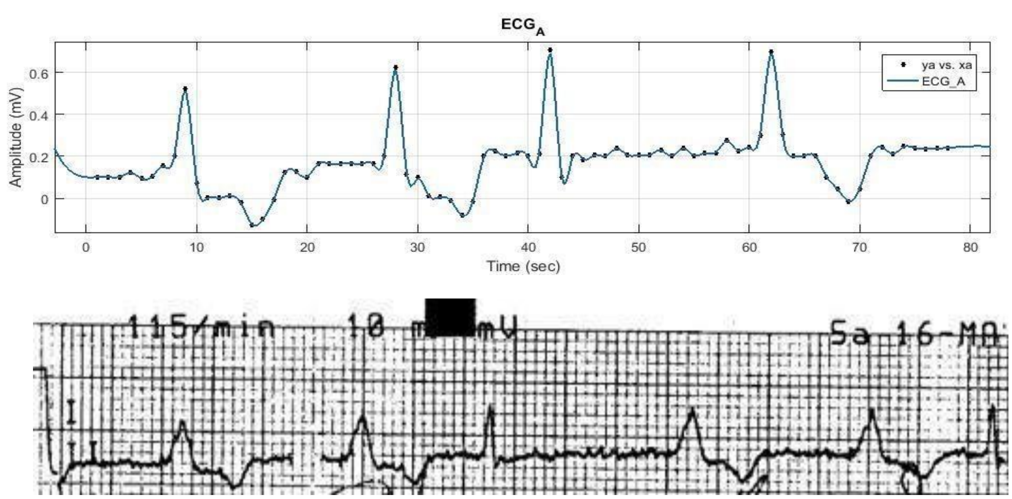

Figure3.15: ECG of a 94 years old lady given by (a) Matlab and (b) by the original ECG

There is no use to calculate the frequency of her heart rate because it is extremely instable.

In the next chapter, the performances of the used algorithm are presented.

3.3 Pattern Recognition by using Artificial Neural Networks

There are diverse applications related to Artificial Neural Networks, such as *Neural Networks Clustering*,

Neural Networks Pattern Recognition, and *Neural Networks Time Series*. It was proved that Artificial Neural Networks (NN) are also good at recognizing patterns (the example provided in Math Works is about classifying a tumor as benign or malignant, based on the uniformity of cell size and the clump thickness). [60]

As suggested in *NN Pattern Recognition* instructions, the chosen tool is *nprtool GUI* (as it is described in *NN Pattern Recognition Tool* in Matlab).

The first important operation is to define the input data set. In our case this is the data from our eight patients' ECGs. More specific, it is the amplitudes in mV of those ECGs.

The input vector must be arranged as columns in a matrix. The next operation is to set target vectors which indicate the classes to which the input vector is assigned. In this case, there are only two classes: each scalar target value must be either 0 or 1. [60]

The way these target vectors are constructed is the following: a value 0 is associated with the negative polarity of T waves and the value 1 is given to the positive polarity of T waves (as it should be in the normal cases). Another target vector can be built by giving 0 value to the normal clean signal without alarm and 1 for the bad unwanted signal. These two target vectors can be combined in only one row matrix.

The inputs are classified in several different classes using one element (being either 1 or 0). The entire process is described by the following steps:

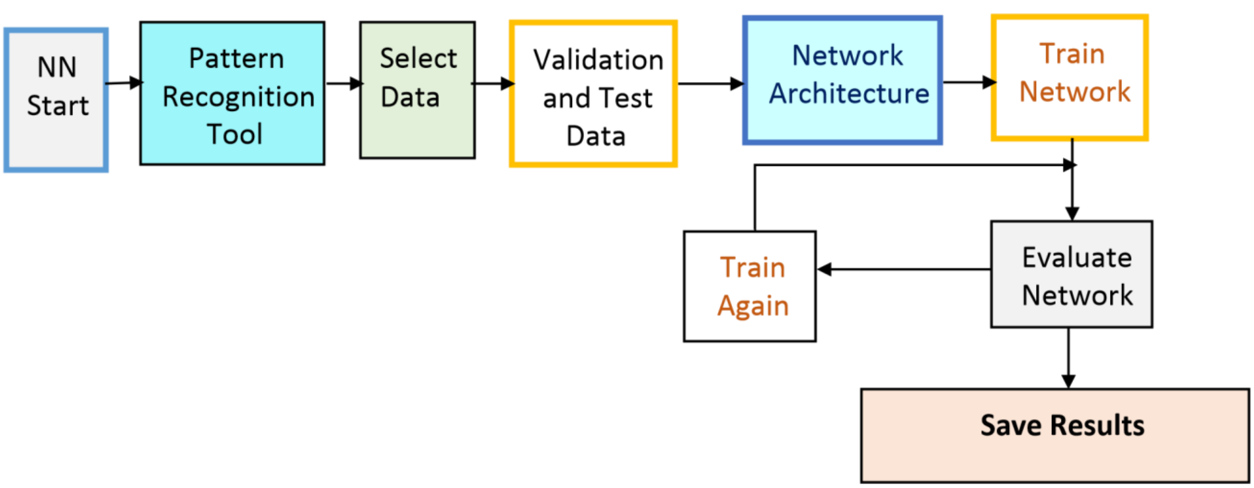

Figure 3.16: Block-diagram of NN Pattern Recognition Tool

Regarding the studied ECGs, the input for the *NN Pattern Recognition* tool is the new built matrix M1 that represents the ECG impulses; to be more specific every row of this matrix corresponds to a 25 units (impulse) that is the equivalent of one second's representation. After gathering all the data from all our eight patients we obtain a matrix with 25 rows and 29 columns.

The target vector is the matrix O1 which has 2 rows and 29 columns.

The typical network that is used for pattern recognition is a two-layer feedforward network. It uses a sigmoid transfer function in the hidden layer and a *SoftMax* transfer function in the output layer. The sigmoid function was largely described in Chapter 2.

The MatlabWorks recommendation is to use 70% of samples for the network training, 15% for validation, and 15% of samples for testing. The network training is adjusted according to its errors. The validation samples are used to measure the network generalization and to close the training when generalization stops improving. The testing samples have no effect on training and provide independent measurement performances during and after training. [60] The first training set is used to compute the gradient and updating the network weights and biases. The error on the validation set is monitored during all the training process. This error should normally decrease during the initial phase of training, as does the training set error. However, when the network begins to over fit the data, the error on the validation set generally begins to increase. All these percentages of using the database can be changed according to the user's ideas. The defaulted ten hidden nodes are sufficient. [60]

In our case, the devised architecture has 25 inputs, 10 hidden neurons, and 2 outputs. The number of hidden neurons can also be changed; there could be hidden neurons involved but, if the number of hidden neurons is increased, that does not mean that the network will automatically perform better. [60]

A good evaluation of these numbers and their performance can be done once the network is trained. The training process is using scaled conjugate gradient backpropagation. The backpropagation learning technique was also largely described in Chapter 2. The trainings are automatically stopped when generalization stops improving, as it is indicated by a growth in the cross-entropy of the validation samples. The network weights and biases are kept at the minimum of the validation set error. The minimizing Cross-Entropy results demonstrates we are dealing with a good classification. Zero values mean there is no error. [60]

The number of output neurons is set to 2 and this is equal to the number of elements mentioned in the target vector (matrix O1).

Once the architecture is built, the number of iterations needed to get the best result are calculated.

In our case, there were seven iterations required. The numbers are shown in the following figure:

Figure 3.17: NN Architecture and Training

As it is shown in figure 3.17, in the *NN Pattern Recognition Tool* is an option called *Confusion*. In our case, while clicking on "Confusion":

Figure 3.18: The Confusion matrices for Network's Training, Validation, and Testing

In figure 3.18 there are the confusion matrices for training, testing, and validation. The correct responses are illustrated in green squares, the incorrect ones in red squares. The blue squares are demonstrating the overall accuracy.

There is also the possibility to see the training performance graph, which in our case looks as follows:

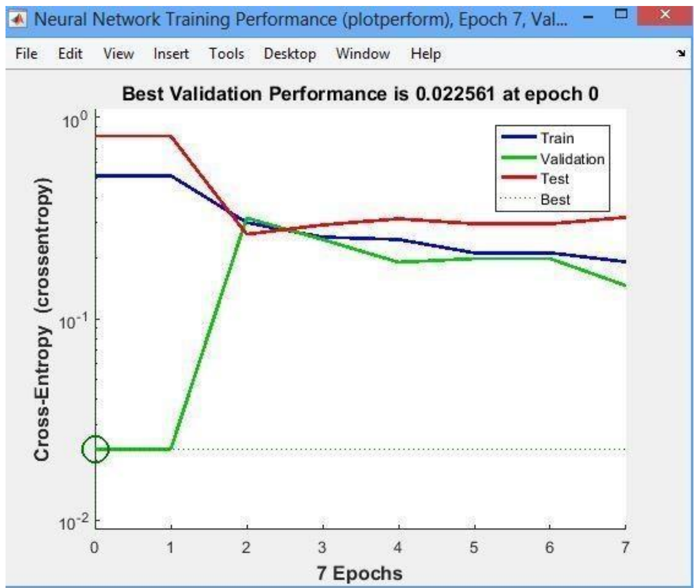

Figure 3.19: The best validation performance graph

According to figure 3.19, at this point, the performance of the entire network process must be evaluated. The network can be tested against new data. If the user is displeased with the network's performance then he / she can train the network again. Modifications can be done, including the increasing or decreasing of number of hidden neurons.

Since the results are good, they can now be saved and the application can be closed.

Chapter 4 Results and Analyses

4.1 Performances Analyses

The first paragraph of this chapter is about the fitting curve presented in Fig 3.3. The Fourier mathematical model chosen for that extracted OMW proved to be reliable with errors between 0.01 and 0.1 for the arbitrary OMW PP's amplitude.

Most of this chapter is dedicated to the analysis of eight ECGs presented and partially analyzed in chapter 3.

All the signals from all the ECGs did not need to be filtered because they were already clean. All the signals from 1995-2014: Dean Jenkins and Stephen Gerred ECG Library and all the signals coming from the other four patients were initially filtered. The filter was already mentioned for the Electrocardiograph1200G device. On another ECG (precisely ECG_bM) it was clearly mentioned that they used two filters: one for the general neighborhood supply electrical network and another one for the measuring device itself.

At the end of this chapter, after digging into performances analyses, two filtering possibilities are presented for an ECG with added noise and another normal noisy ECG. The noisy ECG is taken from 1995-2014: Dean Jenkins and Stephen Gerred ECG Library.

The algorithm that was designed, developed, and described in the previous chapter could provide information mainly about three major components: the average frequency of the heart rate considering the time differences between the R peaks, the zero-crossing points in our ECGs, and if there was any '***Alarm***' given (because if the negative polarity of the T waves).

It is important to underline that there was never a constant frequency. If we exclude the 55 years old patient with a crushing pain chest and the 94 years old lady who had a very irregular heart bit, the period of the most patients was almost constant, it presented very little variations (e.g. between 0.04 and 0.08 sec).

The zero-crossing points present very little interest for our algorithm and practically none for the performance analysis. They are mentioned briefly in the following data tables that are built in this chapter.

The ratio function was made only to model the first period of ECGs and it was composed by two other functions. The two functions parameters are respecting the equation (3.11) (from chapter 3) but they are not used in the first, nor in the second algorithm.

The main goal of this first algorithm was to see if the system can provide us with alarms in case of stroke's predetection or not.

The next table reveals the performance analysis of the first declared electrocardiogram (ECG_M). The other seven tables are shown in Appendix 2.

Table 2: ECG's parameters of a 70 years old man

Average frequency [Hz]	Smoothing parameter	Number of zero-crossing points	T waves negative polarity	Display Alarm	Ratio function f =f1+f2	
					f1 parameters	f2 parameters
0.9259	0.9987671887508507	6	No	No	r_{11}=1.17e+05 r_{12}=-5.405e+05 q_{11}=-6.279e+05 q_{12}=7.395e+06 q_{13}=-1.96e+07	r_{21}=0.1752 r_{22}=2.157 r_{23}=7.297 r_{24}=1.209 q_{21}=7.212 q_{22}=0.4504 q_{23}=67.56

A summary of studied patients (including their predetection of stroke alarms and diseases) is detailed in the next table:

Table 3: Table resuming patients' ECGs, predetection of stroke, and diseases

Patient	T waves negative polarity	Display alarm	Certified Disease	Name of the patients' ECG
Patient 1	No	No	N.A.	ECG_M
Patient 2	No	No	Diastolic dysfunction relaxation delayed type	ECG_D
Patient 3	Yes	Yes	Acute myocardial infarction	ECG_79
Patient 4	No	No	N.A.	ECG_C
Patient 5	No	No	Hypertension - left anterior hemi block	ECG_84
Patient 6	Yes	Yes	Acute inferior myocardial infarction	ECG_55
Patient 7	No	No	N.A.	$ECG_b M$
Patient 8	Yes	Yes	Unknown	ECG_A

Table 2 shows that our algorithm constantly displayed the alarm every time when signals with T-wave polarity were negative. The tables from Appendix B show the performance analysis of this mentioned algorithm applied to all our electrocardiograms.

To filter ECG waves, we first need a noisy one. Noise is added to the ECG of a 79 years old.

This was already plotted in Figure 3.10a in Chapter 3.

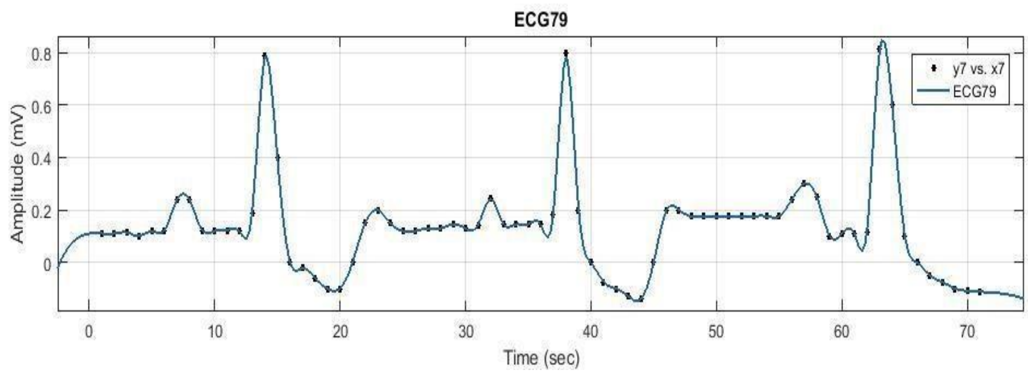

Figure 3.10a from Chapter 3

Noise is added (by using the function ***imnoise*** that is in *Image Processing Toolbox* from Matlab). It can add the following types of noise: “Gaussian”, “localvar”, “poisson”, “salt & pepper”, and “speckle”. For our ECG, the Gaussian noise was selected. Our new noisy function adds Gaussian white noise to our function (the default is zero mean noise with 0.01 variance).

Our new noisy function is shown in Figure 4.1:

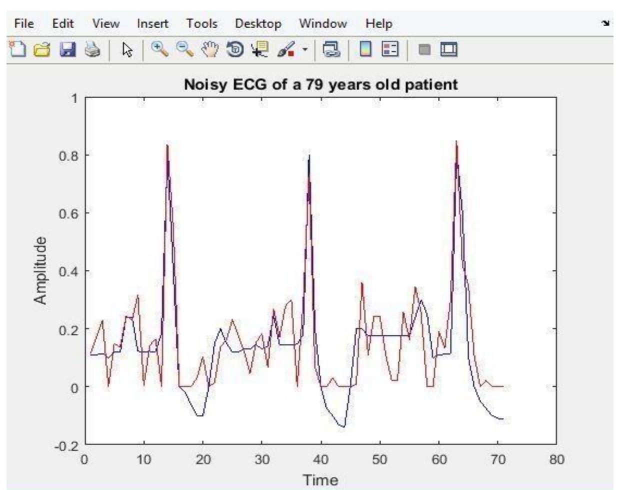

Figure 4.1: The noisy ECG of a 79 years old patient in red and the original filtered ECG in blue

4.2 Filters

This signal is filtrated by using the filter Savitzky-Golay. [61]

The idea is to fit subsets of points with a low-degree polynomial. Signal Processing Toolbox encompasses function *sgolay* that helps to calculate the weight coefficients of the Savitzky-Golay filter and function *sgolayfilt* for data smoothing. Any function y that would be defined as *y=sgolayfilt (x, order, framelen)* applies a Savitzky-Golay FIR smoothing filter to the data in vector x. The polynomial order (*order*) must be less than the frame length (*framen*). The framen must be odd and if order is equal to framelen-1 the filter crops no smoothing. The length of x must be greater or equal to *framelen*. [61]

A very good filter result for the drawn yn function is given by y7_noisy=sgolayfilt (y7_noisy, 4, 5). It is shown in figure 4.2:

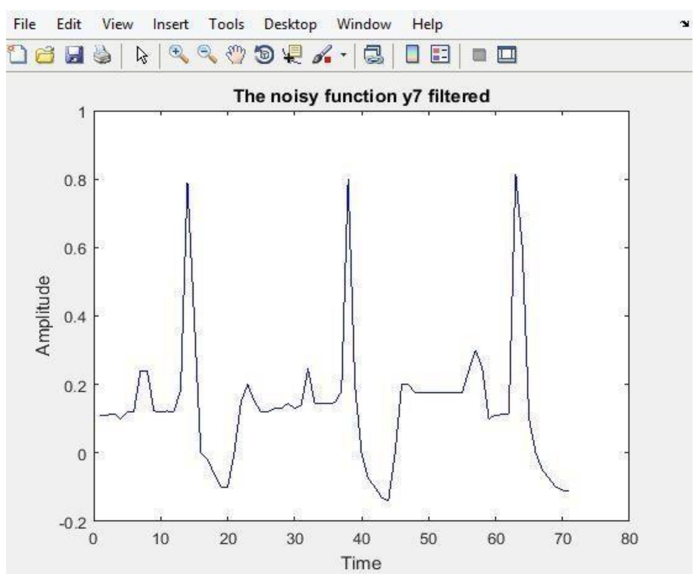

Figure 4.2: The noisy ECG of a 79 years old patient filtered with Savitzky-Golay filter

When dealing with a patient who is suffering acute myocardial infarction, the importance of obtaining a clear and solid signal does not need to be demonstrated.

The last ECG that is filtered is the normal ECG from 1995-2014: Dean Jenkins and Stephen Gerred ECG Library which was shown in figure 2.5 (Chapter 2).

The ECG was plotted in the same way that the other ECGs have been plotted in Chapter 3. In figure 4.3 the *lead I* and *lead II* can also be seen.

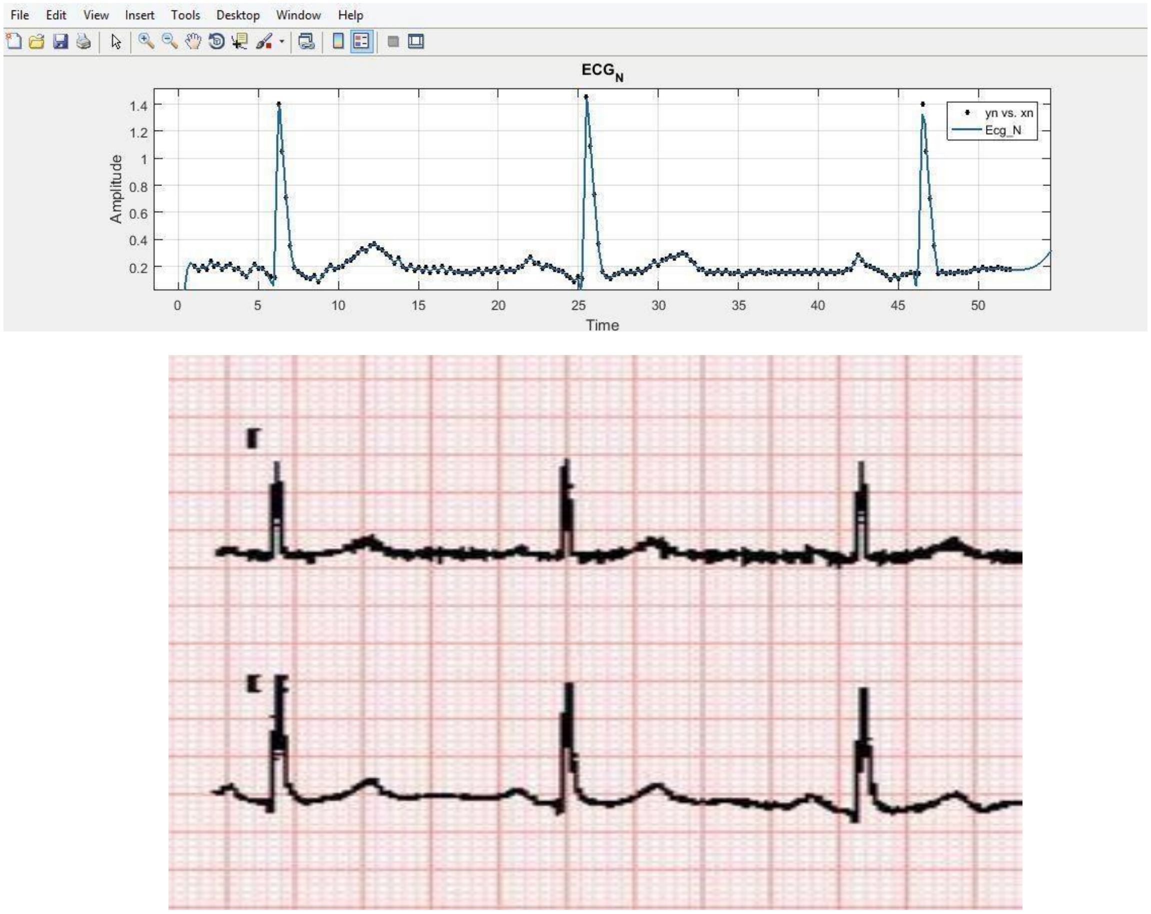

Figure 4.3: A normal given ECG by (a) Matlab graph and (b) by the original ECG lead I&II

Source: ECG Library 1995 - 2014. Dean Jenkins and Stephen Gerred

The signal given by *lead I* is filtrated by using the same filter, Savitzky-Golay. Above it can be seen a two-dimensional image resulted from a set of data distorted by random noise. The purpose is to smooth this data.

This filter needs to be applied to the signal given by *lead I* (represented by yn function; it is shown in figure 4.3– *lead I*). The best smoothing filter result for the drawn yn function is given by yn_filtered=sgolayfilt (yn, 4, 5).

The filtered function is plotted in blue color while the original building points of yn are plotted in red, as shown in figure4.4:

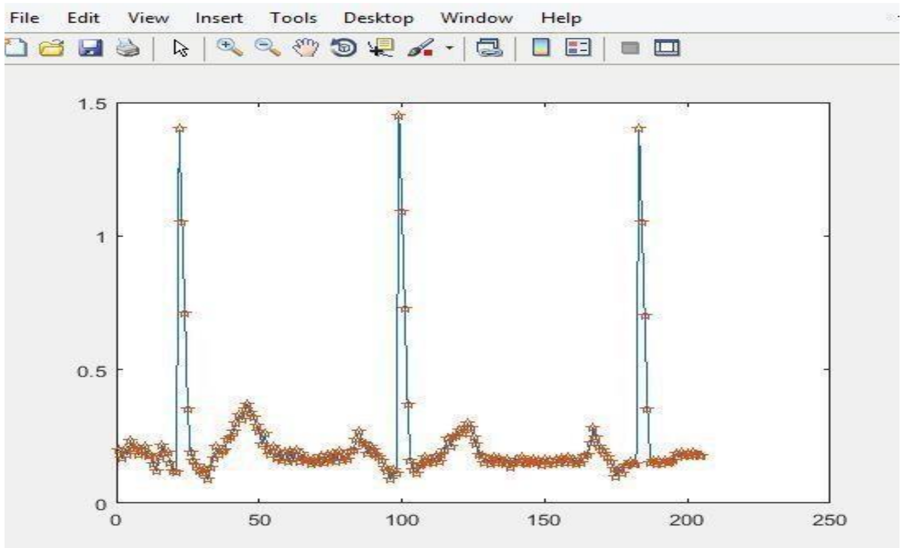

Figure 4.4: The original yn function in red color and the filtered function in blue color after using the *sgolayfilt* function

Since the figure above does not clearly show the filtered function, figure 4.5 shows only the filtered function:

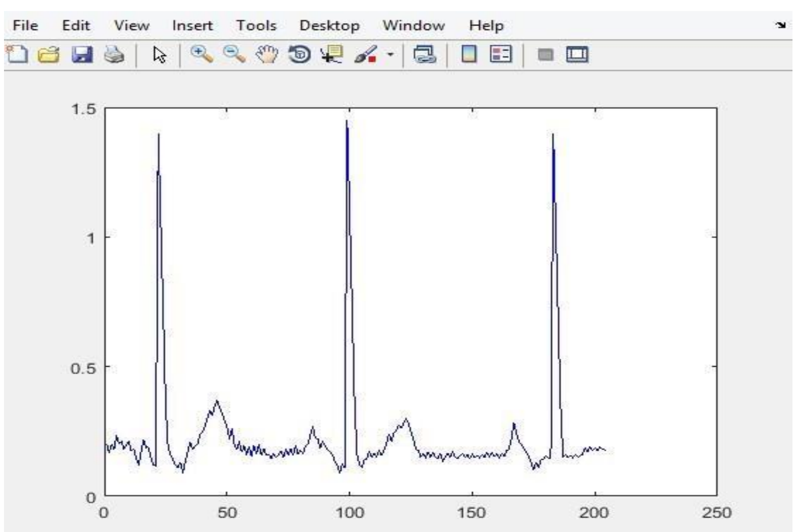

Figure 4.5: The filtered function in blue color after using the *sgolayfilt* function

One hundred units of the horizontal axis correspond to one second in real time while in the initial ECG 25 units of the same horizontal axis correspond to one second. Various filters were created in time. The low pass band filter was considered one of the basics filters.

The filtering function *filter* was also tested. This function is about a one-dimensional digital filter which filters data described by two vectors. The filtered function is presented in figure 4.6:

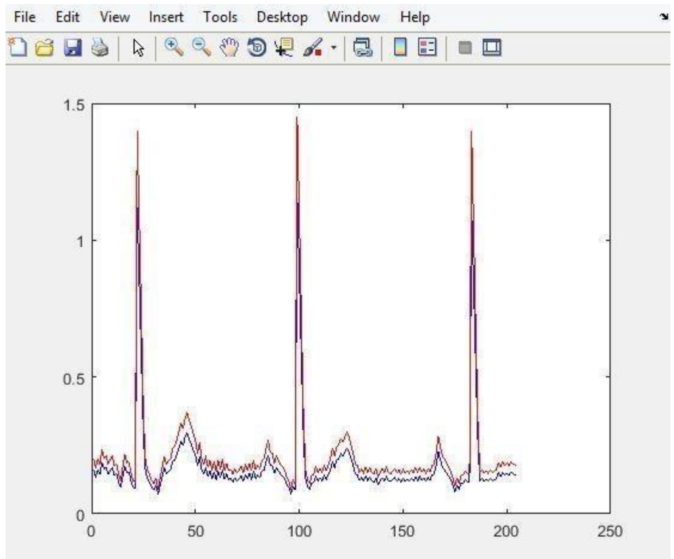

Figure 4.6: Function yn filtered with one dimensional filter

Artificial Neural Networks can be used as estimators. When opening the *Neural Network Fitting Tool,* the command *nftool* can be used. Artificial Neural Networks can fit any practical function. In the normal ECG case, we need to fit xn input values to the yn targets. A two-layer feed-forward network with a specific sigmoid number of hidden neurons and linear output neurons can fit multidimensional mapping complex problems (as it was mentioned before in our case it is a two-dimensional problem). [62]

The number of hidden nodes is set at 10 as well and the next step is the training which stops automatically when the generalization stops improving.

The Levenberg-Marquand backpropagation training algorithm is recommended for most problems and this one is applied first in our normal ECG case. The Levenberg-Marquardt algorithm was selected to train our neural network in a faster way. [63] Our network is trained until the validation error failed to decrease. Under Plots pane after clicking on Fit the following figure appears:

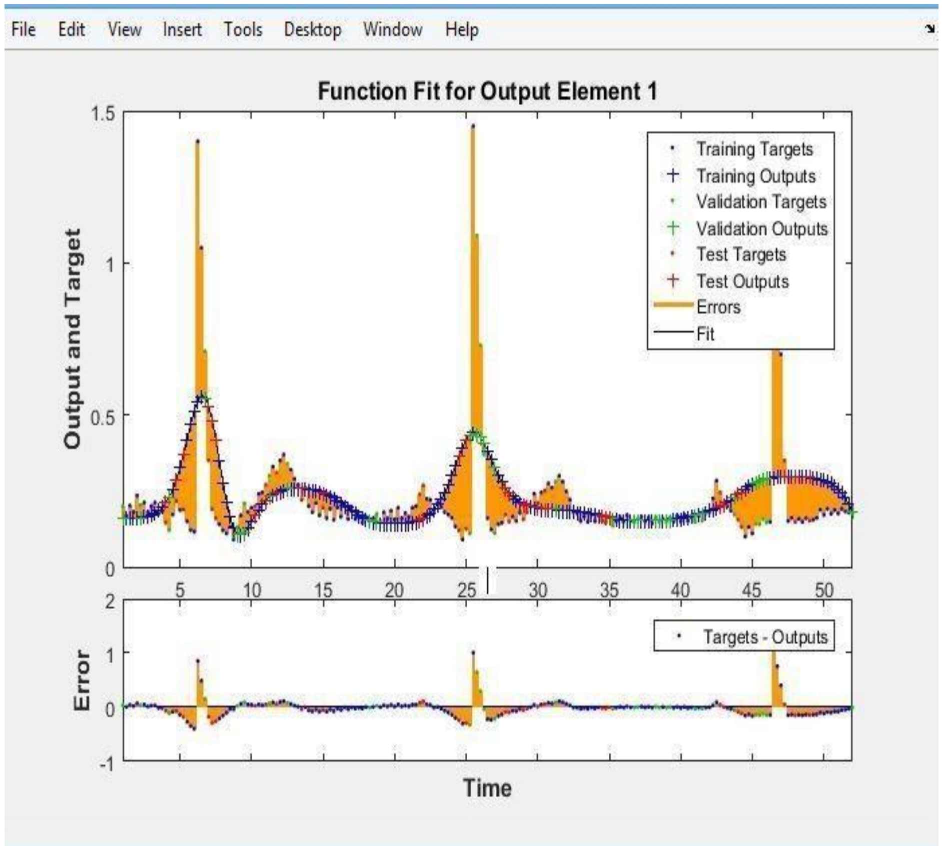

Figure 4.7: Artificial Neural Networks fitting plot for ECG_N by using 10 hidden nodes and Levenberg-Marquand training algorithm

The result is not satisfactory: the amplitude of the blue line is too low and the line is too smooth.

The best result is given by using 80% data for training, 10% data for validation and 10% data for testing. The number of hidden neurons is set to 20 and the network is trained and retrained. The neural network training is presented in figure 4.8:

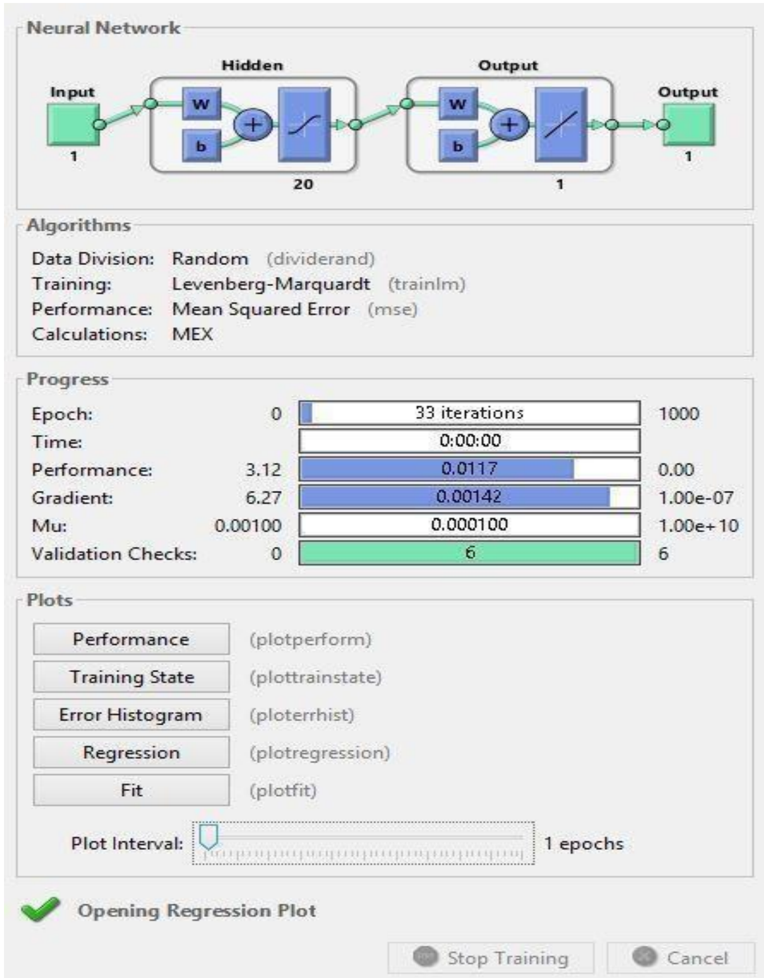

Figure 4.8: The NN architecture including the used algorithm and the obtained progress

As shown in figure 4.8 under *Plot* pane after clicking on *Regression* another plot is displayed with respects to targets for training, validation, and test sets. For a perfect fit, the data should fall along 45-degree line. A reasonable good fit is R values in each case that are 0.93 and above. [62]

Our regression plot looks as it follows:

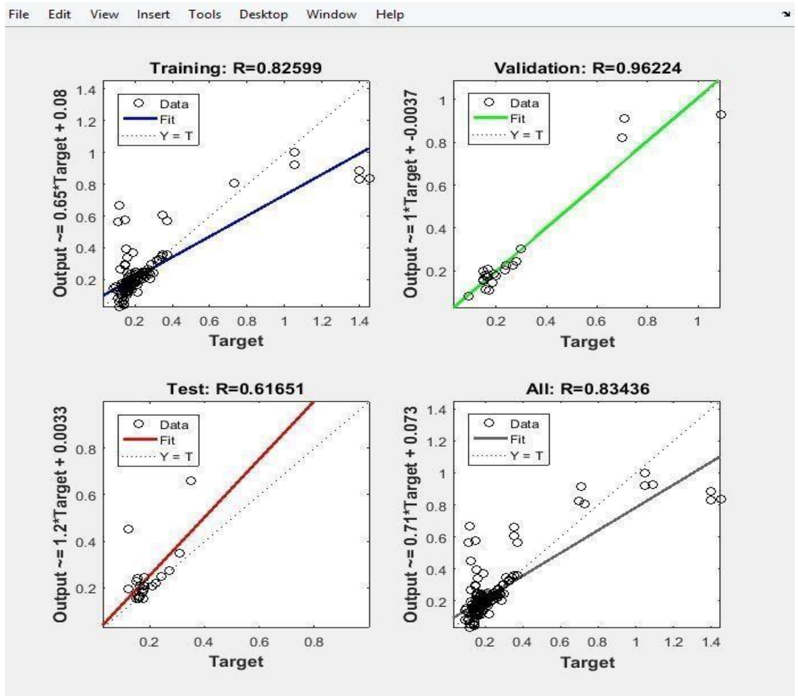

Figure 4.9: The regression plot for ECG_N

Under *Plot* pane the view of the *Error Histogram* can provide additional verification of network performance as follows:

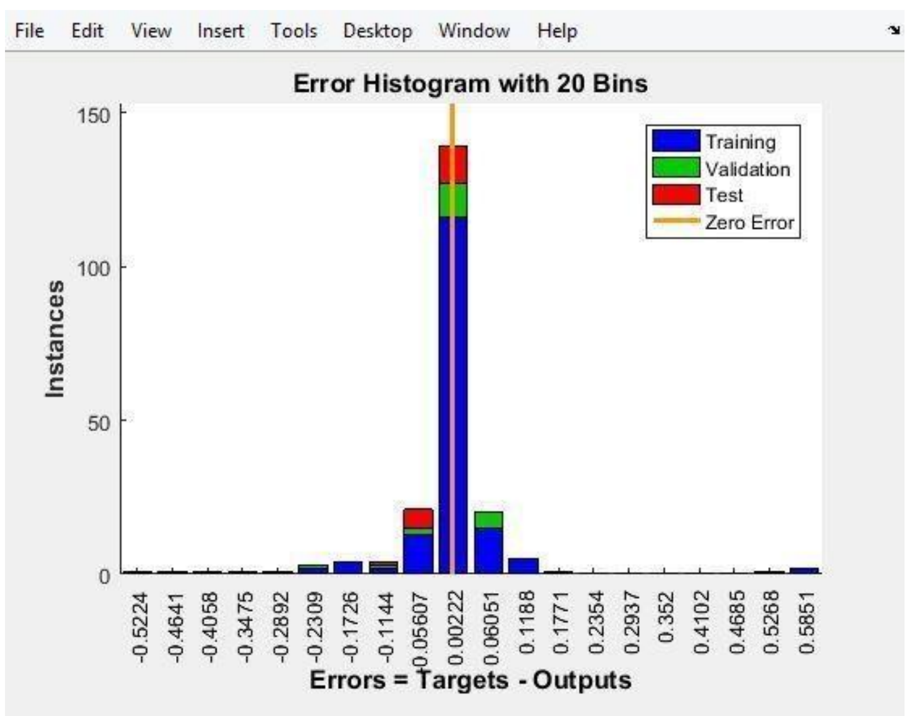

Figure 4.10: The Error Histogram for ECG_N

If the results are satisfactory they are saved. The plot of this neural network training and retraining process is shown in figure 4.11:

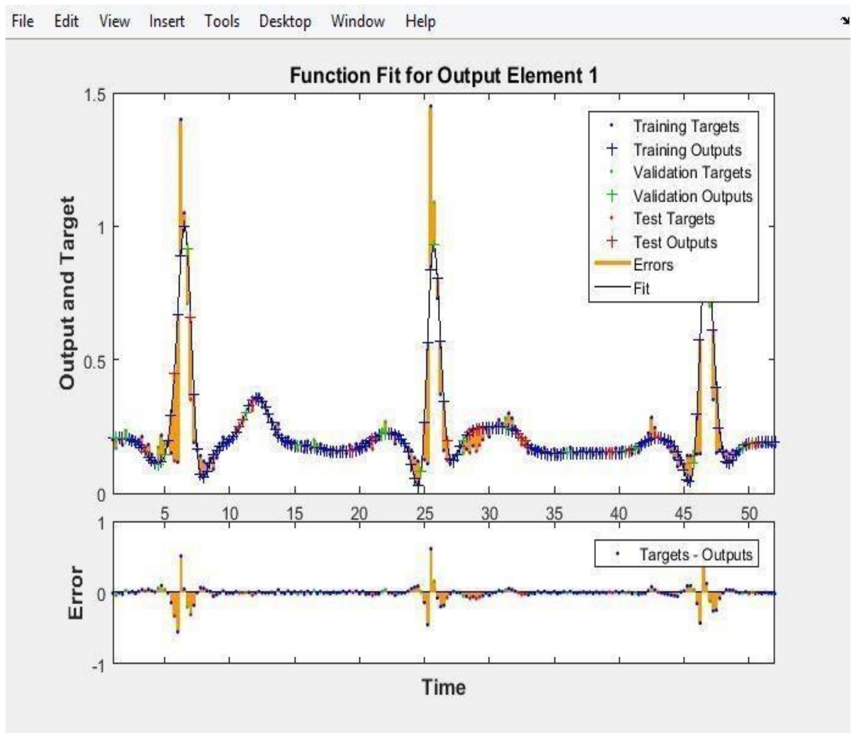

Figure 4.11: Artificial Neural Networks fitting plot for ECG_N by using 20 hidden nodes and Levenberg-Marquand training algorithm

When a network has noise, the algorithm *Bayesian Regularization* is recommended. This algorithm takes more time. A Bayesian analysis is a complex one: it needs to compute a posterior distribution which is an up-dated distribution of the given data. [63]

The *posterior* is composed of:

- A *likelihood* function (which contains the information that the sample offers about the parameters)
- *Prior distributions* (the distribution of the parameters believed by the general specialist before observing the data)

After running the *Bayesian Regularization* algorithm, the following result was obtained:

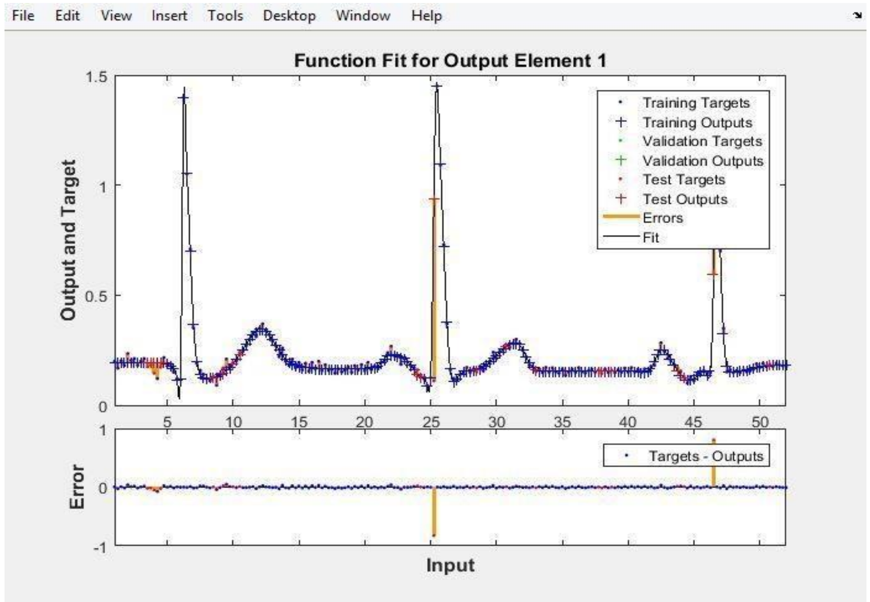

Figure 4.12: Artificial Neural Networks fitting plot for ECG_N by using 20 hidden nodes and Bayesian Regularization training algorithm

The last algorithm can reach the original amplitudes of the normal ECG and it has less errors. The regression plot for Bayesian Regularization algorithm looks as it follows:

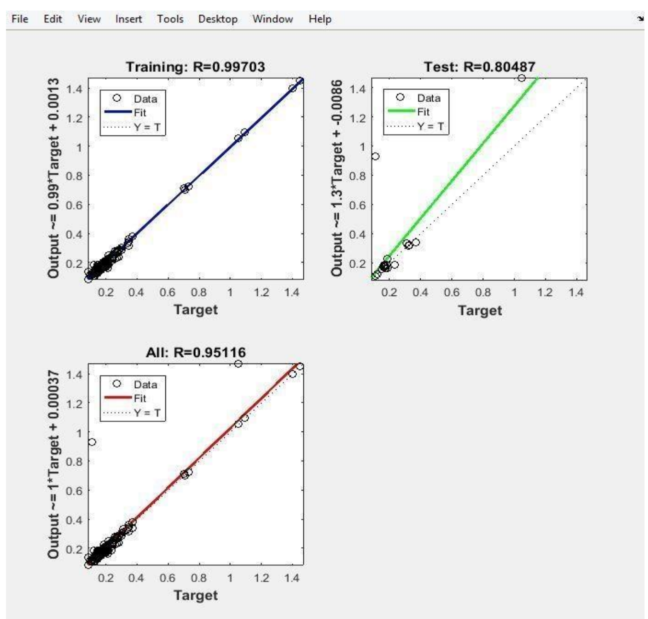

Figure 4.13: The Regression plot for ECG_N after running Bayesian Regularization algorithm

The Artificial Neural Network architecture and the obtained progress for the Bayesian Regularization (BR) algorithm is shown in figure 4.14:

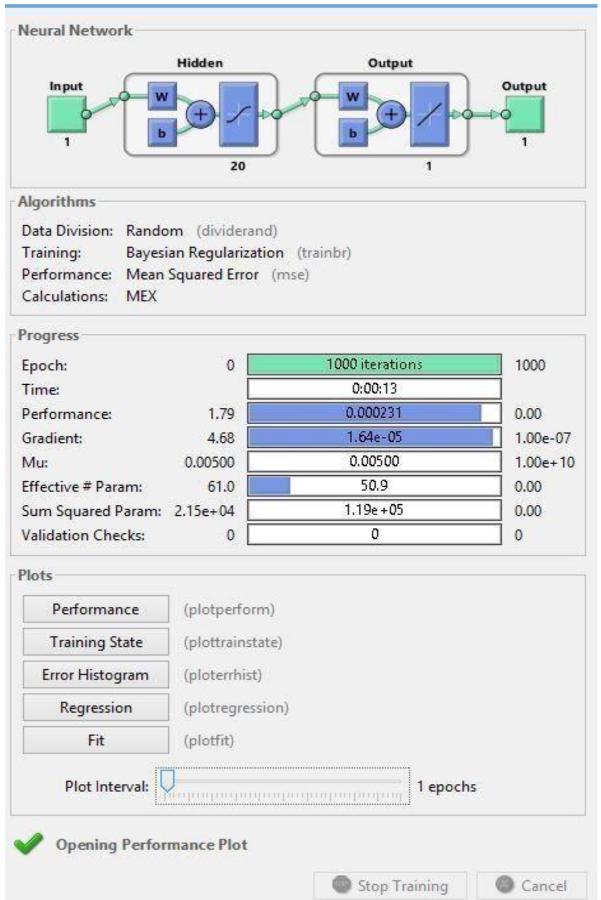

Figure 4.14: The Artificial Neural Network architecture including the used algorithm and the BR obtained progress

4.3 Comparisons of the used filters and the two predetection of stroke models

In the last two chapters, an interesting variety of different and complex cases was analyzed. There were three healthy patients with good and clear electrocardiograms, two patients with other medical issues, and three patients with ECGs that finally led to predetection of strokes. The electrocardiogram of 84 years old lady with hypertension showed that hypertension does not always conduct to predetection of stroke but the recording her ECG was the right thing to do.

The complete electrocardiograms of the patients who are not included in the 1995-2014: Dean Jenkins and Stephen Gerred ECG Library are shown in Appendix A.

For the major component of this thesis given by the predetection of stroke two major models were presented in the previous two chapters, with a visible elaboration in Chapter 3. Those two models are considered after a short analysis about filters.

Previously two filters were used. Since the results from the one-dimensional filter were not impressive, in this chapter only the Savitzky-Golay is cited.

The filter was applied to specific functions from our various ECGs. Their results were good, clear filtered signals resulted after its application.

The Savitzky-Golay filter is a good fit for our signals. It is easier to be manipulated, there are only two mathematical parameters that could be modified, and there is little time needed for its implementation; therefore the chosen filter for our ECGs is the *Savitzky-Golay filter*.

In this chapter, after filtering a noisy electrocardiogram, two NN algorithms were used for curve fittings.

The first algorithm used was Levenberg-Marquand. While implementing the neural network fitting tool as an estimator, it was obvious that the first result could not be accepted because of the amplitude and the horizontal smooth line. It was noticed that satisfactory results are coming after 30 iterations, in our case we had 33 iterations. As recommended in MathWorks, the algorithm Bayesian Regularization was implemented. [63] As it is presented in figure 4.14 from chapter 4, there were 1000 iterations necessary to get the best result for this process. Even if it took more time, the final filtered signal was more than satisfactory.

If we compare figure 4.13 and 4.9 from the previous chapter, the Regression plot looks a lot better for the Bayesian Regularization algorithm than Levenberg-Marquand algorithm.

The first applied model for predetection of strokes included a mathematical modelling of our eight ECGs and the detection of the polarity of their T waves as presented in figure 3.6 from chapter 3. Depending of that declared polarity, the alarms were displayed or not displayed.

The implemented algorithm was more than reliable, the alarm was displayed for all the patients with myocardium problems.

The second model was completely different; it used Artificial Neural Network Pattern Recognition to analyze the ECG pulses. The model computed all the waves decomposed in intervals of one second and built a neural network with 25 inputs, ten hidden nodes, and two outputs as it could be seen in figure 3.17, chapter 3.

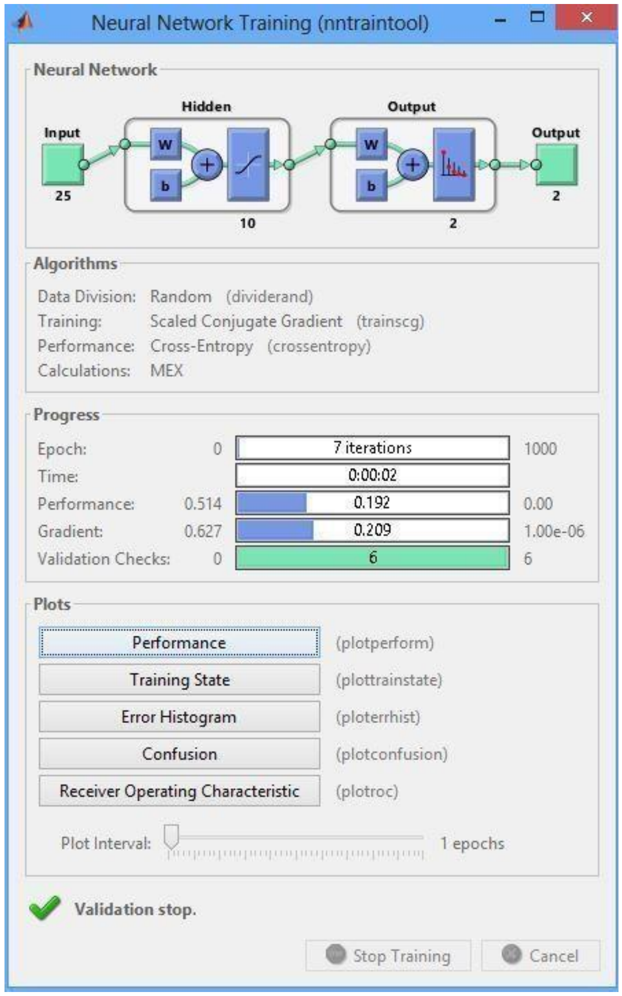

Figure 3.17 from chapter 3

In figure 3.17, before the *Algorithm* pane, the Neural Network architecture of the second model can be seen.

The alarms for this second model are given by the logical zeros values of the output matrix O1. This matrix could have been built with two or only one rows, both would work. In this thesis, the option went for two rows to consider the decomposed pulses and the polarity of T waves.

The Error Histogram for NN Pattern Recognition Algorithm (see the next figure 4.15) shows that the biggest error is 0.9369 while the smallest is 0.04931.

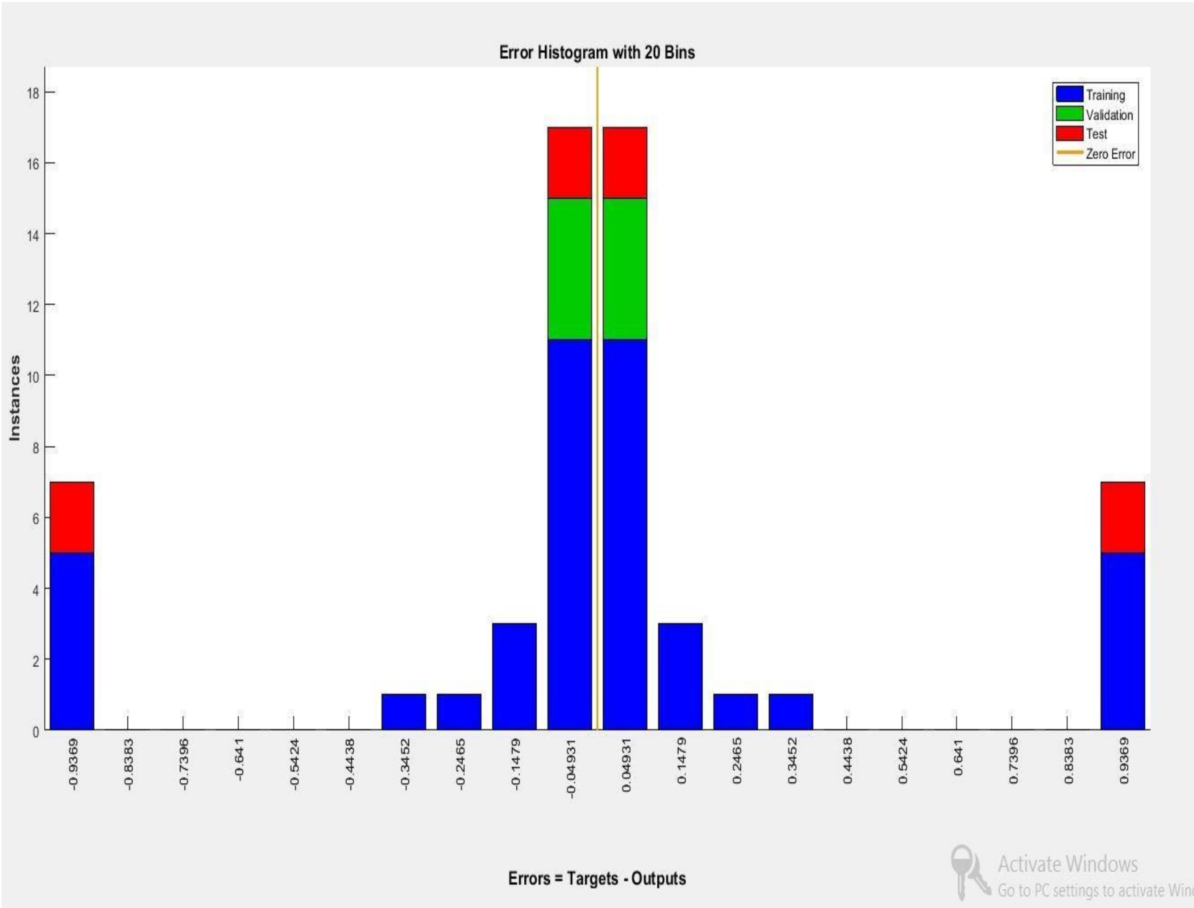

Figure 4.15: Error Histogram of NN Pattern Recognition Algorithm

The main results of the NN Pattern Recognition algorithm for predetection of strokes are presented in Table 4 and 5.

Table 4: The number of analyzed ECG samples by using NN Pattern Recognition algorithm

	ECGs	Number of analyzed ECG samples	Iterations	Training	Testing	Validated
Entry data	8	725	7	507	109	109
Percentage	-	100%	-	70%	15%	15%

In table 4 there are mentioned the 725 analyzed samples resulted from the 9 ECGs. From these 725 analyzed ECG samples, there were used 507 ECG samples for training, 109 ECG samples for testing, and 109 for validation.

Table 5: Main results of NN Pattern Recognition algorithm for predetection of strokes

	Total number of T-waves	Inverted T waves	Detected Inverted T-waves	Correct detection
Entry data	29	7	7	
Percentage	100%	24.14%	24.14%	100%

From 29 detected T waves there are seven T waves that have negative polarity so 24.14 is the percentage of inverse T waves of all analyzed T waves.

4.4 Model Selection

The first model is presenting a few advantages: it is dealing with each individual ECG, it is easier to build and it is giving a specific alarm for a specific client.

One disadvantage of this first model is that depending on the data source, the threshold values needs to be changed accordingly but, despite of the very large variety of data (including different amplitudes, different frequencies, different number of R peaks), the main purpose was met: the alarms were always displayed when this operation was needed.

If the main criteria for this model is the speed and effectiveness, then model one is the right one. Also, considering all these advantages and disadvantages which were just underlined above the author’s preference goes for the first model.

The use of Artificial Neural Networks becomes remarkable when it comes to nontrivial signals. When the general signal waves is hardly readable on ECGs, the use of Pattern Classification algorithm is appropriate.

If there is a need for improvement, there is minor things that could be improved in the first model.

Improvements can be brought at the second model. The number of columns could be better optimized, as well as the number of hidden nodes.

One problem when using Artificial Neural Networks is that when the user needs to retrain the samples, different results are obtained. The ways that the weights are changed and manipulated cannot be controlled by the user. So, basically speaking, there are no constant results.

The first model is efficient while model two is good for data optimization.

Model one is treating each ECG case by case so it can be used to examine and validate the results found in the second model.

Chapter 5 Conclusions

In the last dozens of years, artificial neural networks were used for the processing of data related to images and signals. The data is generated by various electronic devices recalled in the second chapter of this thesis or from registered sets of pre-existing data.

Various mathematical algorithms were implemented by different authors to evaluate the most important values of electrocardiograms.

In this study, there are two main algorithms and two new mathematical equations: two trigger alarms algorithms for predetection of strokes based on the electrocardiograms and two new mathematical equations related to signal estimation to detect stroke conditions. The ***main point of interest*** for this thesis was to see how the artificial neural networks can influence the predetection of strokes.

The most important things achieved are the following:

- ❖ *The* mathematical algorithm conceived to detect the *polarity of T waves* is successful; it detected all inversed T waves that existed in three ECGs out of nine analyzed ECGs.
- ❖ *The NN Pattern Recognition algorithm* was used to classify the mentioned signal waves: as shown in Table 5, all inverted T waves were classified correctly.
- ❖ *The new mathematical equation* for OMW can be considered the starting point of this thesis

When facing a stroke, the blood pressure is also taken into consideration. In time, several algorithms were implemented by distinguished scientist people for a good estimation of the most important components of the blood pressure: the systolic and diastolic pressure. A reliable model for the estimation of blood pressure components was provided in chapter 3. The parameters of the Fourier series describing the oscillometric waves were found. They performed well and proved to be reliable when the implementation of the respiration effects for two models took place. The extraction of the breathing effects for the oscillometric waveforms was done in other studies.

In this thesis, the impact that the breathing effects have on electrocardiograms were observed but not extracted because they had no influence over the pre-stroke detection studied here.

The filtering methods presented in chapter 4 were conceived for pre-processing noisy ECG signals. The acquisition of the data base was made by using pre-filtered electrocardiogram, such that applying these filters had a minimal impact over the global study; still it is important to have reliable filters when dealing with noisy signals to attain accurate alarms.

The results obtained in chapter four support the use of the Savitzky-Golay filter. Managing neural networks for fitting purposes proved to be challenging; with the selected data, a network was created and its performance was evaluated by using mean square error and regression analysis. It was obvious that the best fitting results are not acquired in the first case (with mean square error). Nerveless it is interesting to develop estimating algorithms by operating artificial neural networks.

The electrocardiograms and the physiological signals are difficult to be reproduced or modelled. They all have their unique nature. For plotting the ECGs, the best option was the smoothing spline function. The first pulse of ECGs was built with rational functions and for consistency reasons, it was kept only this function (named f(x)) for all the electrocardiograms. That does not mean that other mathematical function could not have been used. For instance, for our 51 years old patient, for the second function a second-degree polynomial function was a better fit. Because those mathematical functions were not very consistent for our electrocardiograms, they have not been incorporated into algorithms.

The backpropagation algorithm proved to be a good method for our biomedical signals classification since any new data was going to get similar outputs for the already trained signals.

For this thesis, when choosing an algorithm for the predetection of strokes it was easy to pick the first algorithm because it was direct, simple, and especially case oriented. It is not correlated to the artificial neural networks, it was the first mathematical model presented for our electrocardiograms in chapter three. Still the use of Artificial Neural Networks is superior to the mentioned algorithm when it comes to nontrivial signals.

The comparison of the algorithms for electrocardiograms is difficult because they are very different and they both have their own advantages and disadvantages. The main discussion about this aspect was generated in chapter four.

For future predetection of stroke alarms and other heart dysfunctionalities, the advantages of these both algorithms could be considered.

Limitations

The main limitations of this thesis are the followings:

- The number of the analyzed ECGs was limited to nine
- The variation of the main ECGs parameters such as R peaks and waves amplitudes, frequencies, and polarities; in general, these mentioned parameters are unpredictable
- The use of only *lead I* in all these electrocardiograms: other signals could have been identified on other leads but they will probably need different algorithms
- The copy-right issues: the permission for using specific figures was not given so some of them were drew by the undersigned

This study does not have to be considered a clinical trial because it was not done on a large number of patients. Ideally it would have been applied on a greater number of ECGs.

Future Work

When using Artificial Neural Networks, it is mandatory to deal with the world of different probabilities.

As reminded the data set was partially provided by ECG Library 1995-2014: Dean Jenkins and Stephen Gerred and from other five patients. Those electrocardiograms have the same scale and the data was easy to be collected. If these algorithms are going to be applied on different potentially data then different results are going to be obtained and the main parameters of our algorithms (e.g. thresholds) might need to suffer minor or major changes.

As it is written in chapter two, often the electronic devices that make available medical data have different scales.

More complex algorithms could be incorporated when dealing with electrocardiograms. Different T wave and other ECG's wave morphologies could be studied. As mentioned in chapter 1, in case of a myocardial ischemia, the T wave may become flattened, tall, inverted, or biphasic. [73]

Other algorithms could incorporate these changes or a part of these changes, including the use of Artificial Neural Networks.

Recent experiments are indicating notable promise in identifying diseases and predicting health outcomes. A new system made at the University of Nottingham in the UK can scan patients' medical data and predict who would have a stroke or heart attack in the next ten years. [78]

We know from various publications that some institutions are already using Artificial Neural Networks for the classification of the entire electrocardiogram. [46]

Steven Weng tested different learning machines tools on medical records (on over 375 000 patients across the UK). The accuracy of usual guidelines had a score of 0.728 while the machine learning models went from 0.745 to 0.764 and this best result came from a machine learning model "called neural networks". Almost 5000 patients who suffered a stroke or heart attack (the exact number is 4998) were predicted out of 7404 cases; this included 355 more than the standard method could predict. The use of artificial intelligence pattern recognition could provide more accurate results. [78]

In chapter 2 it was presented a history of the human medicine. Back in time errors of the medical devices were tolerated and the readings accuracy came later. Nowadays certain errors given by Neural Networks are expected. It is good to have small errors.

In the future, these errors are certainly going to be reduced, proved that science's progress has only one direction.

Appendix A

The complete and partial electrocardiograms of the patients studied in this thesis

ECG_M

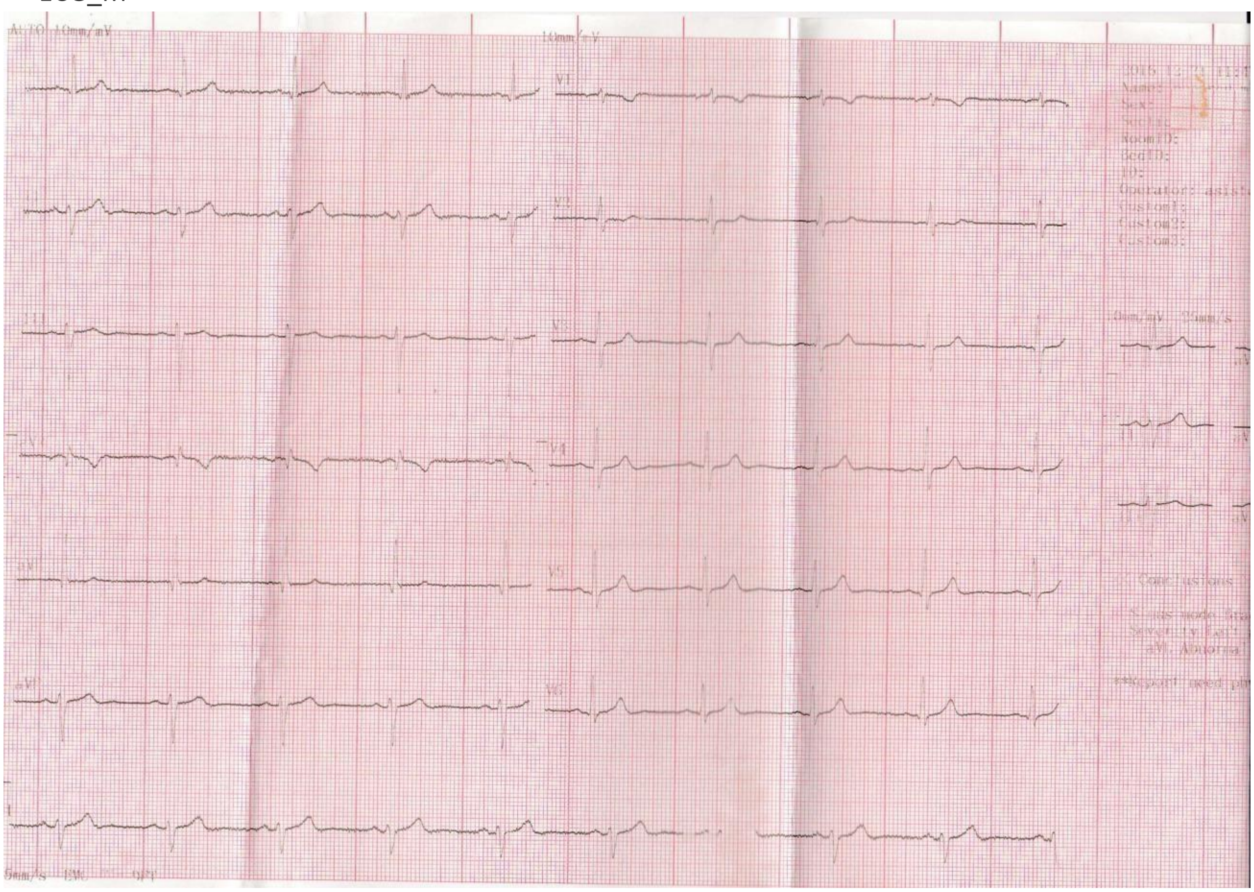

ECG_D

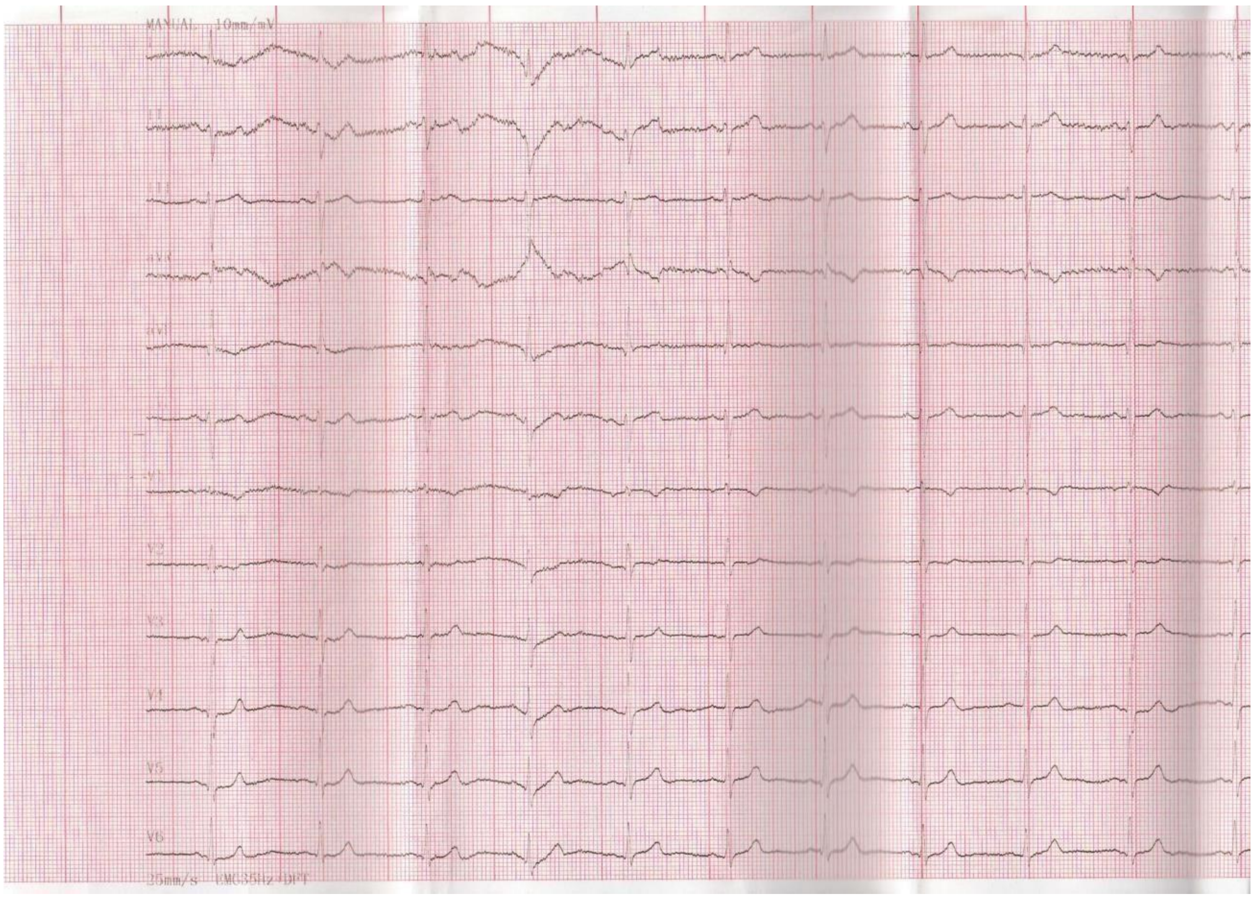

ECG_C

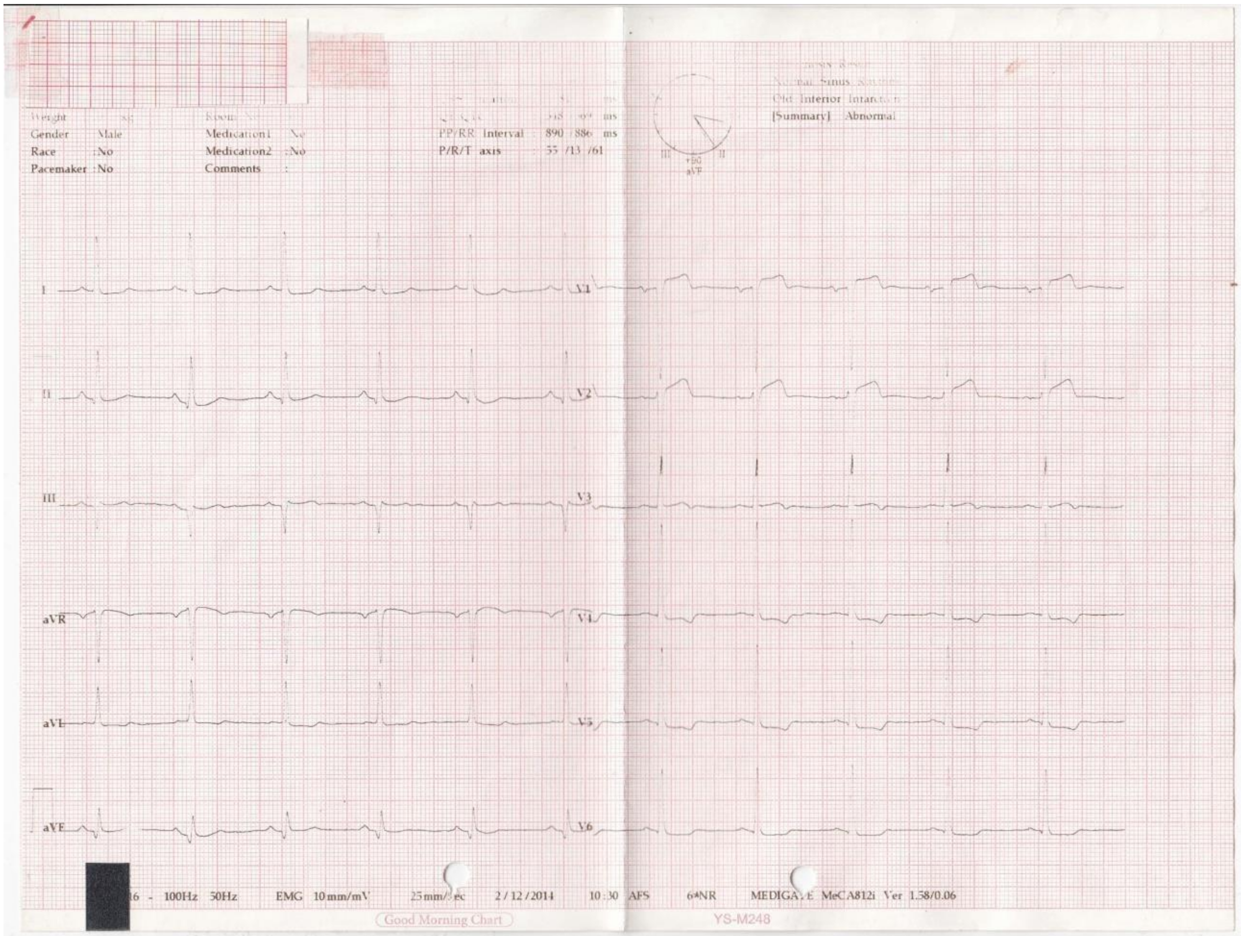

Gender Male
Race :No
Pacemaker :No
Medication2 :No
Comments :
PP/RR Interval : 890 /886 ms
P/R/T axis : 55 /13 /61
Old Interior Infarction
[Summary] Abnormal
I
II
III
aVR
aVL
aVF
V1
V2
V3
V4
V5
V6
[redacted] 16 - 100Hz 50Hz EMG 10mm/mV 2 / 12 / 2014 10:30 AFS 6*NR MeCA812i Ver 1.58/0.06
Good Morning Chart
YS-M248

ECG$_b$M

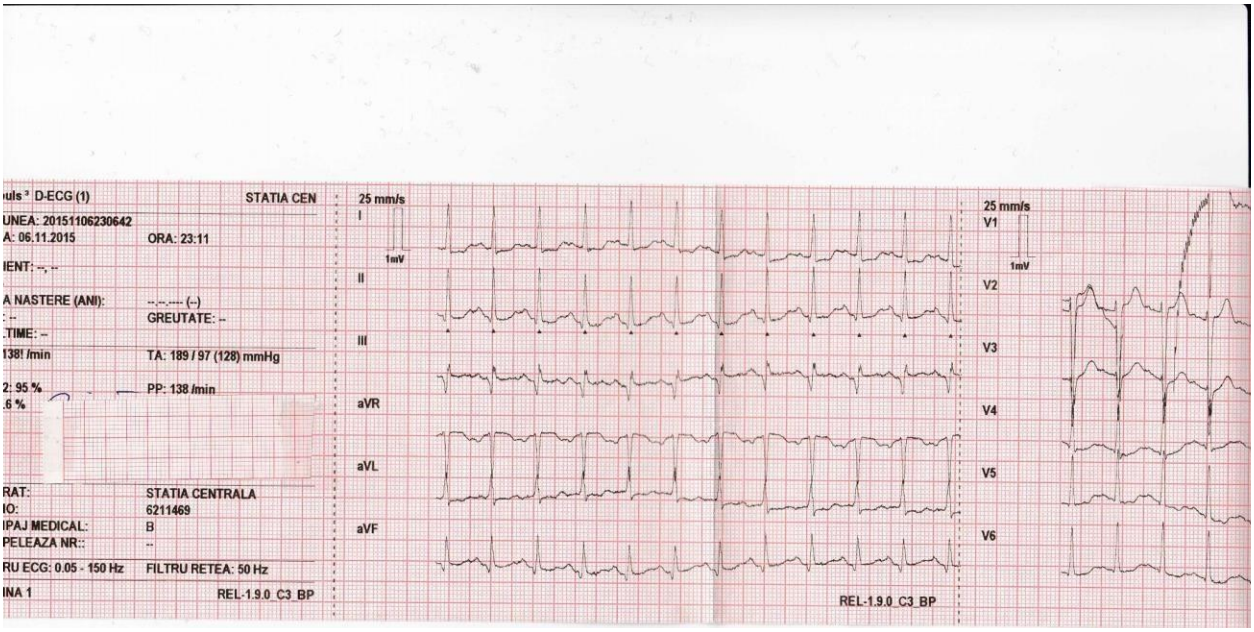

uls ³ D-ECG (1)
STATIA CEN
UNEA: 20151106230642
A: 06.11.2015
ORA: 23:11
IENT: --, --
A NASTERE (ANI):
--.--.---- (--)
GREUTATE: --
.TIME: --
138! /min
TA: 189 / 97 (128) mmHg
2: 95 %
PP: 138 /min
.6 %
RAT:
STATIA CENTRALA
IO:
6211469
IPAJ MEDICAL:
B
PELEAZA NR::
--
RU ECG: 0.05 - 150 Hz
FILTRU RETEA: 50 Hz
INA 1
REL-1.9.0_C3_BP
25 mm/s
I
1mV
II
III
aVR
aVL
aVF
REL-1.9.0_C3_BP
25 mm/s
V1
1mV
V2
V3
V4
V5
V6

ECG_A

115/min
10 mm/mV
Sa 16-MA -15 0
60/min
10 mm/mV
Sa 16-MAY-15 08:30:25
89/min
10 mm/mV
aVR
V2
aVF
V3
m/s
P8000
1e32 C
0.05-35Hz
F50 CMID25 mm/s
P8000
1e3
C
0.05-35Hz
F50 CMIDR Marino
u 25 25 mm/s
P8000
1e3
Art. No. 2.157 026
Art. No. 2.157 026
Art. No. 2.157 026
Art. No. 2.157 026

Appendix B

Tables of blood pressure and the electrocardiogram parameters of the studied patients

Table 1: Low, medium, and high values of blood pressure

Categories	Systolic / Diastolic
Low risk	120 / 80
Medium risk	121-139 / 80-89
High risk	140+ / 90

Table 2: ECG's parameters of a 70 years old man

Average frequency [Hz]	Smoothing parameter	Number of zero-crossing points	T waves negative polarity	Display Alarm	Ratio function f =f1+f2	
					f1 parameters	f2 parameters
0.9259	0.9987671887508507	6	No	No	r_{11}=1.17e+05 r_{12}=-5.405e+05 q_{11}=-6.279e+05 q_{12}=7.395e+06 q_{13}=-1.96e+07	r_{21}=0.1752 r_{22}=2.157 r_{23}=7.297 r_{24}=1.209 q_{21}=7.212 q_{22}=0.4504 q_{23}=67.56

Table 3: Table resuming patients' ECGs, predetection of stroke, and diseases

Patient	T waves negative polarity	Display alarm	Certified Disease	Name of the patients' ECG
Patient 1	No	No	N.A.	ECG_M
Patient 2	No	No	Diastolic dysfunction relaxation delayed type	ECG_D
Patient 3	Yes	Yes	Acute myocardial infarction	ECG_79
Patient 4	No	No	N.A.	ECG_C
Patient 5	No	No	Hypertension - left anterior hemi block	ECG_84
Patient 6	Yes	Yes	Acute inferior myocardial infarction	ECG_55
Patient 7	No	No	N.A.	ECG$_b$M
Patient 8	Yes	Yes	Unknown	ECG_A

Table 4: The number of analyzed samples by using NN Pattern Recognition algorithm

	ECGs	Number of analyzed ECG samples	Iterations	Tested	Trained	Validated
Entry data	9	725	7	507	109	109
Percentage	-	100%	-	70%	15%	15%

Table 5: Main results of NN Pattern Recognition algorithm for predetection of stroke

	Total number of T-waves	Inverted T waves	Detected Inverted T-waves	Correct detection
Entry data	29	7	7	
Percentage	100%	24.14%	24.14%	100%

Table 6: ECG's parameters of a 64 years old man

Average frequency [Hz]	Smoothing parameter	Number of zero-crossing points	T waves negative polarity	Display Alarm	Ratio function f =f1+f2	
					f1 parameters	f2 parameters
1	0.99876718875085	3	No	No	r_{11}=449.7 r_{12}=1.57e+04 r_{13}=1.356e+05 q_{11}=-211.4 q_{12}=8085 q_{13}=1.211e+05 q_{14}=6.68e+05	r_{21}=0.0621 r_{22}=0.1188 r_{23}=7.341 q_{21}=-19.81 q_{22}=123.3

Table 7: ECG's parameters of a 79 years old man

Average frequency [Hz[	Smoothing parameter	Number of zero-crossing points	T waves negative polarity	Display Alarm	Ratio function f =f1+f2	
					f1 parameters	f2 parameters
1.0417	0.997969062115129	6	Yes	Yes	r_{11}=-0.4702 r_{12}=18.17 r_{13}=234 r_{14}=1022 q_{11}=-45.68 q_{12}=771.9 q_{13}=-5760 q_{14}=1.631e+04	r_{21}=-11.2 r_{22}=879.3 r_{23}=2993 r_{24}=1967 q_{21}=334.8 q_{22}=145.8 q_{23}=937.1 q_{24}=173

Table 8: ECG's parameters of a 39 years old woman

Average frequency [Hz]	Smoothing parameter	Number of zero-crossing points	T waves negative polarity	Display Alarm	Ratio function f =f1+f2	
					f1 parameters	f2 parameters
1.1364	0.9987671887508	1	No	No	r_{11}=214 r_{12}=7877 r_{13}=6.668e+04 q_{11}=-51.11 q_{12}=1568 q_{13}=-3.252e+04 q_{14}=241e+05	r_{21}=325.3 r_{22}=364.3 r_{23}=1649 q_{21}=-15.53 q_{22}=0.5877 q_{23}=2193 q_{24}=-6378 q_{25}=1.167e+04

Table 9: ECG's parameters of an 84 years old lady

<table>
<tr><th rowspan="2">Average frequency [Hz]</th><th rowspan="2">Smoothing parameter</th><th rowspan="2">Number of zero-crossing points</th><th rowspan="2">T waves negative polarity</th><th rowspan="2">Display Alarm</th><th colspan="2">Ratio function f =f1+f2</th></tr>
<tr><th>f1 parameters</th><th>f2 parameters</th></tr>
<tr><td>1.3889</td><td>0.9992518992959787</td><td>13</td><td>No</td><td>No</td><td>r_{11}=0.6693
r_{12}=-2.952
r_{13}=1.774
q_{11}=-7.306
q_{12}=10.45
q_{13}=9.466
q_{14}=5.663
q_{15}=4.153</td><td>r_{21}=130.7
r_{22}=488.8
r_{23}=415.7
q_{21}=1683
q_{22}=-8843
q_{23}=1.344e+04</td></tr>
</table>

Table 10: ECG's parameters of a 55 years old man

<table>
<tr><th rowspan="2">Average frequency [Hz]</th><th rowspan="2">Smoothing parameter</th><th rowspan="2">Number of zero-crossing points</th><th rowspan="2">T waves negative polarity</th><th rowspan="2">Display Alarm</th><th colspan="2">Ratio function f =f1+f2</th></tr>
<tr><th>f1 parameters</th><th>f2 parameters</th></tr>
<tr><td>0.7576</td><td>0.99796906211513</td><td>9</td><td>Yes</td><td>Yes</td><td>r_{11}=239 r_{12}= -4820
r_{13}=2.42e+04
q_{11}=872.8 q_{12}=-2.047e+04
q_{13}=1.164e+05</td><td>r_{21}=0.09034
r_{22}=-1.064
r_{23}=3.787
q_{21}=15.54
q_{22}=68.52
q_{23}=-39.61</td></tr>
</table>

Table 11: ECG's of a 51 years old man

Average frequency [Hz]	Smoothing parameter	Number of zero-crossing points	T waves negative polarity	Display Alarm	Ratio function f =f1+f2	
					f1 parameters	f2 parameters
2.2727	0.9987671887508	1	No	No	r_{11}=-144.2 r_{12}=-665.7 r_{13}=9248 q_{11}= -61.54 q_{12}=1146 q_{13}= -9873 q_{14}=2.845 e+04 q_{15}=9161	r_{21}=41.35 r_{22}=308.4 r_{23}= -168.1 q_{21}=1866 q_{22}= -947.8

Table 12: ECG's parameters of a 94 years old lady

Average frequency [Hz]	Smoothing parameter	Number of zero-crossing points	T waves negative polarity	Display Alarm	Ratio function f =f1+f2	
					f1 parameters	f2 parameters
Irregular	0.99796906211513	7	Yes	Yes	r_{11}=-42.79 r_{12}= -848.7 r_{13}=4212 q_{11}= 18.68 q_{12}=38.57 q_{13}= -6929 q_{14}=3.961 e+04	r_{21}=0.01339 r_{22}= -.1379 r_{23}=0.3339 r_{24}= -0.0902 q_{21}= -11.15 q_{22}=32.39

References:

[1] John Paul Rosendall, Amanda J. Sheppard, Dalla Lana, Elly Berger (Chief of Editors), "AboutKidsHealth" Published and last revised, August 19, 2015. Online available at:

{http://www.aboutkidshealth.ca/En/HowTheBodyWorks/IntroductiontotheHeart/Anat omyo fth

[2] A. Castiglioni, "A History of Medicine" Castiglioni A.-2nd ed. Krumbhaar EB, TR. New York; Alfred Knopf, 1947.

[3] Heart & Vascular Team, "HealthEssentials - Busting 5 Myths about Blood Pressure and Heart Rate" February 24, 2014. Online available at:

{ http://health.clevelandclinic.org/2014/02/busting-5-myths-about-blood-pressure-andhearthttp://health.clevelandclinic.org/2014/02/busting-5-myths-about-blood-pressure-and-heartrate/rate/}

[4] National Stroke Association team, "Understanding stroke – What is stroke?" ® Hope After Stroke. Accessed in March 2017. Online available at: http://www.stroke.org/understand-stroke/what-stroke

[5] Dennis Thompson, "Too Many Stroke Victims Don't Get Clot-Buster Drug"– WebMD – February 23, 2017. Online available at:
http://www.webmd.com/stroke/news/20170223/toomany-stroke-victims-dont-get-clotbusting-drug-study#1

[6] WebMD team, "Stroke Overview", 2016. Online available at: http://www.webmd.com/stroke/

[7] Robert Berkow, Mark H. Beers, Robert M. Bogin, Andrew J. Fletcher "Merck Manual of Medical Information", Home Edition, page 74, 1997.

[8] American Heart Association, "How High Blood Pressure Can Lead to Stroke". Online available at:

http://www.heart.org/HEARTORG/Conditions/HighBloodPressure/LearnHowHBPHar msYour
He alth/How-High-Blood-Pressure-Can-Lead-to-
Stroke_UCM_301824_Article.jsp#.WPDdn_nyuM8

[9] N.M. Naqvi, M.D. Blaufox," Blood Pressure Measurement – An Illustrated History" - The Parthenon Publishing Group, New York, pages xiii, 5, 60, 58, 67, 7, 78, 82, 1998.

[10] Heart & Stroke team, "High Blood pressure". Online available at:

{http://www.heartandstroke.com/site/c.ikIQLcMWJtE/b.3484023/k.2174/Heart_diseas e___High__blood_pressure.htm

[11] Scott Reule and Paul E. Drawz, "Heart Rate and Blood Pressure: Any Possible

Implications for Management of Hypertension?" PMC – US National Library of Medicine National Institutes of Health, Published in final edited form as: Curr Hypertens Rep. 2012 Dec; 14(6): pages 478-484, December 1, 2013. Online available at: http://www.ncbi.nlm.nih.gov/pmc/articles/PMC3491126/

[12] R. Dulbecco, "Encyclopedia of Human Biology" - 2nd ed. San Diego, Calif.: Academic Press; 1997.

[13] Y.K. Anthony Chan, "Biomedical Device Technology: Principles and Design" – Charles C Thomas Publisher, Ltd. Springfield Illinois USA - pages 315, 317, 299, 2008.

[14] National Institute of Health team, "Your Heart's Electrical System" – National Heart, Lung, and Blood Institute – November 17, 2011. Online available at: https://www.nhlbi.nih.gov/health/healthhttps://www.nhlbi.nih.gov/health/healthtopics/topics/hhw/electricaltopics/topics/hhw/electrical

[15] Sarah Perez, "AliveCor unveils Kardia Band, a medical-grade EKG band for Apple Watch", March 16, 2016. Online available at: https://techcrunch.com/2016/03/16/alivecor-unveilshttps://techcrunch.com/2016/03/16/alivecor-unveils-kardia-band-a-medical-grade-ekgband-for-apple-watch/kardia-band-a-medical-grade-ekg-band-for-apple-watch/

[16] Peters TM, Williams JC, Bates JHT "The Fourier Transform in Biomedical Engineering. Boston: Birkhal user", 1998.

[17] E. Balestrieri, "Open Questions on Unified Approach for Calibration of Oscillometric Blood Pressure Measurement Devices," Differences, pages 206–211, University of Sannio and P. Daponte University of Sannio, 2009.

[18] David A. Abolarin, "Non-invasive Estimation of Blood Pressure using Harmonic Components of Oscillometric Pulses", Ottawa, 2015.

[19] Silu Chen, "Improving Algorithms for Oscillometric Blood Pressure Estimation by Suppressing Breathing Effects", page 6, 2010.

[20] J. N. Amoore, "Oscillometric sphygmomanometers: a critical appraisal of current technology," Blood Press. Monit, vol. 17, no. 2, pages 80-86, 2012.

[21] J.N. Amoore, "Extracting Oscillometric Pulses from the Cuff Pressure: Does it Affect the Pressures Determined by Oscillometric Blood Pressure Monitors?" Blood Pressure Monitoring, vol. 11, Oct. 2006, pages 269-279, Online available at:

https://www.ncbi.nlm.nih.gov/pubmed/16932036

[22] V. Jazbinsek, J. Luznik, Z. Trontelj, "Non-Invasive Blood Pressure Measurements: Separation of the Arterial Pressure Oscillometric Waveform from the Deflation Using Digital Filtering," IFBME Proceedings of EMBEC'05, Prague, Czech Republic, November 2005.

[23] Andrew R. Nara, Michael P. Burns, W. Gregory Downs, “Biophysical Measurement Series: Blood Pressure”, page 73, January 1, 1989.

[24] R.I. Kitney and O. Rompelman, “The beat-by-beat investigation of cardiovascular function; measurement, analysis, and applications”– Oxford: Clarendon Press – Oxford, 1987 – pages 59, 148, and 154, 1987.

[25] J.A. Hirsch, B. Bishop, “Respiratory Sinus Arrhythmia in Humans: How Breathing Pattern Modulates Heart Rate,” American Journal of Physiology Heart and Circulatory Physiology, vol. 241, pages 620-629, Oct. 1981.

[26] Dohan James, “Lesson 4: Circulatory System” in BioMed 108 – Human Physiology, Sept. 17, 1999. Online available at: http://www.biosbcc.net/doohan/sample/htm/COandMAPhtm.htm

[27] George B. Moody, Roger G. Mark, Andrea Zoccola, and Sara Mantero, “Derivation of Respiratory Signals from Multi-lead ECGs”, Computers in Cardiology 1985, vol. 12, pages 113-116 (Washington, DC: IEEE Computer Society Press), 1985.

[28] Charles F. Babbs, “Oscillometric measurement of systolic and diastolic blood pressures validated in a physiologic mathematical model”, June 28, 2012. Online available at: https://biomedical-engineering-online.biomedcentral.com/articles/10.1186/1475-925X-1156

[29] Mohamad Forouzanfar, “A Modeling Approach for Coefficient-Free Oscillometric Blood Pressure Estimation”, 2014.

[30] L. T. Hersh, B. Friedman, and R. Medero, “Method for oscillometric blood pressure determination employing curve fitting.” US Patent 5,704,362, Jan. 6, 1998.

[31] Shkti Chatterjee and Aubert Miller “Biomedical Instrumentation”, 1st Ed. New York: DelMar Cengage Learning, 2010.

[32] M. Mafi, S. Rajan, M. Bolic, V. Z. Groza, and H. R. Dajani, “Blood pressure estimation using oscillometric pulse morphology,” Proc. Annu. Int. Conf. IEEE Eng. Med. Biol. Soc. EMBS, pages 2492–2496, 2011.

[33] Health Care Science OCW team, “Introduction to Vital Signs Examination and Evaluation, Measuring Pulse Rate”, pages 2-9, Accessed on February 2017. Online available at: http://healthcaresciencesocw.wayne.edu/vs/4_2.htm

[34] Michael F O’Rourke, Alfredo Pauca and Xiong-Jing Jiang, “Pulse wave analysis”, pages: 507-522, 2001.

[35] Tony J. Akl, Marl A. Wilson, M. Nance Ericson, and Gerard L. Coté, “Quantifying tissue mechanical properties using photoplethysmography”, pages: 2362–2375, July 1, 2014.

[36] Dallas Price, “SSMJ South Sudan Medical Journal – How to read an Electrocardiogram (ECG) Part One: Basic principles of the ECG. The normal ECG”, 2010-2012, May 2010. Online available at: http://www.southsudanmedicaljournal.com/archive/may-2010/howto-read-an-electrocardiogram-ecg.-part-one-basic-principles-of-the-ecg.-the-normalecg.html

[37] Neil Townsend, Michaelmas Term, “Medical Electronics”, pages 52-54, 2001.

[38] J. Allen, “Photoplethysmography and its application in clinical physiological measurement”, Clinical Science, Vol. 103, page 371-377, 2002.

[39] Andrew Houghton, “Making sense of the ECG: A Hands-On Guide, Fourth Edition”, David Gray, page 7, June 4, 2014.

[40] Stephen J. Phillips, “Pathophysiology and Management of Hypertension in Acute Ischemic Stroke”, page 131-136, 1994.

[41] Karen C. Johnston and Stephan A. Mayer, “Blood pressure reduction in ischemic stroke - A two-edged sword?” vol. 61 no. 8 1030-1031, Neurology October 28, 2003.

[42] K.N. Vemmos, K. Spengos, G. Tsivgoulis, N. Zakapoulos, E. Manios, V. Kotsis, M. Daffertshofer, D. Vassiopoulos, “Factors influencing acute blood pressure values in stroke subtypes”, pages: 253-259, April 18, 2004.

[43] Mohamad Forouzanfar, Saif Ahmad, Izmail Batkin, Hilmi R. Dajani, Voicu Z. Groza, and Miodrag Bolic, “Coefficient-Free Blood Pressure Estimation Based on Pulse Transit Time– Cuff Pressure Dependence”, vol. 60, pages: 1814 – 1824, July 7, 2013.

[44] A. Ball-Llovera, R. Del Rey, R. Ruso, J. Ramos, O. Batista, I. Niubo,” An experience in implementing the oscillometric algorithm for the non-invasive determination of human blood pressure”, Proceedings of the Annual International Conference of the IEEE Engineering in Medicine and Biology Society; 2003; pages: 3173-3175, 2003.

[45] J.C. Perfetto, A. Ruiz, J.R. Mazzeo, C. D'Attellis, “Robust algorithm to extract systoles and diastoles from continuous blood pressure signal”, Proceedings of the 25th Annual International Conference of the IEEE Engineering in Medicine and Biology Society; pages 279-282, 2003.

[46] Robnier Reyes Perez, Andrew Marques, Farah Mohamadi, “The application of supervised learning through feed-forward neural networks for ECG signal classification”, Proceeding of the IEEE Canadian Conference on Electrical and Computer Engineering (CCECE), 2016.

[47] S. Colak, C Isik, “Systolic blood pressure classification”, Proceedings of the International Joint Conference on Neural Networks, 2003.

[48] G. Gratze, J. Fortin, A. Holler, K. Grasenick, G. Pfurtscheller, P. Wach, J. Schonegger, P. Kotanko, F. Skrabal, “A software package for non-invasive, real-time beat-to-

beat monitoring of stroke volume, blood pressure, total peripheral resistance and for assessment of autonomic function", pages: 121-142, March 28, 1998.

[49] Simon Haykin "Neural Networks – A Comprehensive Foundation", Pearson Education Upper Saddle River, pages 2, 6, 7, 10, 11, 14, 21, 23; 1999.

[50] Lucas Illing, "Fourier Analysis", page 3, 2008.

[51] ANSI/AAMI SP 10: 2002/(R) 2008 & ANSI/AAMI SP 10: 2002/A1: 2003/(R) 2008 & ANSI/AAMI SP 10: 2002/A2: 2006/(R) 2008, "Manual, electronic, or automated sphygmomanometers", 2008.

[52] MATLAB, "Linear and Non-Linear Regression - Sum of Sines Models", March 2017. Online available at: http://www.mathworks.com/help/curvefit/sum-ofsine.html?searchHighlight=sum%20of%20sine

[53] MATLAB R2016b, "Help – Linear Regression", March 2017.

[54] MATLAB R2016b, "Help – Curve Fitting and Distribution Fitting", March 2017. .

[55] Normal Breathing team, "Normal Respiratory Frequency and Ideal Breathing", NORMALBREATHING.com, site registered in 2004 by Dr. Artour Rakhimov.Online available at: http://www.normalbreathing.com/index-rate.php

[56] Dean Jenkins and Stephen Gerred, "ECG Library - 1995-2014. Dean Jenkins and Stephen Gerred". Accessed in February 2017. Online available at: http://www.ecglibrary.com/ecghome.php

[57] Matlab, The Math Works Inc. team, "The Language of Technical Computing – Computation, Visualization, Programming" – Using Matlab Version 6, page 12-3, October 2, 1996.

[58] Contec Medical Systems team, "Electrocardiograph ECG1200G – User Manual" – Contec Medical Systems Co., Ltd., page 20, March 2014.

[59] Robert O. Bonow, James E. Udelson, "Left Ventricular Diastolic Dysfunction as a Cause of Congestive Heart Failure: Mechanisms and Management – Annals of Internal Medicine", September 15, 1992. Online available at: http://annals.org/aim/article/705803/leftventricular-diastolic-dysfunction-cause-congestive-heart-failure-mechanisms-management

[60] Matlab, The MathWorks, Inc. team, "MathWorks – Classify Patterns with a Neural Network" – 1994-2017: The MathWorks, Inc.: Online available at: https://www.mathworks.com/help/nnet/gs/classify-patterns-with-ahttps://www.mathworks.com/help/nnet/gs/classify-patterns-with-a-neural-network.htmlneuralnetwork.html

[61] Matlab, The MathWorks, Inc. team," MathWorks – Signal Processing Toolbox – Functions – sgolay" – Introduced before R2006a - 1994-2017 The MathWorks, Inc.

Online available at: https://www.mathworks.com/help/signal/ref/sgolay.html (March 2017)

[62] Matlab, The MathWorks, Inc. team," MathWorks – Neural Network Toolbox – Function
Approximation and Nonlinear Regression – Fit Data with a Neural Network" - 1994-2017 The MathWorks, Inc. : Online available at: https://www.mathworks.com/help/nnet/gs/fitdata-with-a-neural-network.html (March 2017)

[63] Matlab, The MathWorks, Inc. team, "MathWorks – Econometrics Toolbox – Time Series Regression Models – Bayesian Linear Regression Models" - 1994-2017 The MathWorks, Inc.: Online available at: https://www.mathworks.com/help/econ/what-is-bayesian-linear-regression.html

[64] A.J. Thomas, "MEDICWIZ" – Concise Health Insights –Editorial Team, medically reviewed by Dr. AJ Thomas MS, April 3, 2016: Online available at: https://www.medicwiz.com/medtech/diagnostics/10-types-of-ecg-devices-for-heartrhythmhttps://www.medicwiz.com/medtech/diagnostics/10-types-of-ecg-devices-for-heartrhythm-monitoringmonitoring

[65] W. Perry Dickinson, "Medscape – Myocardial Infarction After Stroke", July 19, 2003.
Online available at: http://www.medscape.com/viewarticle/458114

[66] Better Health team, "Better Health Channel – ECG test" – Heart Foundation 2016, page 2, February 2017. Online available at: https://www.betterhealth.vic.gov.au/health/conditionsandtreatments/ecg-test

[67] Statistics Canada, "Health Fact Sheets – The 10 leading causes of death, 2012" December 10, 2015. Online available at: http://www.statcan.gc.ca/pub/82-625x/2015001/article/14296-eng.htm

[68] Government of Canada, "Health Status of Canadians 2016: Report of the Chief Public Health Officer – How we are unhealthy?" page 17, December 15, 2016- Online available at: http://www.healthycanadians.gc.ca/publications/department-ministere/state-publichealth-status-2016-etat-sante-publique-statut/page-17-eng.php

[69] Feroze Rafey, Arpan V. Prabtu, and Agarwal Nitin, "Stroke Education is Underrepresented in U.S. Undergraduate Clinical Curricula", page 435, April 2017. Online available at:

http://journals.lww.com/academicmedicine/Citation/2017/04000/Stroke_Education_Is_Underr epresented_in_U_S_.24.aspx

[70] Paul D. White, Howard B. Sprague, "The New England Journal of Medicine – Medical Progress – Cardiovascular Review for 1933", vol. 211, No 22, page 1019, November 1934.

Reproduced with permission from "Medical Progress – Cardiovascular Review for 1933" -Copyright Massachusetts Medical Society

[71] David F.M. Brown, Farouc A. Jaffer, Joshua N. Baker, and Edip Gurol, "The New England Journal of Medicine – Case 28-2003 – Old Man with Cardiac Arrest after an Acute Myocardial Infarction", page 1047, September 12, 2003.

Reproduced with permission from Case 28-2003-Old Man with Cardiac Arrest after an Acute Myocardial Infarction-Copyright Massachusetts Medical Society

[72] My EKG team, "How to place Electrocardiogram Electrodes", My ECG – The Web of the Electrocardiogram, Accessed on April 2017. Online available at: http://en.my-ekg.com/basicprinciples/electrodes-ekg.html

[73] Kevin Channer and Francis Morris, "ABC of clinical electrocardiography – Myocardial ischemia", British Medical Journal 2002, April-June, No 324, page 1023, April 2002.

[74] Peter Libby, "Mechanism of Acute Coronary Syndromes and Their Implications for Therapy", The New England Journal of Medicine, page 368, May 23, 2013.

[75] Mohamed Abdelazez, Adrian D. C. Chan, Homer Yang, "Gating of False Alarms in Myocardial Ischemia Monitoring Using ST Segment Deviation Trend Estimator", page 332-327, 978-15090-2984-6/17/$31.00 ©2017 IEEE, 2017.

[76] V.C. Cavalcanti Roza, Ana Maria de Almeida, Octavian Adrian Postolache, "Design of an Artificial Neural Network and Feature Extraction to Identify Arrhythmias from ECG", pages 391396, 978-1-5090-2984-6/17/$31.00 ©2017 IEEE, 2017.

[77] C-H Lin, "Frequency-domain features for ECG beat discrimination using grey relational analysis-based classifier," Computer and Mathematics with Applications, vol. 55, page 680-690, 2008, April 10, 2007. Online available at: http://www.sciencedirect.com/science/article/pii/S0898122107005019

[78] Eliza Strickland, "AI Predicts Heart Attacks and Strokes More Accurately Than Standard Doctor's Method", 1 May 2017. Online available at:

http://spectrum.ieee.org/the-human-os/biomedical/diagnostics/ai-predicts-heart-attacksmore-accurately-than-standard-doctor-method

[79] Jason Brownlee, "How to Implement the Backpropagation Algorithm from Scratch in Python," November 7, 2016. Online available at:

https://machinelearningmastery.com/implement-backpropagation-algorithm-scratch-python/

[80] Matt Mazur, "A Step by Step Backpropagation Example," March 17, 2015. Online available at: https://mattmazur.com/2015/03/17/a-step-by-step-backpropagation-example/

[81] Revindra Kumar Garg, Steven R. Levine "Neurology MedLink – Stroke associated with myocardial infarction", April 10, 1995, last updated May 14, 2017. Online available at: http://www.medlink.com/article/stroke_associated_with_myocardial_infarction

[82] Daniel E Becker, "Fundamentals of Electrocardiography Interpretation", page 53-64, 2006. On-line available at: https://www.ncbi.nlm.nih.gov/pmc/articles/PMC1614214/